Title
Clonal behavior of germ cells during male sex differentiation

Permalink
https://escholarship.org/uc/item/4pj57336

Author
Nguyen, Daniel

Publication Date
2017

Peer reviewed|Thesis/dissertation

Clonal behavior of germ cells during male sex differentiation

by

Daniel Hoang Nam Nguyen

DISSERTATION

Submitted in partial satisfaction of the requirements for the degree of

DOCTOR OF PHILOSOPHY

in

Biomedical Sciences

in the

GRADUATE DIVISION

of the

UNIVERSITY OF CALIFORNIA, SAN FRANCISCO

ACKNOWLEDGEMENTS

This thesis is merely mine to write about, but the work described within belongs to many besides myself. If we stand on the shoulders of giants, I hope I have not been too burdensome on the climb up. To my many colleagues along the way – you are the real giants.

My foremost thanks goes to my advisor, Diana Laird, for inspiring myself and this work. Diana has been steadfast in her encouragement and motivation for my research as well as my personal and professional development. Her intelligence, creativity, and patience have provided me room to explore and an endless supply of interesting questions to consider. For a scientist so well versed in a wide range of model organisms, Diana may be most expert in humans – her mindfulness about her science and her scientists has helped us all improve to better achieve our goals. Our lab is a wonderful environment because of her. Diana, I am grateful you welcomed me into your lab and home. I am a far better scientist and person because of it.

I have had the good fortune to receive exceptional training and advice from many mentors along the way. I would like to first acknowledge my thesis committee, Marco Conti and Todd Nystul, for their unwavering guidance and extraordinarily helpful insight as this thesis project has grown and changed throughout the years. Their commitment to my success and the development of this work is humbling. I am honored to have worked with them.

I must also thank my former PI, Tamara Alliston, who not only inspired me to pursue a graduate degree but also provided the emotional support that allowed me to dedicate myself to it. Her faith in me helped shepherd me through my own adversity and I owe so much of my

accomplishments in graduate school to her compassionate encouragement. I am so grateful to have her nearby to share in personal and academic successes.

For all the endless hours spent in lab, none of it would be possible without the amazing people I have been privileged to work with on a daily basis. You make the long days and nights not merely enjoyable but truly memorable. If I cannot mention you all – you are certainly every much a part of this as I am. To Andrea, Ripla, Mehlika, Boris, Rebecca, Bikem, Jen, Brandon, Estelle, and all who came before and all who are yet to come – you have made Laird Lab my home. I treasure our conversations and activities and I am so excited to see your future successes. I simply hope I can return a fraction of all the you have so richly provided me.

To my non-scientist friends, I apologize for disappearing for all these years. This thesis proves, perhaps, that all those times I've reneged on socializing were not in vain. As you can now see, my mouse obligations were quite real. I still am amused by your efforts to translate my research to others. Thank you for providing some brevity to remind me that science is an amazing endeavor, even when egregiously miscommunicated. To Esther, Al, my high school friends, Jon, Greg, Vijay, Austin, Anand, and my other college friends: I have some free time finally – is Bootie still around? I'm so glad you were also in San Francisco to help keep me sane and in good spirits.

Lastly, all this is dedicated to my family. To Christina, my sister: you are such an inspiration to me. I am so proud of you and all you've accomplished. And thank you for always providing me with laughter. It's more meaningful than you might know, even though you know everything. To my mother, Thu: your bravery towers over anything I've had to face. This thesis is a reflection of the strength you've endowed in me and the love with which you've raised me. I can never thank you enough. And lastly, to my father, Long, my first and most beloved teacher. You always loved showing me how things worked and I secretly delighted in learning from you. And still to this day, and even beyond, I keep learning from you. I'm so thankful for that. I may have started graduate school without you, but along the way, I've found you. I'm forever on your shoulders.

ABSTRACT

Natural selection is the process by which variation within a population is assessed and resolved, leading to success of certain individual winners over losers. Though this principle is well studied at an organismal level, cellular populations are also subject to selection as they navigate through developmental transitions. Germline development in the fetal period is complex and diverse, necessitating that germ cells complete numerous cell state transitions to appropriately prepare for gametogenesis in the adult. The events of fetal germ cell development can therefore function as selective barriers that assess developmental competency in a germ cell population. Here, we examine how fetal events in male germ cell development contribute to the variation in a germ cell population. We utilize clonal labeling and various analyses at a cellular resolution to determine the heritable basis for winner germ cells that successfully complete development versus losers that fail to do so.

We identify apoptosis as a major selective process that nonrandomly eliminates germ cells. We show that apoptosis is due to cell-intrinsic properties rather than extrinsic causes. Clonal labeling reveals that specific clonal populations are removed by apoptosis. We further analyze by apoptotic germ cells within an entire population by single-cell RNA sequencing to identify characteristics associated with developmental losers. We find that fidelity to the male sex differentiation program is a highly heterogeneous attribute discerning winner germ cells from those eliminated by apoptosis. When we extend our assessment of germ cell heterogeneity over developmental time, we identify an early differentiating population that is resilient to apoptosis and more capable of suppressing transposons.

These results indicate that variation in germ cells is revealed during male differentiation to lead to highly divergent outcomes. This variation is clonal in nature and therefore heritable. The consequence of developmental selection acting on this germ cell heterogeneity is predicted

to benefit germ cell function. In this sense, fetal development improves germ cell quality by serving as a natural selection process.

TABLE OF CONTENTS

LIST OF TABLES

LIST OF FIGURES

CHAPTER 1: INTRODUCTION

Natural selection is the process by which variations among individuals produce differential success, eventually leading to population wide changes that are responsible for diverse speciation seen today. A key requirement for natural selection is phenotypic diversity that can be assessed for fitness differences. When combined with a heritable basis for phenotypic diversity – such as through genetic or epigenetic differences – selection can lead to population-level changes over time. This principle has been well-established and studied at an organismal level, but investigating cellular selection has long proven elusive due to difficulties in both assessing variation and tracking outcomes. New advances for cellular analysis such as clonal labeling and single-cell sequencing have begun to shed light into the selection criteria and outcomes among many cell populations, including tumors and adult stem cells (Snippert et. al, 2010, Patel et. al, 2014, Kumar et. al., 2017). However, the germline is unique among these cellular settings in that any heritable differences that arise among individual cells can only be transgenerationally fixed if they occur in germ cells. For this reason, variation among germ cells is subject to two modes of natural selection: one at the organismal level, to determine if a heritable change provides a fitness benefit to the soma, and second at the germ cell level, to determine if such a change assists in the success of a germ cell in progressing through all the stages of germ cell development to the end goal of gametogenesis.

Germ cells undergo diverse cell state transitions to prepare for eventual gametogenesis, which occurs in the fetal period in females but is delayed until adulthood for spermatogenesis. Progress through these diverse developmental challenges can further segregate germ cells based on competence. The variety of cell behaviors required to complete this journey can thoroughly examine germ cells for genetic variation in a sort of developmental selection.

Prior to sex determination, which occurs around e12.5 in mice, germ cells are sexually undifferentiated and their development is largely identical. Germ cells are specified from a

population of about 40 cells at 7.25 (Saitou et. al., 2012). Termed primordial germ cells (PGCs), this population undergoes migration through the hindgut shortly after specification, onto the dorsal mesentery at e9.5, and finally conclude their migratory journey by colonizing the gonadal ridge at e10.5 (Molyneaux et. al., 2001, Seki et. al., 2007). Simultaneous to this migratory cell state, epigenetic reprogramming via genome-wide DNA demethylation is ongoing to erase genomic imprinting (Saitou et. al., 2012). Upon colonizing the gonadal ridge, PGCs from both sexes transition to a proliferative phase while preparing for sex differentiation. This next step occurs at 13.5 and is dependent on the sexually dimorphic somatic environment (Koopman et. al, 1991). In females, retinoic acid from the soma initiates meiotic entry (Koubova et. al., 2006) while in males, Cyp26b1 degrades retinoic acid and promotes a male fate (Saba et. al., 2014).

As this work is primarily concerned with male germ cell development, this discussion will be subsequently restricted to developmental events leading to spermatogenesis. Beginning as early as e11.5, male fate differentiation is also initiated by FGF9 signaling from the newly-formed Sertoli cells (Bowles et. al., 2010) and further reinforced by Nodal signaling, which is expressed in developing male germ cells at e12.5 and binds to Cripto, a Nodal receptor induced by FGF9 (Spiller et. al., 2012). Nodal signaling in turn promotes expression of *Nanos2* beginning at e13.5, a master male germ cell regulator that locks in male fate (Suzuki et. al., 2008). Mutations in *Nanos2* lead to male germ cells failing to mitotically arrest and entering meiosis instead. This occurs even in a male somatic environment; therefore, *Nanos2* expression is necessary for intrinsic commitment of male germ cells to the male lineage.

Germ cell proliferation, which continues from e9.5 up through e13.5, begins to cease as early as e12.5 (Cantu, et. al., 2016, Western et. al., 2008), although mitotic arrest does not occur synchronously throughout the entire population (Spiller et. al, 2009). By e14.5, most male germ cells are quiescent in G_0/G_1 arrest until shortly after birth, when neonatal germ cells – now termed prospermatogonia – move to the periphery of the testis cord, resume mitosis, and initiate

spermatogenesis (Nagano et. al., 2000, Western 2008). Activin receptors such as ALK4/ALK7 are required for entry into mitotic arrest (Miles et. al., 2013) and Activin knockout studies report overproliferation of germ cells by e15.5 (Mendis et. al., 2011). Mitotic arrest is associated with the male sex differentiation program; *Nanos2* is required for maintenance of an arrested state, although it is not necessary for the initial entry into mitotic arrest (Saba et. al., 2013).

Apoptosis is a major event during germline development, in both the fetal and postnatal periods (Mori et. al., 1997, Rodriguez et. al., 1997, Wang et. al., 1998). In fetal testes, apoptosis has been described to occur in a wave that begins between e12.5 and e13.5 (Coucouvanis et. al., 1993) and continues until e17.5. Germ cell apoptosis is controlled by a balance of proapoptotic (*Bad, Bax*) (Knudson et. al., 1997) and antiapoptotic *Bcl* family members (Rucker et. al., 2000). Disruption of *Bcl-x* results in severe loss of germ cells by e13.5 and ultimately results in sterility. *Bax* mutants are also sterile, although characterization of male germ cell defects has only been during adult spermatogenesis and little is known about the fetal role of *Bax*. However, these studies demonstrate that apoptosis is a finely regulated balancing act between antagonistic apoptosis regulators. As germ cells progress toward e13.5, *Bax* expression increases, rendering the germ cell population more primed to undergo cell death (de Felici et. al., 1999).

Germ cells also undergo extensive epigenetic reprogramming during the fetal stage. Global DNA demethylation is initiated as early as e8.0 (Seki et. al., 2007) and continues through e13.5 (Yamaguchi et. al., 2013). Repressive histone marks such as H3K9me3 and H3K27me3 are also lost as well (Hajkova et. al., 2008). This extensive epigenetic reprogramming involving both DNA demethylation and polycomb mark erasure is unique to the germline (Hajkova et. al., 2011). The function of this reprogramming is to reset the epigenome in a naïve state and clear both genomic imprinting and any accumulated epigenetic marks that may have been acquired between specification and sex differentiation – including epimutations. However, epigenetic reprogramming also exposes germ cells to reactivated expression of transposable elements (TEs)

that are ordinarily repressed by methylation (Bourc'his and Bestor., 2004). Therefore, careful control over the timing and loci-specificity of epigenetic reprogramming adds further levels of regulation and complexity to fetal germ cell development. Importantly, any differences in competency in navigating fetal developmental challenges could affect the fidelity of epigenetic reprogramming and cause populations of germ cells that lag behind to acquire heritable aberrant epigenetic marks.

To determine the contributions of these key developmental events to the composition of the germ cell pool in the fetal period, we sought to examine population changes among germ cells using a high-resolution approach with clonal labeling and single-cell transcriptional analysis. These techniques permitted us to assess developmental heterogeneity within a dynamic germ cell population and uncover how variable developmental maturity across germ cell subpopulations is associated with different outcomes including apoptotic elimination and genomic protection against transposable elements.

CHAPTER 2: Fetal germ cell apoptosis is clonal and selects against aberrantly undifferentiated male germ cells

INTRODUCTION

Over the course of thousands of millennia, developmental biology has produced complex structures and organisms out of chaotic primordia. As impressive as the finished product may be, the process of development is not the model of relentless efficiency - rather, it's consistently and extremely wasteful. To produce an organism, development is rife with examples of overproduction followed by culling. Indeed, waste is a persistent and universal theme across numerous organisms, particularly during the rigorously demanding morphogenetic and differentiation processes that define embryonic development. The removed populations of cells represent both an energetic and time cost. Many theories attempt to explain why excess numbers of cells are developmentally useful. Overproduction may provide a buffering reservoir of cells to increase a system's robustness. Cell competition may also benefit from a larger, more diverse pool of competitors. A general developmental principle is that the elimination of cells is a form of selection, which implies a reduction from a more heterogeneous population to a more homogeneous one.

In the mammalian germline, the theme of overproduction and elimination is prominent regardless of sex or age. Both male and female germ cells are subjected to multiple events that reduce germ cell populations. These have an important functional role – bypassing apoptosis results in male sterility (Rucker et. al., 2001) or increases the likelihood of reproductive defects in oocytes (Perez et. al., 1997). However, the severe requirement for apoptosis specifically in males suggests that programmed cell death is integrally linked with reproductive fitness. In males, large-scale apoptosis is reported at several stages. Prior to sex differentiation, apoptosis eliminates fetal germ cells that fail to migrate correctly (Runyan et. al., 2006). Fetal male germ cells also are subjected to an apoptotic wave between e13.5 to e17.5 (Coucouvanis et. al.,1993, Wang et. al., 1998). Later apoptotic events are coincident with spermatogenesis in the juvenile males between

10 to 30 days of age (Russell et. al, 2002). Male germ cell apoptosis is dependent on several common apoptotic mediators, such as the pro-apoptotic gene *Bax* that is antagonized by the pro-survival family of *Bcl-2* genes (Rucker et. al, 2000). While previous studies using *Bax* mutant mice have investigated the effects of knocking out apoptosis on adult spermatogenesis (Knudson et. al., 1995), little is known about the effects on fetal male germ cells. Given the complex developmental journey of fetal germ cells, this population represents an attractive timepoint for apoptotic selection to act upon.

In the postmigratory phase of germ cell development, PGCs undergo massive epigenetic reprogramming consisting of genome-wide DNA demethylation, imprint erasure, and changes to histone modifications (Hajkova et. al., 2011). These epigenetic changes prepare male germ cells for sexual differentiation to the male lineage, suppression of the female program, and genome defense by regulating transposable elements. At e12.5, sexual differentiation occurs and female germ cells enter meiosis. In contrast, male germ cells continue proliferation until they mitotically arrest at e13.5 (Western et. al., 2008). Epigenetic reprogramming continues through mitotic arrest, with male germ cells beginning to express piRNA genes to further regulate transposons (Seisenberger et. al., 2012, Molaro et. al., 2014, Aravin et. al., 2009). These diverse developmental transitions illustrate the dynamic requirements expected of germ cells to appropriately respond to the variety of extrinsic and intrinsic cues coordinating their maturation. While germ cells that fail in migration are known to be eliminated by apoptosis, the fate of aberrant germ cells in the post-migratory fetal period is not well understood. However, the presence of a significant apoptotic wave in the male germline represents an intriguing possibility for differences among germ cells to be surveyed and selected among.

We investigate the role of fetal apoptosis in the male germline and discover that apoptosis non-randomly eliminates populations of spatially grouped germ cells. Using clonal labeling, we are able to determine that this clustered apoptosis is driven by intrinsic, heritable properties rather

than location or physical connections among germ cells. We examine the transcriptional diversity of germ cells during the apoptotic wave at a single-cell level to identify *Trp53* as a differentially expressed gene among apoptotic cells. Furthermore, we discover wide variation in male differentiation that may underlie susceptibility to apoptosis. These findings elucidate the functional role for fetal male germ cell apoptosis in guarding against developmentally compromised germ cells, which we can distinguish by inappropriate transposon regulation.

RESULTS

Wholemount imaging of the fetal germ cell apoptotic wave reveals clustered apoptosis

A hallmark of development is the exquisite spatiotemporal coordination of maturing cellular populations within growing tissues. To better understand the paradigms that guide development, it is essential to contextually understand populations in their surroundings. This principle motivated our approach to investigating the developmental role of apoptosis in the fetal germline. The wave of germ cell apoptosis in fetal testes has been described as a sustained elevation in germ cell death from embryonic day (e) 13.5 through e17.5 (Coucouvanis et. al., 1993) although earlier studies examined apoptosis in disaggregated testes or tissue sections – neither preserves the spatial relationships of the intact testis. Such information can identify global patterning of developmental events, like the well-established anterior-posterior wave of meiosis in the female gonads at the same fetal stage (Menke et. al., 2003). To examine the spatial distribution of germ cell apoptosis in the intact testis, we stained testes from e12.5 to e17.5 embryos with cleaved-PARP (cPARP) for wholemount imaging. We quantified germ cell apoptosis by coincidence of cPARP and the germ cell marker TRA98 and notably found apoptosis to peak at 2-4% of cells at e13.5, earlier than described (Coucouvanis et. al., 1993) and subside more rapidly, returning to pre-wave levels at e15.5 (Fig. 2.1A). Altogether, we estimate that the net effect of this fetal apoptotic wave is a 15% reduction in germ cells, as determined by enumerating the total germ cell counts at e17.5 in wild-type compared to *Bax* mutant testes in which apoptosis is blocked (Knudson et. al., 1995) (Fig. 2.1B).

Intriguingly, wholemount immunofluorescence revealed that dying germ cells were present in local clusters (Fig. 2.1C) but these clusters did not display any polarized localization such as that of meiotic entry (Menke et al., 2003; Yao et al., 2003; Bullejos and Koopman, 2004; Koubova et al., 2006, 2014). To assess the extent of this clustering, we analyzed the spatial distribution of apoptotic germ cells using 3D coordinates extracted from wholemount staining (Fig.

Figure 2.1
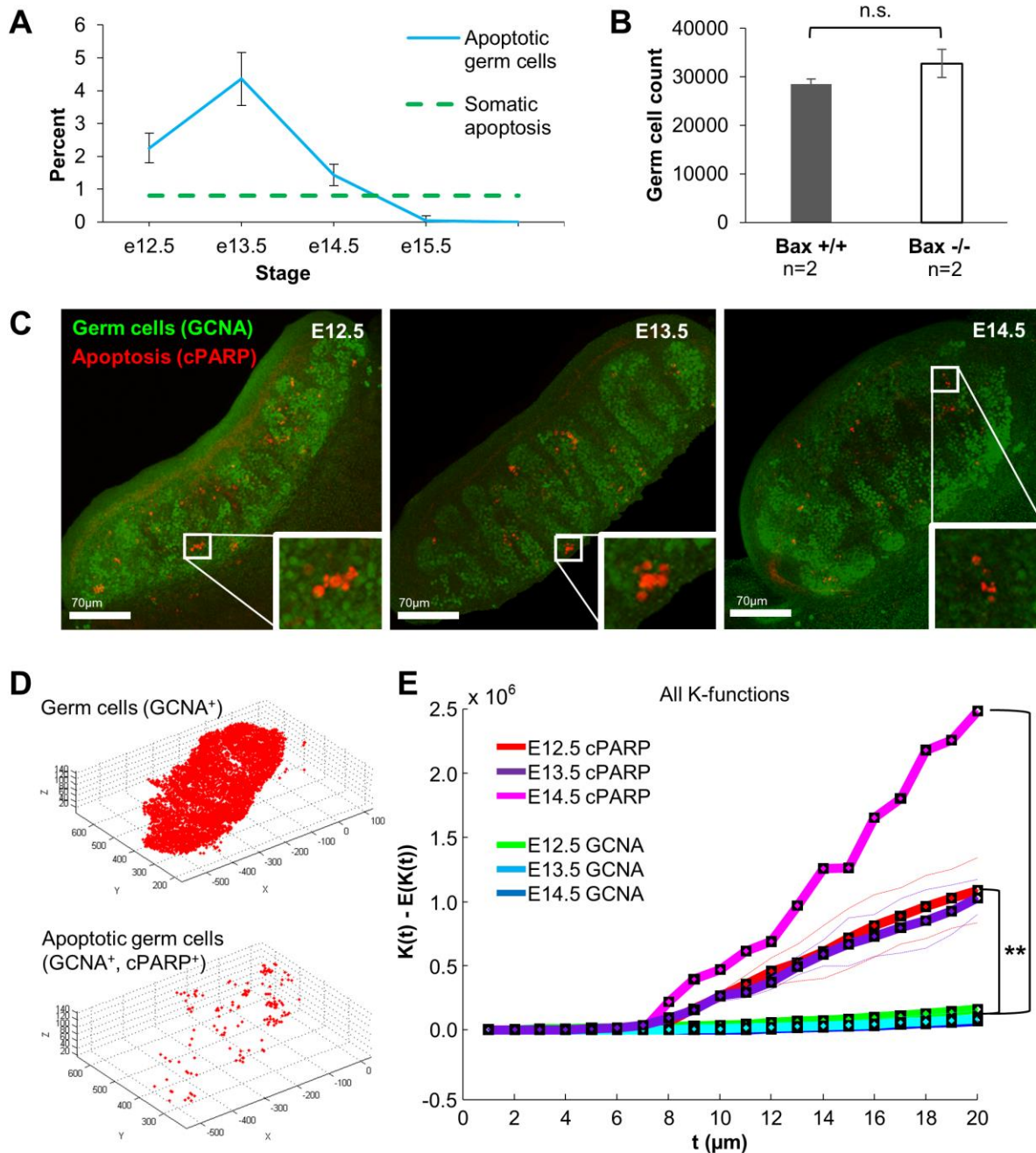
Figure 2.**1**: (**A**) Frequency of apoptotic germ cells during the apoptotic wave, detected by cleaved-PARP and TRA98 staining in wholemount testes between e12.5 to e15.5. n-4 for each timepoint. Somatic apoptotic rate is an average reported value across several somatic compartments between e12.5 to e16.5.(Foley et. al., 2002). (B) Total germ cell counts in littermate Bax^{+/+} and Bax^{-/-} e17.5 testes by TRA-98 wholemount staining. (C) Wholemount staining of TRA98-positive germ cells with cleaved-PARP across e12.5-e14.5, with examples of clustered apoptotic germ cells highlighted (inset). (D) Distribution of germ cells and apoptotic germ cells plotted using coordinates extracted from wholemount imaging of an example e13.5 testis. Distributions were used for spatial clustering analysis (E) Ripley K-factor analysis of apoptotic germ cell distributions compared to total germ cell distributions. Plot depicts deviation from randomness, k(t)-E(K(t)). Dashed lines indicate 95% confidence interval. **p<0.001

2.1D). Apoptotic germ cells displayed a significantly increased degree of clustering compared to the distribution of all germ cells. This clustered apoptotic distribution was sustained from e12.5 through e14.5 (Fig. 2.1E), suggesting that locally coordinated germ cell death is a key feature of the apoptotic wave. Subsequent timepoints contained insufficient numbers of apoptotic germ cells to conclusively analyze for spatial clustering. Altogether, the statistically significant degree of clustered apoptosis demonstrates that local populations of germ cells are selectively eliminated by the apoptotic wave.

To determine whether organization of apoptotic clustering extends beyond local-scale interactions, we sought to investigate how the tissue-wide distribution of apoptotic populations compares to known developmental gradients, such as the anterior-posterior axis, or to distinctive tissue environments, such as along vasculature like the coelomic vessel that spans the testis. We identified apoptotic clusters as discrete points and evaluated the spatial distribution for the resulting point processes (Fig. 2.S1A). Apoptotic germ cell clusters were highly similar in distribution to simulated random distributions and significantly different from simulated clustered or polarized distributions, confirming an absence of higher-level organization at the level of the entire testis (Fig. 2.S1B). This result further implies that distance from vasculature does not correlate with apoptotic cluster location, which we confirmed by measuring the distance among apoptotic clusters and PECAM-marked vasculature (data not shown). These findings indicate that germ cell apoptosis occurs independently of location within the fetal testis.

On a smaller scale, interactions between cell types can be highly influential in directing apoptosis. In the testis, germ cells are supported by Sertoli cells that are diverse in their contributions to germ cell development in both the fetal and adult period. Sertoli cells assist germ cells both indirectly through secretion and directly via desmosomes (Kopera et. al., 2010). Sertoli cells also form the testis cords that begin to organize and encapsulate germ cells in the fetal testis beginning at e12.5. Defects in Sertoli cells can lead to dysfunctional germ cells and infertility,
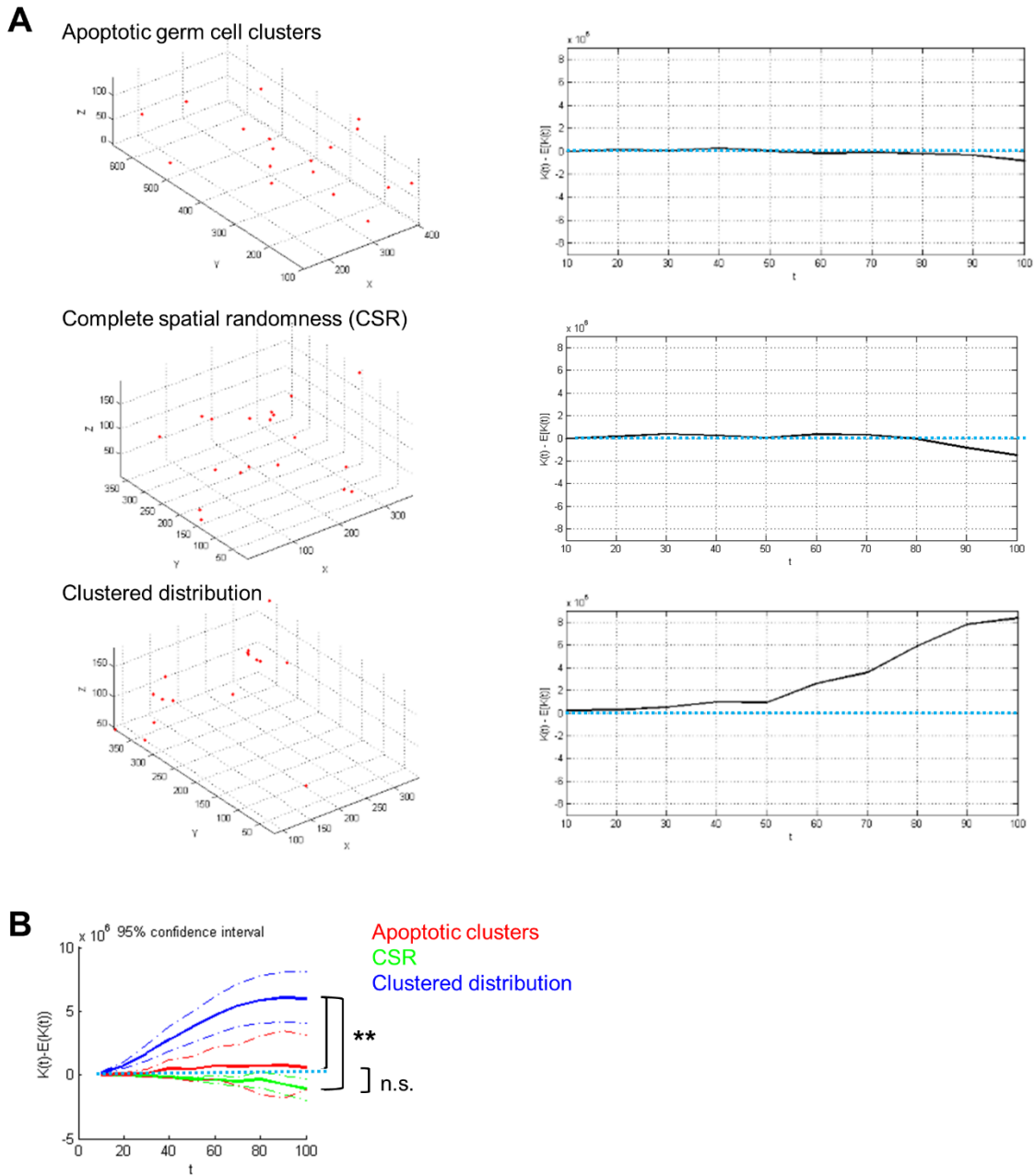
Figure 2.S1

Figure 2.**S1**: (A) Apoptotic germ cells were grouped into local clusters based on proximity to other apoptotic germ cells and and the individual cluster centroid was calculated for a single e13.5 testis. The 3D coordinates of each cluster's centroid was plotted for Ripley K-factor analysis. Apoptotic germ cell cluster distribution (top) compared against simulated distributions for an equivalent number of points under non-clustered (CSR) and clustered distributions. Graphs depict deviation from randomness, K(t)-E(K(t)) with a completely ideal random distribution K(t)-E(K(t)) equal to zero indicated by dashed line. (B) Apoptotic clustering comparison performed for n=5 e13.5 testes and 100 simulations of CSR and clustered distributions for an equivalent number of clusters. **; $p<0.001$

demonstrating the essential role of these "nurse" cells to germ cell development (deRooij 2009). Our observation of clustered apoptosis could potentially be indicative of local Sertoli cell environments that are poorly supportive of germ cell survival. To investigate whether clustered apoptosis is related to aberrant Sertoli cell interactions, we examined the Sertoli-germ cell relationship in apoptotic versus non-apoptotic testis cords. A prevailing hypothesis in the adult testis is that an optimal Sertoli:germ cell ratio must be maintained during spermatogenesis, with imbalances corrected by germ cell apoptosis (Kimura et. al., 2003). In counting Sertoli and germ cells within apoptotic cord sections (Fig. 2.S2A), we found no evidence for such a ratio to control local germ cell apoptosis (Fig. 2.S2B). Furthermore, we measured the distance between apoptotic germ cells and nearby Sertoli cells to investigate if remote germ cells were more susceptible to dying but found no such distance-apoptosis relationship to exist (Fig. 2.S2C). Neither Sertoli cell ratio nor proximity were associated with apoptotic germ cells, providing further evidence against an environmental cause for locally clustered germ cell death. Whether at a cellular level via Sertoli cell interactions, or at a tissue-level, our results indicate that extrinsic guidance of germ cell death is not primarily responsible for the observed clustering – which argues instead for germ-cell intrinsic apoptotic mechanism.

Clustered apoptosis is not mediated by intercellular bridges among germ cells

Germ cells possess the unique cellular ability to form stable intercellular bridges that are byproducts of incomplete cytokinesis (Greenbaum et. al., 2011). These 1-3μm wide bridges enable cytoplasmic contents ranging from mRNA to proteins to flow among interconnected cells (Pepling et. al., 1998). Groups of germ cells physically linked by bridges are termed germ cell cysts. Such connectivity can potentially coordinate cellular events; indeed, apoptosis has been described to occur synchronously among interconnected spermatogonia in the adult mouse testis (Hamer et. al., 2003). While these bridges begin to form as early as e10.5, their contribution to
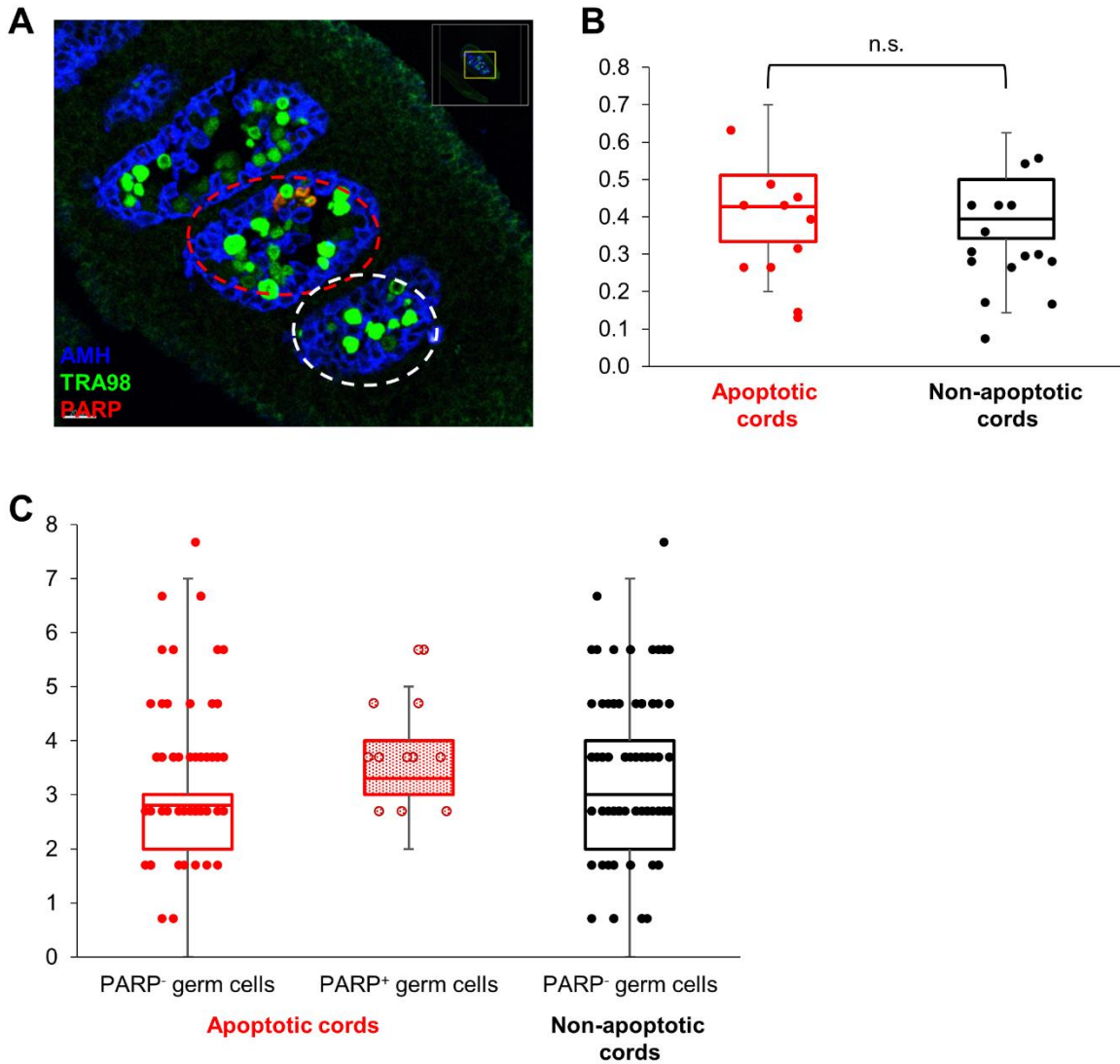
Figure 2.S2

Figure 2.**S2**: (A) Section of e13.5 testis stained for Sertoli cells (AMH), germ cells (Tra98), and apoptosis (cleaved-PARP). Apoptotic cords are defined as cords containing any apoptotic germ cells (red outline) in contrast to non-apoptotic cords (white outline). (B) Ratio of total germ cells to Sertoli cells in both apoptotic and non-apoptotic cords sections, p-value: 0.584. (C) Average numbers of Sertoli cells in direct contact with each germ cell in both apoptotic and non-apoptotic cords. Sertoli cell contacts were further distinguished between apoptotic (PARP+) and non-apoptotic (PARP-) germ cells. Apoptotic cords are plotted in red and cords without apoptosis are plotted in black plot. For all 3, p>0.25.

and necessity for synchronized apoptosis during the fetal apoptotic wave remains unclear. Because cytoplasmic sharing could facilitate the spread of apoptotic signals among neighboring fetal germ cells, we sought to investigate the role of these bridges in producing locally clustered patterns of apoptosis. We utilized a knockout mutant, *Tex14*, which lacks an essential component of the intercellular bridge and fails to form these connections (Greenbaum et. al., 2011). *Tex14*^{-/-} males were found to be infertile, though defects were only characterized during adult spermatogenesis. However, cytoplasmic sharing via bridges exists far earlier in male reproductive development, from e10.5 through the fetal apoptotic wave, suggesting that intercellular connections may have an earlier role in organizing fetal germ cell behavior. Therefore, we hypothesized that disrupting intercellular bridges should desynchronize apoptosis, reducing both local clustering and the overall testis-wide frequency of germ cell death, as dying cells would function as independent units in the initiation and execution of apoptosis.

We examined fetal *Tex14*^{-/-} testes at the e13.5 peak of the apoptotic wave for clustering of apoptotic germ cells. From wholemount imaging, we observed no significant difference in apoptosis (Fig. 2.2B) in *Tex14*^{-/-} testes compared to wild-type littermates. Importantly, we still observed grouping of cleaved-PARP-positive germ cells into local clusters (Fig. 2.2A). Spatial analysis of apoptotic germ cell distributions indicated that clustering was slightly reduced in *Tex14*^{-/-}, but the difference was insignificant compared to wild-type and heterozygote littermates (Fig. 2.2C). Therefore, bridges may marginally increase the overall degree of clustering but are ultimately not required for this phenomenon. It is important to note that apoptosis may occur in an asynchronous but still locally clustered manner such that, over a longer period of observation, nearby cells may eventually also undergo apoptosis. However, the persistence of simultaneous apoptotic clustering in *Tex14*^{-/-} implies that individual, unconnected cells can still die in a synchronized manner.

Figure 2.2
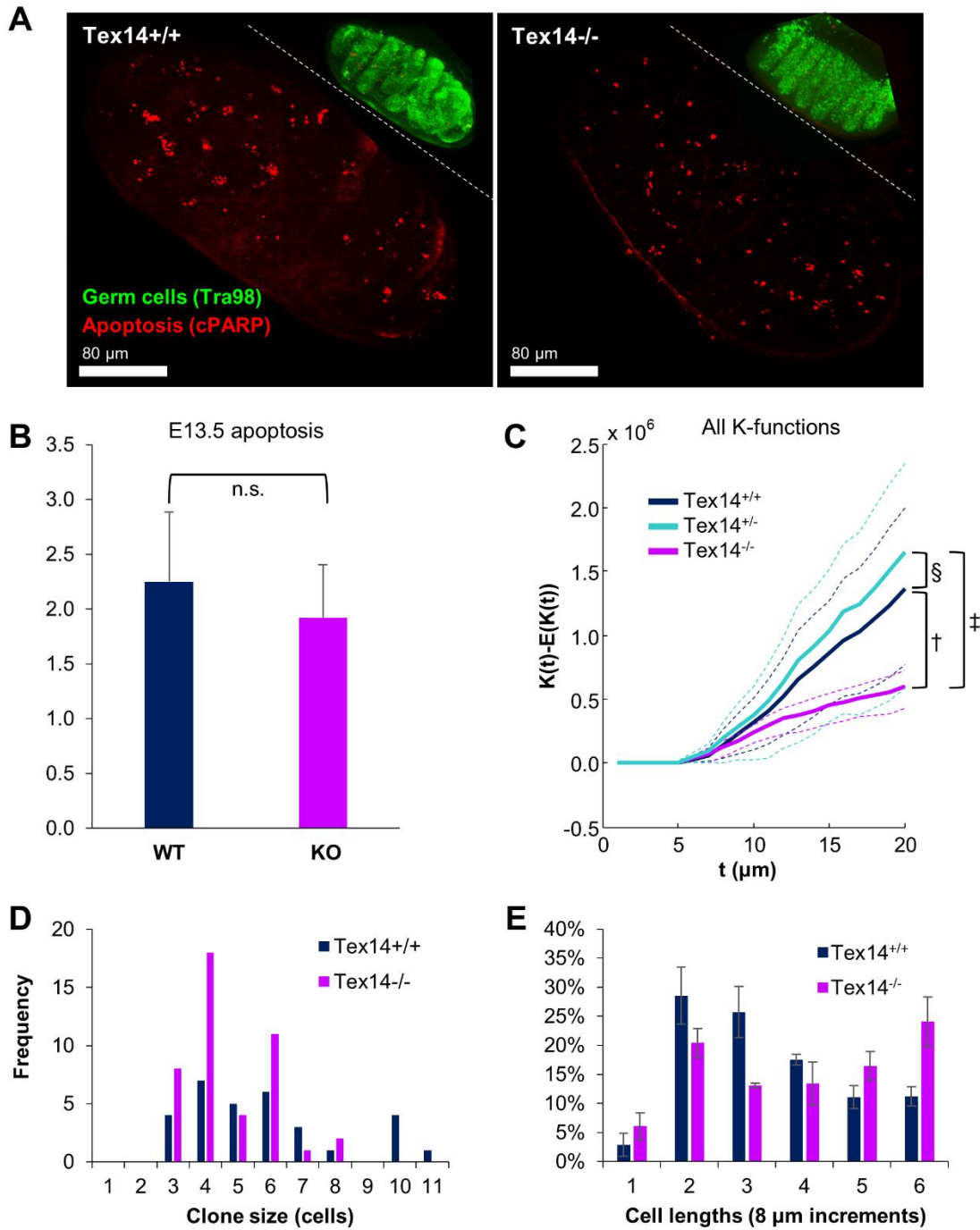
Figure 2.2: (A) Wholemount imaging of e13.5 Tex14$^{+/+}$ and Tex14$^{-/-}$ testes stained for germ cells (Tra98) and apoptosis (Cleaved PARP). (B) Apoptotic germ cell percentage at e13.5 in Tex14$^{+/+}$ and Tex14$^{-/-}$, n-4 for each genotype. p-value = 0.4486. (C) Ripley k-factor analysis of apoptotic germ cell distributions in Tex14$^{+/+}$ and Tex14$^{-/-}$ e13.5 testes. n=4 for each genotype. Dashed lines indicate 95% confidence interval for each distribution. t = search radius; †p = 0.172; ‡p = 0.246; §p = 0.94. (D). Apoptotic cluster size by number of PARP$^+$ germ cells in Tex14$^{+/+}$ and Tex14$^{-/-}$ e13.5 testes. (E) Centroid-to-centroid distance among all apoptotic germ cells at e13.5.

While the absence of intercellular bridges did not alter the distribution of apoptosis, we sought to investigate the contribution of bridges to the physical dimensions of apoptotic clusters. Based on the ability for cytoplasmic contents to diffuse across these bridges, we anticipated that bridges would facilitate the propagation of apoptotic signals to produce larger clusters. We found that the median cell number of apoptotic germ cells in each cluster declined in e13.5 *Tex14*^{-/-} (Fig. 2.2D) from 4.84 cells per cluster in wild-type to 3.66 cells per cluster, suggesting that apoptosis was confined to fewer cells in each cluster. There was a notable absence of larger clusters numbering above 8 apoptotic cells in size in *Tex14*^{-/-} compared to wild-type. Together, these results indicate that intercellular bridges are necessary for the wider spread of apoptosis among nearby cells to produce larger synchronized apoptotic clusters.

While apoptotic germ cell clusters were smaller in constituent size, the distance between apoptotic cells of the cluster also increased in *Tex14*^{-/-} (Fig. 2.2E). This could result from apoptosis skipping intermediate cells due to the lack of bridges enforcing contiguity of apoptosis. Alternatively, apoptosis may occur more asynchronously in *Tex14*^{-/-} due to more stochastic variation among individual cells. Without bridges to equalize apoptotic signals in neighboring cells, *Tex14*^{-/-} germ cells may undergo apoptosis in a more disjointed manner. We did not observe an increase in germ cell spacing (data not shown), so this result cannot be solely explained by an overall increase in germ cell dispersion in *Tex14*^{-/-}. Although the loosely dispersed apoptotic clusters in *Tex14*^{-/-} are also smaller in apoptotic cell number, the overall effect on apoptotic germ cell frequency is insufficient to significantly reduce apoptosis. This may be due to increased dispersion blending individual apoptotic clusters such that the overall number of apoptotic germ cells remains consistent but that clusters are more likely to overlap in *Tex14*^{-/-}.

Our data show that intercellular bridges promote tight coordination of apoptosis to enhance clustered apoptosis, but are ultimately dispensable for ensuring a common apoptotic fate within these clusters. Combined with our observation that apoptosis is location-independent,

these results further establish that apoptotic fate is a cell-autonomous property, despite apoptosis occurring in groups of dying, nearby cells.

Clonal apoptosis eliminates entire germ cell clones

The observation that germ cell apoptosis is non-random, location-independent, and yet clustered suggests that some locally-restricted property promotes synchronous apoptosis of proximal cells. Although we determined that such apoptotic organization is not provided by physical linkages via intercellular bridges, clonal expansion of germ cells can also provide spatial organization due to the sessile nature of germ cells prior to the fetal apoptotic wave. After migrating to the gonadal ridge at e10.5, primordial germ cells become immotile and resume heightened proliferation (Runyan et. al., 2006). As this stationary population undergoes several rounds of division, the resulting progeny from each settler germ cell remains nearby, ultimately producing contiguous clonal populations that can be mapped by Tex14$^+$ bridges and clonal labeling (Mork et. al., 2012). If the susceptibility to apoptosis is clonal, the resulting pattern of cell death would appear spatially clustered. Therefore, we sought to examine apoptosis in a clonally-labeled background. We predicted that apoptosis would follow clonal boundaries such that local clusters of apoptosis would be monoclonal.

To determine the clonality of apoptosis, we utilized a multicolor clonal labeling system, *R26R-Confetti* (Snippert, et. al., 2010), in conjunction with a germ cell-specific *Pou5f1 Cre-ER* (Greder et. al., 2012) for inducible recombination. The *Confetti* locus can express four distinct colors to allow for labeling and distinction of multiple clones in a testis. This permits both interclonal and intraclonal analyses with much greater efficiency. We induced recombination at e10.5 as germ cells begin colonizing the gonadal ridge and analyzed the distribution of apoptosis within clonally labeled populations at e13.5 (Fig 2.3A). Interestingly, each instance of local

Figure 2.3
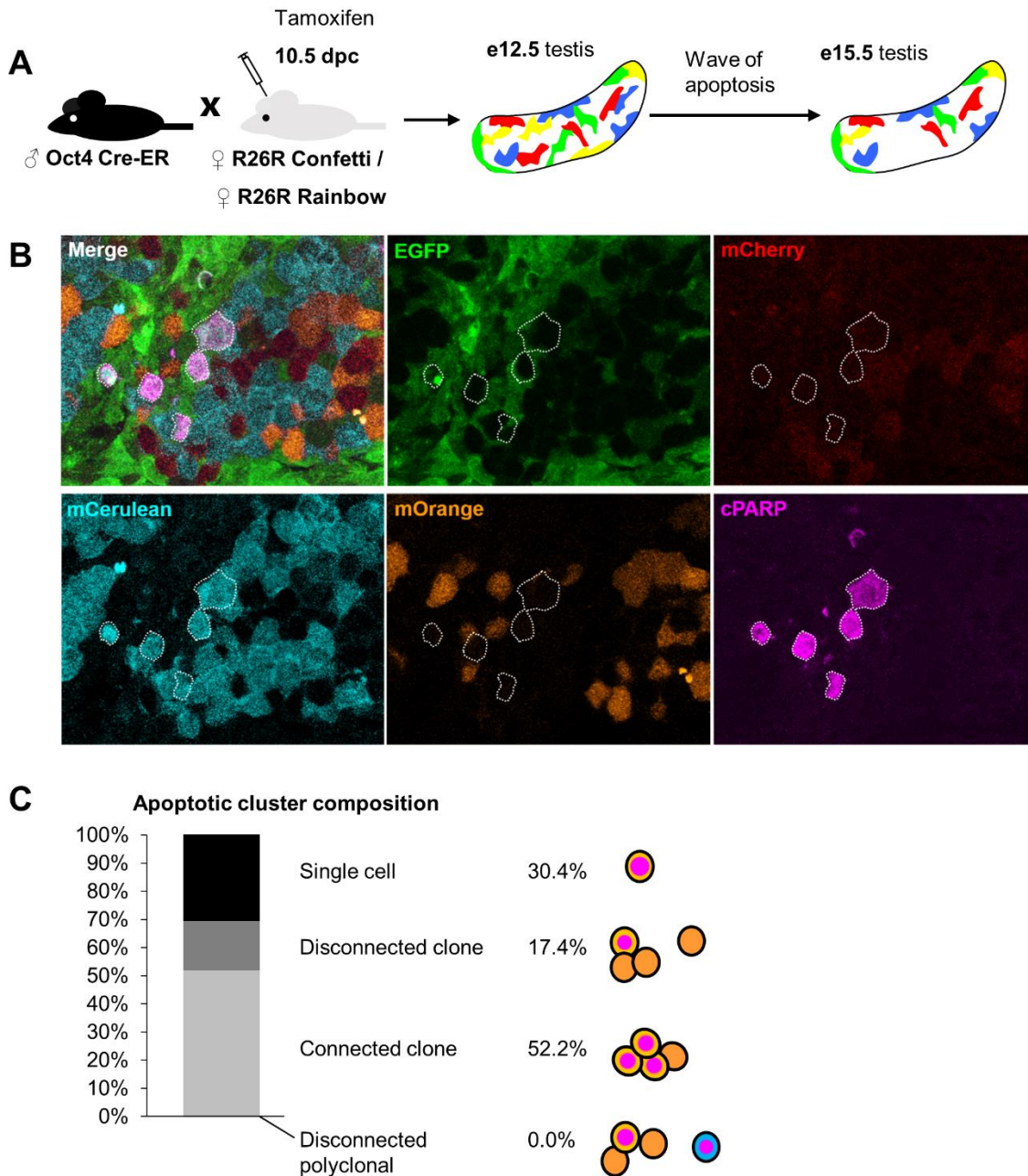
Figure 2.3: (A) Multicolor clonal labeling system to investigate germ cell apoptotic clustering. *Confetti* and *Rainbow* females are crossed to *Oct4Cre-ER* males and recombination is initiated at e10.5 when germ cells colonize the gonads. Clonal analysis is performed throughout the wave of apoptosis from e12.5 to e15.5 to evaluate apoptosis among clonal populations as well as to compare clonal growth and persistence. *(B)* Multicolor clonal labeling from e13.5 testes in *Rainbow*. A mOrange clone is outlined, exemplifying clonal restriction of apoptosis. (C) Apoptotic germ cell clusters (n=86) were analyzed to determine the frequency of each type of apoptotic distribution.

apoptotic germ cell clustering was confined to a single color (Fig 2.3B). Even when a clone harboring apoptotic germ cells was surrounded by and interspersed with differently labeled clones, apoptosis did not cross clonal boundaries (Fig 2.3B). We categorized the instances of clustered apoptosis in labeled cells and confirmed that monoclonal clustered apoptosis was a frequent event but clustered apoptosis spanning multiple clones did not occur (Fig 2.3C). The absence of multicolored local apoptosis also refutes the possibility that local, diffusible factors could coordinate apoptosis. Such a model would not strictly adhere to clonal boundaries; rather, apoptosis would follow an extrinsic gradient that should cut across multiple clones. The robustly monoclonal apoptosis we observed in apoptotic clusters instead argues that a heritable and clonally variable property renders cells of certain clones more susceptible to apoptosis.

Using multicolored clonal labeling, we also evaluated how clonal parameters such as clone size change as a result of apoptosis. Germ cells are highly proliferative between e10.5 to e13.5, so our labeling scheme would produce sizeable populations before peak apoptosis occurs in germ cells at e13.5. We assessed clone size from e12.5 through e15.5 and observed an unexpected diversity of clone sizes ranging from a single cell to over 40 cells large (Fig. 2.3D). However, the median clone size of 8 was unchanged throughout the apoptotic wave. This is consistent with a model of total clone loss, where apoptosis eliminates every cell of a clone. This contrasts with a model of partial clonal apoptosis in which a portion of cells in a clone is eliminated but a small remainder persists. Such a process would produce an accumulation of smaller clones and a decrease in average clone size during the window of apoptosis. Rather, the result of consistent median clone size suggests that apoptotic clones are entirely removed. This also implies – importantly – that, in regard to eventual apoptotic fate, individual cells of a clone behave uniformly. Over the entire window of the apoptotic wave, we account for variation in apoptotic synchronization at any particular timepoint so that by e15.5, all cells from an apoptotic clone will have succumbed to their apoptotic fate and so the entire clone is eventually eliminated.

Figure 2.3
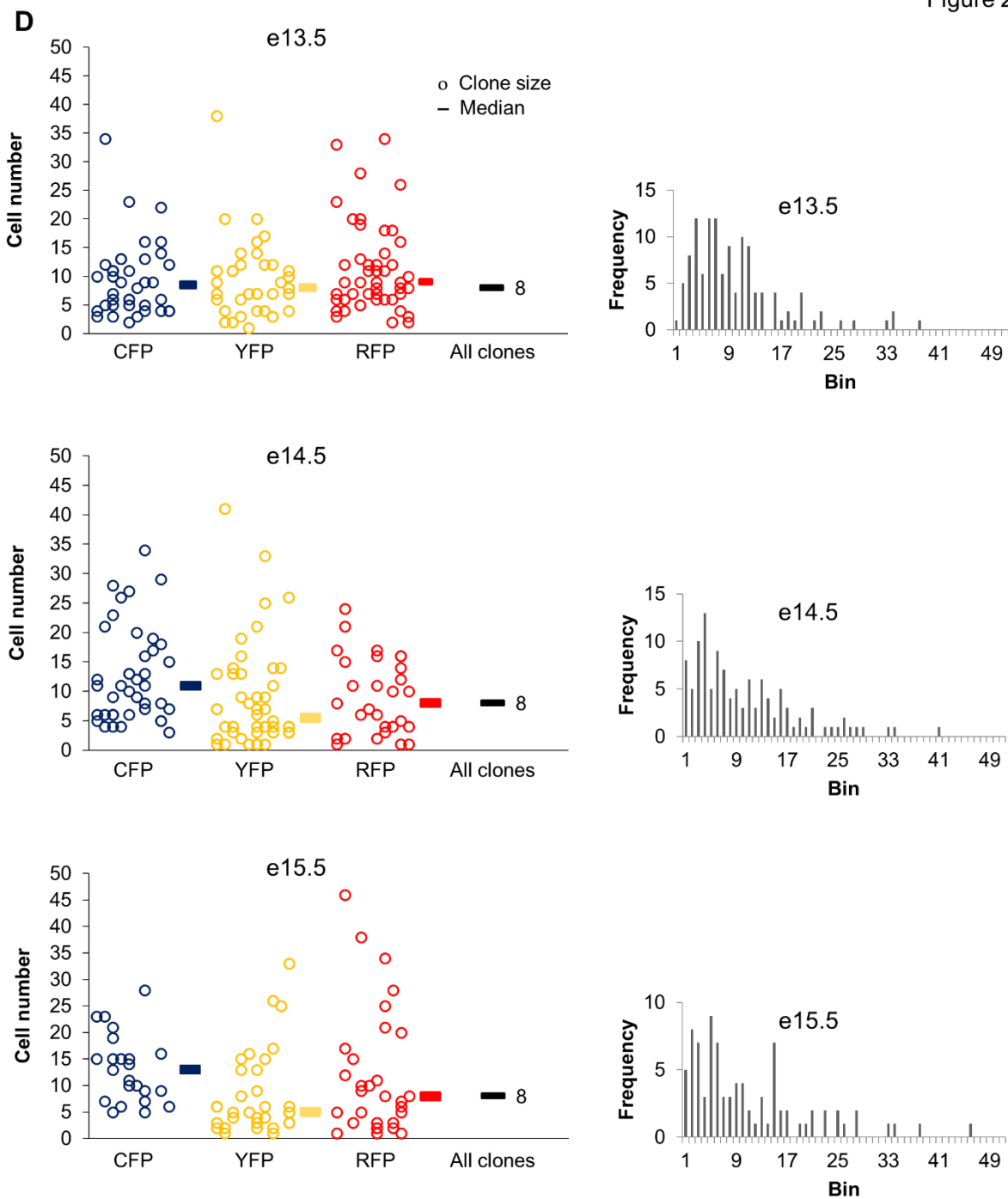
Figure 2.**3**: (D) Clone size distributions for each stage between e13.5-e15.5, organized by clonal label. Each circle represents the size of an individual clone. Median clone size is indicated by bars, both for individual colors and an overall median. Histograms indicate the distribution for all clones together at each time point.

Single-cell transcriptional profiling identifies aberrant transposon regulation in a pro-apoptotic population

Our evidence of clonal, apoptotic germ cell populations suggests that a heritable susceptibility to apoptosis underlies clonally distinct outcomes during fetal development. Whether suchheritable properties stem from genetic or epigenetic differences, we anticipated that these differences would manifest as divergent transcriptional states distinguishing apoptotic from non-apoptotic populations. Indeed, our *Confetti* system affirmed that significant clonal differences existed and would be obfuscated in pooled analyses. To capture the transcriptional diversity present across all fetal germ cells, as well as identify the transcriptional signature of an apoptosis-vulnerable population, we employed single-cell RNA sequencing of *Oct4-GFPΔPE* male germ cells sorted from an e13.5 testis and filtered to exclude cells not expressing the germ cell marker *Pou5f1.* We performed our analysis on the 10X Chromium platform to ensure maximal coverage and inclusion of rare subpopulations such as the putative pro-apoptotic germ cell clones.

From 2,606 e13.5 germ cells from a single testis, we first asked how many transcriptionally distinct subpopulations could be distinguished. We first searched for variably expressed genes across all individual cells and detected 961 such genes (Table 2.S1). We then performed principal component analysis and clustered cells based on their distribution in PCA space. This produced nine significantly discrete subpopulations (Fig. 2.4A). To investigate our hypothesis that the subpopulation of apoptotic germ cells is transcriptionally distinctive, we evaluated expression of classical apoptotic markers such as *Bax* and caspase-family members for elevated expression in a particular cluster of cells. Surprisingly, expression of these pro-apoptotic genes was mostly homogenous across the nine identified cell subpopulations (Fig. 2.S4A). In agreement with known expression profiling of *Bax* (Rucker et. al., 2000) we detected high expression of this critical apoptotic mediator in all e13.5 germ cells, indicating that the entire population were primed for

Figure 2.4

A

B

Bad

Bax

Log Mean Normalized Expression

Cluster ID

C

Expression

Cluster ID

	71
	13
	52
	78
	66
	61
	230
	18
	109

D

Gene	myAUC	Avg difference
Rhox9	0.951	1.043709
Rhox6	0.908	0.884445
Rhox5	0.883	0.70985
Ckb	0.847	0.627378
Grn	0.822	0.506767
Fabp5	0.786	0.501563
Lefty2	0.776	0.493282
Dppa5a	0.878	0.49267
Hmgn5	0.781	0.492525
L1td1	0.808	0.482669
Pdgfa	0.794	0.461845
Txn1	0.79	0.457538
Arpc1b	0.787	0.432513
Tdh	0.76	0.43195
Ung	0.761	0.421766
Nsmce4a	0.768	0.417079
Lgals1	0.733	0.409712
Ifitm3	0.749	0.373949
Gmnn	0.717	0.357053
Rest	0.771	0.353994
Grhpr	0.75	0.341488
Map1lc3b	0.79	0.339889
Dynll2	0.733	0.321525
Trp53	0.733	0.314233
Pmm1	0.768	0.31151

E

Trp53 expression by cluster

Log Normalized Expression

Cluster ID

Figure 2.**4**: (A) t-SNE plot of 2606 e13.5 male germ cells with clustered populations by differentially expressed genes. (B) Averaged expression of apoptotic genes that are differentially expressed across clusters. Bars indicate mean expression for that cluster. (C) Positive and negative transcriptional markers of each population organized as a clustered heatmap. Colored bars indicate cluster ID with total numbers of markers per population indicated to the right of the heatmap. (D) Top 25 markers of cluster 5, sorted by average difference in expression in cluster 5 compared to all other germ cells. (E) Log-normalized Expression of *Trp53* by individual cell, organized by cluster. Mean expression for each cluster is indicated by dashed line.

Figure 2.4

F

G
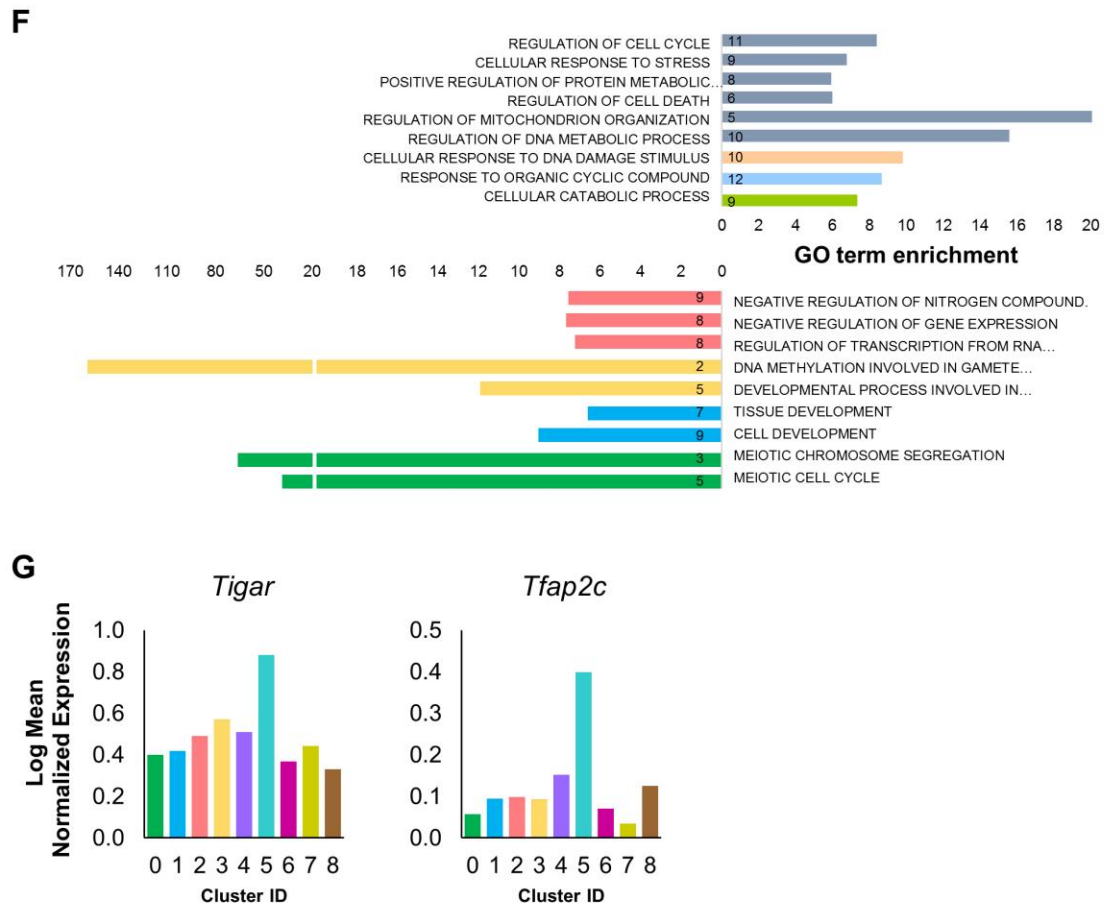
Figure 2.4: (F) Gene ontology enrichment for positive and negative markers of *Trp53*^(high) cluster 5. GO categories are colored and grouped by semantic similarity. Enrichment is calculated by overrepresentation of genes in the list of cluster 5 markers and compared to the expected frequency of genes for that GO category. (G) Averaged expression of p53-downstream genes that are differentially expressed across clusters. Bars indicate mean expression for that cluster.

Figure 2.S4
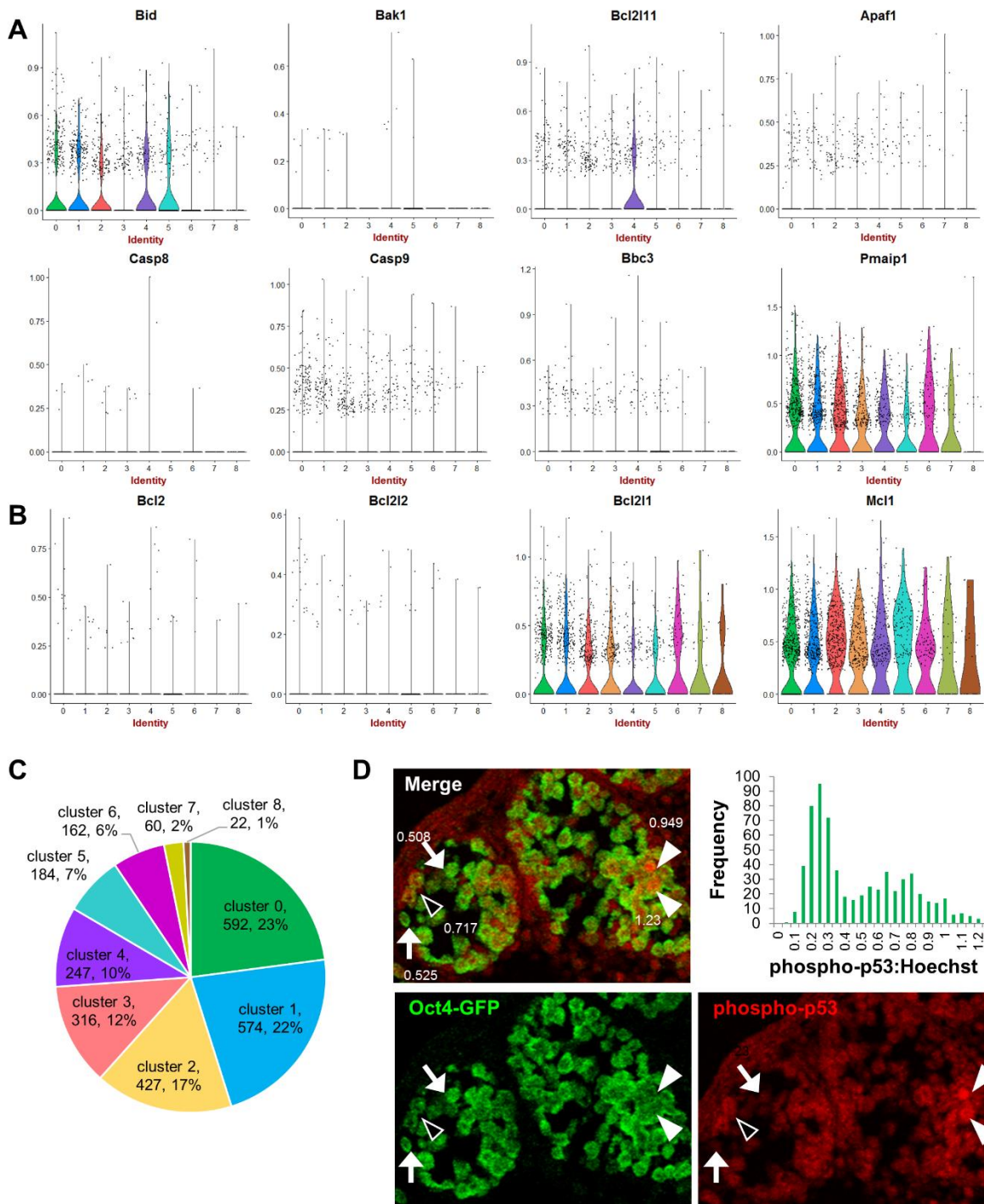
Figure 2.**S4**: (A) Cluster average expression for pro-apoptotic genes. (B) Cluster average expression for Bcl2 family member pro-survival genes. (C) Cluster size in cell number and as a percentage of total germ cells analyzed for single-cell RNA sequencing. (D) Heterogeneous phospho-p53 staining in e13.5 testes. White arrowheads, phospho-p53-high cells; black arrowheads, intermediate phospho-p53 cells; white arrows, low phospho-p53 cells. phospho-p53 intensity was normalized to Hoechst (DNA) intensity and annotated next to each selected cell. Histogram depicts the distribution of this normalized phospho-p53 value across all germ cells.

apoptosis. We did detect two pro-apoptotic genes that were enriched in several subpopulations: *Bad* and *Bid*, both BH3-only family members whose products antagonize the prosurvival Bcl2 proteins (Lomonosova et. al., 2008) (Fig. 2.4B). However, neither gene was exclusively specific to any single subpopulation. We also investigated if downregulation of pro-survival genes such as Bcl2 family members *Bcl2* and *Bcl-xl (Bcl2l1)* could also identify an apoptosis-susceptible population. While some Bcl2 family members such as *Bcl-xl* were more highly expressed than others, no pro-survival gene was significantly up or down-regulated in any single subpopulation (Fig. 2.S4B). These results indicate that, as far as the expression of apoptotic regulators is concerned, germ cells are mostly similar at a transcriptional level and are all competent to die at e13.5.

To discover other differentially expressed genes and networks that could modulate susceptibility to apoptosis, we identified up- and down-regulated genes that were statistically robust and unique markers of each detected population (Fig 2.4C). Examination of these markers highlighted a population (cluster 5) identified by high expression of *Trp53*, a well-documented regulator of apoptosis (Benchimol et. al., 2001) (Fig. 2.4D). Although p53, the protein encoded by *Trp53*, is commonly regulated post-translationally by phosphorylation, elevated p53 is associated with a relative decrease in cellular fitness, consistent with its known function as a sensor of cellular stress and DNA damage (Bondar et. al., 2010). In e13.5 germ cells, the population marked by high Trp53, henceforth referred to as Trp53^{high}, expresses nearly twice the average level of *Trp53* mRNA (Fig. 2.4E). Trp53^{high} represents 6% of the total germ cell population, which is similar to the 4% fraction of cleaved-PARP expressing apoptotic germ cells observed in wholemount testes at the same stage (Fig. 2.S4C). Interestingly, this Trp53^{high} population corresponded to the same population that expressed the highest levels of *Bad* and *Bid*, both of which are known transcriptional targets of p53 (Jiang et. al., 2006, Sax et. al., 2002).

To validate the activity of p53 in this *Trp53^high^* population, we stained for p53 phosphorylation in e13.5 testes sections. This revealed heterogeneous p53 activation among germ cells; interestingly, the distribution of phospho-p53 high and low populations appeared clustered with contiguous populations suggestive of clonal populations (Fig. 2.S4D). Quantitative immunofluorescence analysis confirmed the heterogeneity of this distribution, with the highest-staining cells expressing at least a twofold higher level of phospho-p53. While single-cell RNA sequencing does not permit simultaneous detection of clonal relationships, the co-expressed markers specific to this *Trp53^high^* population can be assessed on a clonal background to determine the clonality of *Trp53* status and its relationship to clonally grouped apoptosis.

To further characterize *Trp53^high^* germ cells, we examined other markers that were strongly associated with this population defined by elevated *Trp53*. Using a receiver operating curve (ROC) test to assess true positive versus false positive rates for marker classification of each clustered population, we generated a list of 91 genes that were either up or downregulated in this *Trp53^high^* population. Gene ontology analysis of these markers revealed several categories related to apoptosis, including regulation of cell death, DNA damage response, and the cellular stress response (Fig. 2.4F). P53 is known to regulate these processes (Fridman et. al., 2003); accordingly, we confirmed that several p53-induced genes, such as *Tigar* and *Tfap2c*, were among those specifically upregulated in this Trp53^high^population (Fig 2.4G). Because these genes are downstream targets of phospho-p53, this indicates that p53 activity is higher in the *Trp53^high^* population. Both p53 targets have established roles in apoptosis regulation (Bensaad et. al., 2006, Schemmer et. al., 2013), further suggesting that this *Trp53^high^* population identified by these genes is comprised of germ cells with increased susceptibility to apoptosis.

In addition to this distinctive *Trp53* signaling, we sought to determine what other robust gene networks might further distinguish this germ cell subpopulation from the entire pool. The most significant positive markers of this *Trp53^high^* population (myAUC score > 0.9) were two *Rhox*

family members, *Rhox6/9* (Fig. 2.4D). *Rhox6/9* is equally expressed in germ cells at e11.5 but becomes sexually dimorphic in its expression; at e13.5, it is restricted to female germ cells (MacLean et. al., 2005). Upon examining *Rhox6*/9 expression in the single-cell male dataset, we found a tenfold increase in Rhox6/9 in the *Trp53^high^* population but minimal expression in any other population (Fig. 2.5A). While the latter is consistent with *Rhox 6/9* expression in e13.5 male germ cells, the unusually high and population-specific levels of *Rhox6/9* in *Trp53^high^* cells represent a developmentally aberrant profile for male germ cells at this stage.

To assess the developmental progression of Trp53^high^germ cells, we examined markers of male differentiation. Male germ cells at e13.5 should downregulate markers of pluripotency, mitotically arrest, and begin expressing male-lineage restricted genes while suppressing female genes. Based on inappropriate *Rhox 6/9* expression, we anticipated that Trp53^high^cells would fail to express *Nanos2*, a major developmental marker of male lineage-commitment that begins to be expressed at e13.5. We first confirmed that *Nanos2* is detected at this stage and determined that high *Nanos2* expression is a marker of a single subpopulation (cluster 6) (Fig. 2.5B). We next confirmed that that *Nanos2* was indeed absent in the Trp53^high^subpopulation, although this was not uniquely so (Fig. 2.5B). Several populations (e.g. clusters 0-2) expressed *Nanos2* at a low level and are likely cells in a developmental transition between immature germ cells and more sex-differentiated ones.

Indeed, we detected multiple other male markers that are co-enriched with *Nanos2* in population 6 and reciprocally absent in the Trp53^high^population (Fig. 2.5C). These include several Tudor-domain containing genes such as *Stk31*/*Tdrd8* and *Tdrd5*, as well as *Mael* and *Piwil2/Mili*. Interestingly, these genes are involved in piRNA biogenesis and transposon suppression (Aravin et. al., 2009), both of which are critical to further development of maturing male germ cells into successful spermatocytes. piRNA mutants are male-infertile (Houwing et. al., 2007), so the striking absence of piRNA genes in Trp53^high^ germ cells could indicate a further deviation from the

Figure 2.5
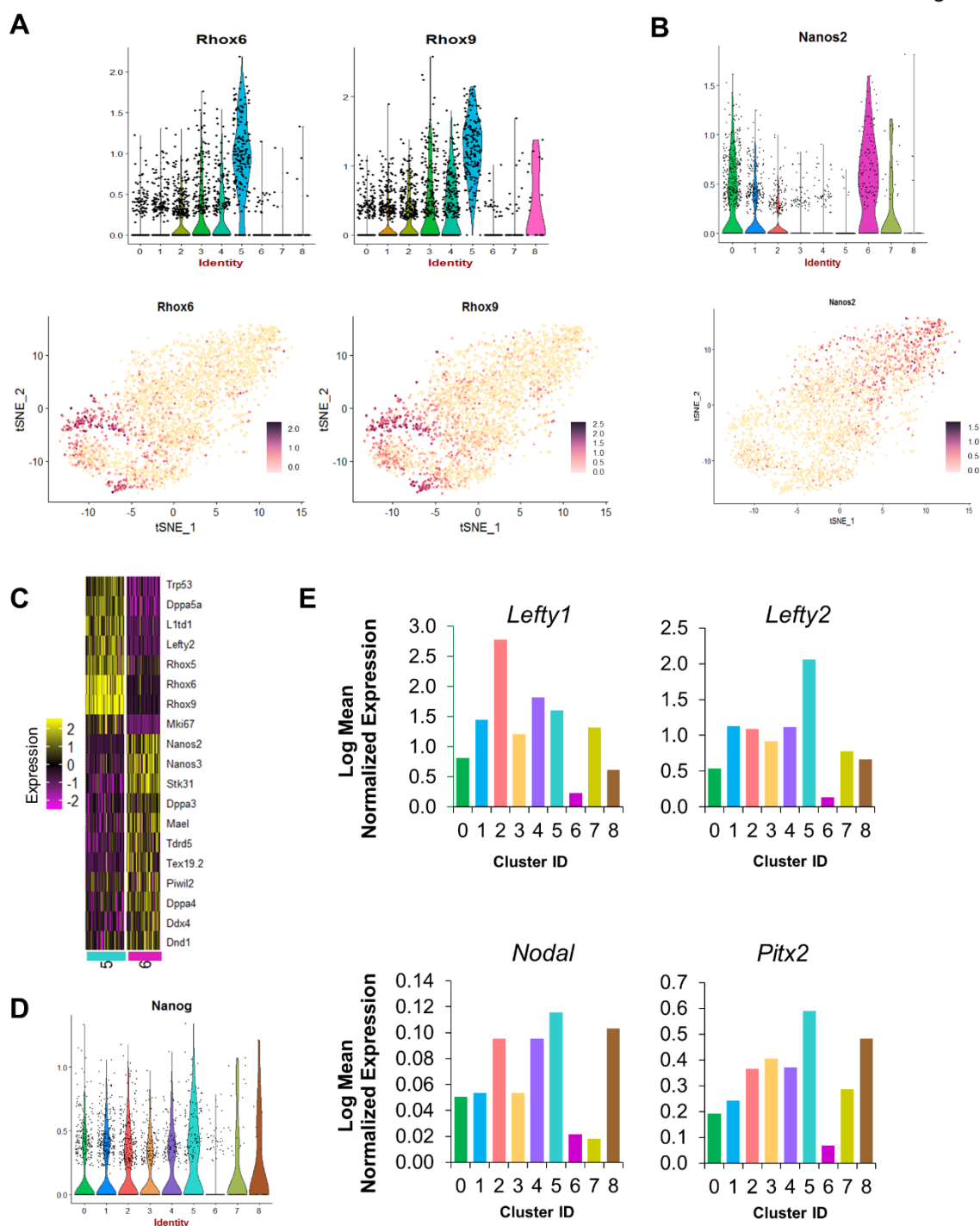
Figure 2.**5:** (A) Cluster average expression for *Rhox* genes (top) with expression of *Rhox* genes plotted onto t-SNE (bottom) distribution, showing germ cell developmental extremes at a whole-population level. (B) Cluster average expression for male differentiation marker *Nanos2* and expression projected onto t-SNE distribution. (C) Clustered heatmap of makers distinguishing *Trp53*^high^ (cluster 5) from a *Trp53*^low^, *Nanos2*^high^ population (cluster 6). (D) Cluster expression of pluripotency gene *Nanog.* (E) Cluster average expression of *Nodal* and Nodal-target genes, *Lefty1/2, Pitx2*.

male differentiation program in addition to the aberrant expression of female-specific *Rhox* genes. Expression of pluripotency markers such as *Nanog* is also higher in this *Trp53*^{high} population (Fig. 2.5D) but significantly diminished upon male differentiation as expected in the *Nanos2* population. The stark contrast between the *Trp53*^{high} and *Nanos2*^{high} populations in terms of groups of key male markers suggests that germ cells expressing relatively higher levels of *Trp53* belong to a clearly distinct, developmentally immature state. Considering the pro-apoptotic inclination of this *Trp53*^{high} population, our transcriptional profiling of single cells illuminates the associated developmental irregularities in male commitment and transposon regulation that may contribute to increased apoptotic susceptibility.

We also noted several other unique markers of the *Trp53*^{high} germ cells such as *Lefty2* that varied in a population-specific manner. *Lefty2* is a downstream target of Nodal signaling (Brennan et. al., 2002), so high *Lefty2* in this *Trp53*^{high} subpopulation implies that Nodal signaling is also elevated alongside *Trp53*. We investigated other readouts of Nodal signaling, including *Nodal, Lefty1,* and *Pitx2* for similarly population-specific expression (Fig. 2.5E). While *Pitx2* was found to significantly distinguish the same *Trp53*^{high} population (p= 1.51E-08), *Lefty1* was elevated in other populations and was weakly insignificant as a marker of *Trp53*^{high} cells (p=0.094). *Nodal* was highest in *Trp53*^{high}, but was overall lowly detected in all germ cells. Considered altogether, this panel of Nodal-responsive genes suggests that *Trp53*^{high} cells experience the relatively highest amount of Nodal signaling. The Nodal signaling axis controls developmental progression in male germ cells (Bowles et. al., 2007) and the expression of *Nodal* and its signaling partners and targets adheres to a tightly defined transient pulse that peaks between e12.5 and e13.5 (Spiller et. al., 2012). Nodal signaling is rapidly curtailed in maturing male germ cells after e13.5; therefore, higher Nodal signaling in this *Trp53*^{high} population could reflect a developmentally immature population. Indeed, the Nodal signaling difference is extremely significant when comparing just the *Trp53*^{high} to *Nanos2*^{high} populations, whereupon Nodal signaling is massively enriched in only

Trp53^{high} cells. It is likely that the other cluster populations reflect intermediate states between these two developmental extremes, and are therefore less exaggeratedly different in Nodal signaling.

Overall, our single-cell profiling of e13.5 male germ cells detects distinctive transcriptional identities that reflect a high degree of heterogeneity. Some identities align with known developmental profiles while others, like the *Trp53^{high}* cluster, are indicative of developmentally aberrant programming that predisposes cells for apoptotic elimination. Our data also indidcate that the phase of Nodal response in germ cells can serve as a measure of male differentiation and tie sex maturation to apoptosis.

DISCUSSION

Cell lineages are established from the expansion and maturation of a population of progenitor cells, so embryonic development is highly influential in defining this progenitor pool. This is especially important in the germline where the enduring influence of early germ cells controls gametogenesis and transgenerational inheritance. However, the significance of embryonic development to the composition of the germline remains poorly understood. In particular, although a stereotyped wave of apoptosis in the fetal male germline eliminates a portion of germ cells from any further gamete contribution, little is known about why cells survive or die during this event. Here, we show that this apoptosis acts non-randomly during the temporally-specific wave in fetal testis development, suggesting that the germ cell pool is heterogeneous and undergoes selection. Apoptotic populations are locally clustered but this distribution is not due to extrinsic properties such as environment nor physical interconnectedness via intercellular bridges. Rather, apoptotic clusters are clonal in origin, arguing instead that a cell-intrinsic and heritable property determines whether a clonal population can pass through this apoptotic bottleneck. We discover transcriptional differences relating to male commitment that generate varied states across the germ cell pool. Importantly, we identify p53 and Nodal as key markers that organize germ cells along a differentiation versus apoptosis axis. A tightly coordinated program of male germ cell differentiation utilizes Nodal responsiveness to simultaneously assess developmental progression and preferentially eliminate deviant cell populations in a p53-mediated manner. The net result is that variation in male-developed germ cells is reduced by apoptotic selection, enriching the germ cell pool for cells with higher male differentiation capacity.

A transient progression of Nodal signaling reads out germ cell maturity

We identify significantly heterogeneous germ cell subpopulations during the dynamic midgestational stage in males that represent a developmental spectrum. The endpoints of this spectrum are characterized by dichotomous expression of male differentiation markers and Nodal signaling genes. *Nodal* is a known activator of male development that promotes expression of male-specific markers such as *Nanos2* and *Dnmt3l* (Wu et. al., 2013). *Nodal* and its receptor *Cripto* are transiently upregulated in male germ cells between e11.5 and e13.5. Genetic removal of Nodal signaling delays male germ cell commitment but *Nodal*-null germ cells can still eventually become male. Surprisingly, we find that transcriptional targets of Nodal signaling were inversely related to male-specific gene expression at e13.5. Cells highest in *Nodal* lacked *Nanos2* and instead were defined by high expression of genes associated with a sexually undifferentiated state (*Rhox6/9*). This is likely due to the self-regulatory nature of Nodal signaling (Chen et. al., 2004), in which *Nodal* upregulates its own inhibitor, *Lefty1/2*, in a negative-feedback loop to curtail Nodal signaling. While this paradigm has been well-studied spatially, such tightly-associated negative feedback can also promote a temporally restricted signaling event (van Boxtel et. al., 2015). The acute nature of Nodal signaling, which sharply peaks at e13.5 in male germ cells, is consistent with this model of regulation (Spiller et. al., 2012).

Transcriptional profiling suggests that cells with low Nodal signaling but high expression of male markers such as Nanos2 represent a more developmentally mature population – one in which Nodal signaling has initiated male differentiation but is subsequently inhibited. Conversely, we find that male germ cells that remain high for *Nodal* are associated with markers of pluripotency and a lack of male-specific markers. Such expression is consistent with germ cells that have just begun to respond to Nodal signaling and are beginning to activate male genes. Alternatively, this could also represent a population deficient in dampening *Nodal* in accordance with its negative-feedback autoregulation. Abnormally high and persistent Nodal signaling in germ

cells results in overexpression of pluripotency genes such as *Nanog* (Tian-Zhong et. al., 2016), which further impedes male differentiation. Nodal signaling can thus serve as both an initiator of male germ cell sexual differentiation as well as a measure of appropriate maturation down this pathway. The temporal restriction of Nodal signaling establishes a tight window for germ cells to receive and respond to differentiation signals - and exposes any differences in the capacity to respond to such signals. While competent germ cells can rapidly progress through all the stages of the Nodal signaling progression, our single cell analysis suggests that any developmental aberrations that compromise Nodal receptivity will delay cells in an intermediate Nodal-high state and exacerbate their inadequate differentiation.

Heterogeneous sexual differentiation in male germ cells produces apoptotic winners and losers

The developmental heterogeneity we report at e13.5 through single-cell analysis is evidence that male germ cells do not synchronously differentiate. Considering the significant developmental states that encompass the transition from a sexually naïve germ cell to male commitment, such heterogeneity could be the product of variation in differentiation kinetics. Male germ cells receive initial differentiation factors as early as e11.5 through FGF signaling (Bowles et. al., 2010). Since FGF9 is a secreted factor, it is possible that male differentiation could proceed asymmetrically in the testis depending on local FGF9 gradients, which can exhibit a center-to-pole bias (Hiramatsu et. al., 2010). This would predict that male differentiation would initiate earlier in a same center-to-pole distribution. From our single-cell analysis, we expect apoptotic susceptibility to be associated with immature differentiation. Such a model should concentrate apoptosis at the poles where immature germ cells lag behind in male differentiation. We did not observe any such non-random distributions for apoptosis, although a more careful examination

of early differentiation markers could reveal initial disparities among populations of germ cells at e12.5 that are assessed later during Nodal signaling and the apoptotic wave.

Nodal itself is another secreted factor that promotes male differentiation – however, its expression is limited to germ cells and may be exerting its effects in a highly localized, autocrine manner (He et. al., 2009). Autocrine Nodal signaling could exaggerate differences among germ cell populations, as the first Nodal-expressing cells beginning male differentiation would amplify the Nodal signal, at least initially before the Nodal response is shut off by its negative feedback circuit. For both Nodal and FGF9, examining clonal variation in responsiveness, such as through the common mediator phospho-ERK, could discriminate between clone-extrinsic environmental differences in differentiation signals and clone-intrinsic differences in differentiation capacity. As male differentiation is closely linked to apoptosis, our observation of clonally-restricted apoptosis argues that clones differ in differentiation status and that environmental effects contribute relatively little to these clone-intrinsic differences.

If differentiation signals are provided equally to germ cell populations, an alternative explanation for the observed developmental heterogeneity is that germ cells vary in their responsiveness to these signals, whether that be in sensing the signals or molecular execution of the differentiation program. At e13.5, we did not detect variable expression of FGF9 or Nodal receptors but it is likely that heterogeneity in cellular sensitivity, if it exists, would be present at e11.5 when FGF9 first signals to begin sex differentiation. Another intriguing source of heterogeneity is variation in epigenetic reprogramming. Fetal germ cells undergo extensive epigenetic reprogramming to suppress somatic genes, erase parental imprints, and activate germ-cell specific genes. This is accomplished through DNA methylation and histone marks; accordingly, differentiation defects result from mutations in important DNA methyltransferases (Maatouk et. al., 2006). Epigenetic reprogramming occurs throughout various stages of fetal germ cell development, but the period between gonadal colonization at e10.5 and the apoptotic peak

at e13.5 is notable for a major epigenetic event that includes global DNA demethylation, chromatin and histone modifications, and an essential erasure of imprints that permits sex-specific imprints to be established (Messerschmidt et. al., 2014). Any variation in the completion of this critical epigenetic reprogramming could severely hinder further sexual differentiation. Because epigenetic modifications are heritable through division, these differentiation defects would affect entire populations of clonally related cells, potentially increasing their propensity to undergo apoptosis. In this manner, clonally heterogeneous epigenetic development determines apoptotic susceptibility to ensure that only the most appropriately reprogrammed cells progress. Our report of clonal apoptosis in male germ cells supports such a model of apoptotic selection and a clonal labeling approach will prove useful for investigating specific epigenetic defects that may predict apoptosis. While intercellular bridges may promote synchrony of epigenetic reprogramming within clones due to sharing of cytoplasmic epigenetic regulators, we find that bridges exert a minimal influence on the clustered distribution of apoptosis. The $Tex14^{-/-}$ model is reported to lack bridges and we verify that mutants are TEX14-negative by immunofluorescent staining (data not shown) but it is possible that bridges still exist in the absence of this component. We are imaging fetal male germ cells by electon microscopy to verify that bridge structures are not detected. We can functionally test for bridge deletion by crossing *Tex14-/-* onto an inducible fluorescently labeled background such as *Confetti* to confirm that fluorescent proteins do not diffuse across cells in the absence of bridges. Further studies on a clonally labeled background will also elucidate the extent of developmental and epigenetic coordination provided by these bridges.

A model: p53-mediated cell competition to improve germ cell quality

Evolution by natural selection has three requirements: variation, heritable traits, and differential fitness. In the fetal male germline, one form of variation is the significant developmental heterogeneity present among germ cells at e13.5. If a source of this variable developmental

35

progress is epigenetic, this satisfies the condition for heritability. Our finding of clonal apoptosis further supports this mechanism, with apoptotic susceptibility as the heritable trait common among clone members. Lastly, in the context of the male germline, differential fitness is provided by divergent apoptotic susceptibility among clones. Therefore, the apoptotic wave exemplifies natural selection occurring on a germ cell population.

Our results suggest that a major basis for germ cell selection is developmental maturity. In addition to selecting for cells that can most efficiently and appropriately respond to further male differentiation cues, apoptotic selection may also improve the overall quality of the germ cell pool in several regards. During the period spanned by the apoptotic wave, germ cells are demethylated and are thus vulnerable to transposon expression. The germ line has several methods of defense against transposons, including remethylation that begins at e14.5 (Popp et. al., 2010) as well as the piRNA system (Aravin et. al., 2009). Interestingly, both DNA methylation and piRNA related genes were absent in the population of cells expressing higher levels of apoptotic genes and *Trp53*, suggesting that apoptosis may also discriminate against cells with impaired transposon regulation. Further supporting the connection between apoptosis resistance and male maturation, previous studies showed that apoptotic genes such as *Bax, Bak,* and *Bad* are progressively upregulated in germ cells as they mature between e10.5 and e12.5 but begin reducing in expression in males at e13.5 onwards (Runyan et. al., 2006). The temporal pattern of these apoptotic genes suggests that germ cells are most sensitized to apoptosis at the developmental age of e12.5, but that subsequent sex differentiation in the male is associated with a decreased apoptotic sensitivity. These prior studies only examined expression from pooled germ cells, but our single-cell analysis has demonstrated that subpopulations of germ cells can be at distinct developmental states. Within the e13.5 male germ cells analyzed, the transcriptional profile of the *Trp53^{high}* subpopulation is consistent with an earlier developmental timepoint of e12.5 germ cells, characterized by high pluripotency, high apoptotic expression and low male commitment. The

importance of ensuring swift, unambiguous differentiation is especially relevant to the germline. At e13.5, male germ cells must mitotically arrest and downregulate pluripotency genes (Heaney et. al., 2012); germ cells that fail to do so are more likely to form teratomas (Cook et. al., 2009). Therefore, in a e13.5 context when male germ cells ordinarily secure their sex-differentiated state, apoptosis can preferentially eliminate germ cells that escape developmental regulation, thus pruning the germ cell pool of aberrant cells.

A mechanism through which developmental fidelity can be connected to apoptosis is suggested by our finding of a p53[high] subpopulation within e13.5 male germ cells. Given the role of p53 as a comprehensive cellular stress sensor (Fridman et. al., 2003), its expression may be indicative of stressed or damaged germ cells. Differential cell fitness has been demonstrated when relative differences in p53 level are present. In the hematopoietic system, cells with relatively higher p53 were at a competitive disadvantage that resulted in diminished p53^{high} cells relative to p53^{low} cells (Bondar et. al., 2010). p53 is a transcriptional activator of many pro-apoptotic genes such as *Bax* and *Bad (*Chipuk et. al., 2004), so elevated p53 can upregulate apoptotic mediators to increase a cell's propensity to die. Indeed, we observe higher *Bad* expression in the *Trp53* high population but its expression declines as germ cells progress towards a more male-differentiated, low *Trp53* state represented by the *Nanos2^{high}* population. Given that e13.5 male germ cells are already poised to undergo apoptosis due to increasing *Bax* expression from e10.5 onwards, increasing the pool of Bad available to exert its pro-apoptotic anti-Bcl2 effect may be sufficient to push the balance towards apoptosis. p53 can also serve as a posttranslational activator of apoptotic mediators (Xu et. al., 2003), so increased p53 at the protein level could further activate the high levels of Bax protein already present in all germ cells at this stage. Markers of male differentiation were also absent in the p53[high] population, while pluripotency markers such as *Nanog* were reciprocally highest in this same population. The relative lack of male differentiation, absent transposon suppression, and aberrantly high

pluripotency are hallmarks of the p53[high] population, suggesting that *Trp53* expression may serve as a comprehensive marker of male germ cell maturation that distinguishes between mature surviving germ cells and developmentally flawed germ cells that are set to die. Considering the precision by which Nodal responsiveness distinguishes male-differentiated from immature germ cells at e13.5, this differential *Trp53* expression hints at a common intersection between Nodal signaling and *Trp53* regulation.

Altogether, our results suggest that the temporally coupled activation and suppression of Nodal signaling categorizes germ cells along a developmental timeline that proceeds toward male differentiation (Fig. 2.6). Variation among germ cell clones, potentially due to epigenetic differences, produces distinct responses to Nodal that reveals heterogeneity in differentiation capacity. This switch, toggled by Nodal responsiveness, diverts germ cells onto a pro-survival male differentiation track. Failure to respond precisely is read out as defective differentiation and leads to apoptotic elimination of these germ cells. This coordination of male maturation with apoptotic protection can serve as a quality control mechanism that ensures an agile developmental transition to a male germ cell fate, with any lagging undifferentiated cells detected and marked for elimination.
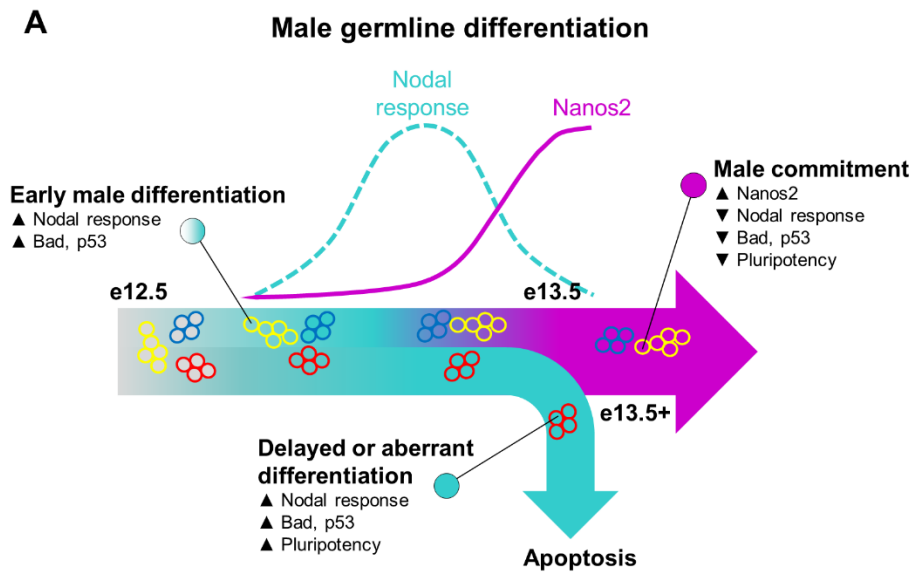
Figure 2.6

Figure 2.6: (A) Model for clonally heterogeneous male differentiation and apoptotic selection against errant male-differentiated populations. Clonally related cells are indicated by red, yellow, and blue outlines. Initial differentiation begins at e12.5 and differentiation progress is depicted on this timeline, proceeding toward male commitment in e13.5 populations. The dynamic pattern of Nodal signaling and Nanos2 expression during this period is included above the timeline. Early male differentiation of germ cells is initiated by a transient wave of Nodal signaling that is accompanied by a general increase in apoptotic sensitivity with higher expression of apoptotic genes and *Trp53*. At e13.5, epigenetic heterogeneity among clones results in variability in differentiation, with most clones appropriately dampening Nodal and increasing *Nanos2* (blue, yellow-outlined clones). Appropriate male differentiation also downregulates apoptotic genes, increasing survival of male germ cells. However, some clones (red outlined) maintain aberrant Nodal signaling and continue to express pro-apoptotic genes along with pluripotency markers. These clones are eliminated by apoptosis, ensuring that aberrant or poor differentiation is excluded in the germline.

MATERIALS AND METHODS

Mice

For WT embryo collection, CD1 females were mated to Oct4-ΔPE-GFP (Szabo, et. al., 2002) males (MGI: 4835542). For clonal labeling, *R26R-Confetti* (Snippert, et. al., 2010) (MGI:104735) and *R26R-Rainbow* (Rinkevich, et. al., 2011) mice (gift from I. Weissman, Stanford University) were outcrossed onto CD1 to generate mixed background homozygous females and then crossed to heterozygous *Pou5f1-cre/Esr*[Greder] (MGI:5049897) males for Tamoxifen-inducible germ-cell specific labeling after e8.5.

Wholemount and Section Imaging

Tissues were fixed in 4% PFA for 2h, washed with PBS, and blocked with 2% BSA, 0.1% Triton X-100 in PBS for 3 hours. Primary antibodies incubation was performed in 0.2% BSA, 0.1% Triton X-100 in PBS for 2 or more days at 4°C, followed by washing with 0.1% Triton X-100 in PBS. Primary antibodies used were [Tra98, Abcam (ab82527), 1:200; cleaved-PARP Alexa 647-conjugated, BD Biosciences(F21-852), 1:20; cleaved-PARP, Cell Signaling (#9544), 1:100;].

Secondary antibody incubation was performed in 0.2% BSA, 0.2% BSA, 0.1% Triton X-100 in PBS. Tissues were washed with PBS and dehydrated through a 25%, 50%, 75%, 100%, 100% methanol series. Tissues were cleared with a 2:1 benzyl benzoate:benzyl alcohol (BABB) solution and imaged in BABB with a *10x*/0.4 *dry* HCX PL APO CS objective on a Leica SP8 upright confocal microscope.

For section immunofluorescence, tissues were fixed in 4% PFA for 2h, washed with PBS, and dehydrated overnight in 30% sucrose at 4C. Tissues were embedded in OCT and flash-frozen and stored at -80C. Thick cryosections were cut at 25um and 50um; otherwise, sections were cut at 8um thickness and affixed to Superfrost Plus slides (Fisher Scientific). Sections were washed with PBS and incubated overnight at 4C with primary antibody in 5% donkey serum, 0.5% Triton

X-100. Sections were washed with PBS and incubated with secondary antibody for 1h at room temperature. Slides were mounted with Vectashield and imaged on a SP5 Leica confocal microscope. For antibodies requiring antigen retrieval, sections were immersed in 10mM sodium citrate and heated until boiling. Sections were washed with PBS and stained with primary antibody as described.

Statistical analysis

Wholemount tissues were stained for makers of apoptosis, germ cells, and nuclei. Objects were identified using the Find Objects function in Volocity (PerkinElmer Improvision) to determine the three-dimensional coordinates of each object centroid. Spatial analysis of clustering was based on the Ripley K function using the RipleyGUI (Hansson et. al., 2013) platform in Matlab. K-function scores were calculated to evaluate deviation (K(t) – E[K(t)]) from an expected random distribution, CSR, which was simulated independently 100 times for each spatial distribution analyzed. The relative degree of clustering for apoptotic germ cells versus all germ cell distributions, or across time points, was tested with the between-treatments sum of squares (BTSS) and compared to a 95% confidence interval for the bootstrapped BTSS value of the null hypothesis.

Apoptotic clonal clusters were identified by detecting two or more apoptotic germ cells with no greater than a 50μm centroid-to-centroid distance between two pairs of cells in the group. This threshold was determined by sparsely labeling *Confetti* x *Oct4*Cre-ER testes at e10.5 when germ cells begin colonizing the gonad as single cells. At e13.5 individual clones were visually distinct and distance between clonally related cells was measure to determine the maximum dispersion of cells within a clone, which was determined to be 50μm. Dispersion principally results from clonal fragmentation; otherwise, clonally related cells remained contiguous or proximal to each other. Two cells greater than 50μm in distance could belong to two separate clones and were excluded from clonal grouping. This does not exclude the possibility that two individual clones

may be adjacent and under this 50µm cutoff; however, apoptotic labeling on *Confetti* testes reveal that such clonal overlap is extremely rare at the administered dose of tamoxifen.

Clonal analysis

R26R-Confetti and *R26R-Rainbow* female mice were mated with *Pou5f1-cre/Esr* males and intraperitoneally injected with Tamoxifen (Sigma, 20mg/ml dissolved in sunflower seed oil) at e10.5. Tamoxifen dosage was scaled to the pregnant female's weight and adjusted to produce distinguishable colored populations (1.25mg and 2.5mg/40g female for *Confetti* and *Rainbow*, respectively). Clonally labeled gonads were dissected and fixed for wholemount staining or section immunofluorescence as described.

To clear tissues and preserve endogenous fluorescence for wholemount imaging, tissues were washed with PBS following secondary antibody incubation and placed in Scale CUBIC Reagent 1[Susaki] overnight. Cleared tissues were imaged in Scale CUBIC Reagent 1 on a white-light Leica SP8 confocal microscope. Excitation for CFP was with a 458nm laserline; GFP and YFP, 514nm white-light; RFP, 561 white-light. Fluorescence was collected for CFP between 465-495nm, airy 1.5; GFP and YFP, 521-555nm; RFP, 565-590nm.

Clonal populations were analyzed using the Cell module on Imaris to identify individual cells of a clone and quantify clone size. Clones were detected by CFP, YFP, or RFP intensity with a threshold set at 2 standard deviations below the median intensity value. Intensity was measured over the cell body with a 1.2um background filter and a 5um minimum cell diameter. Individual cells were separated using a 7um estimated cell diameter. Clonal dispersion was measured with low-dose Tamoxifen to generate sparse, distinguishable clones. Clones were measured at their widest points centroid-to-centroid, inclusive of separated but similarly colored populations, and the maximum observed dispersion was determined to be 50um. For clonal identification, similarly colored cells within the dispersion distance of 50um were considered to be part of the same clone.

Single cell RNA-seq

WT testes from timed matings were dissected in cold PBS and nongonadal tissue removed. Testes were digested in 0.25% trypsin/EDTA at 37C for 20 minutes with trituration every 10 minutes, followed by the addition of 1mg/ml DNAse and further digestion for 10 minutes. An equal volume of fetal bovine serum was added to halt digestion and the digest was strained through a single-cell filter. Dead cells were labeled with Sytox Blue and live germ cells were obtained by sorting on GFP$^+$, Sytox$^-$ into 0.04% BSA. Cells were processed for 10X sequencing by the UCSF Institute for Human Genetics. Cell by gene matrices were obtained by performing CellRanger analysis on 10x reads. Single cell expression data was analyzed using Seurat (Satija, et. al., 2015) to identify differentially expressed genes and perform principal component analysis. Statistically significant principal components ($p<0.05$) were used to cluster cells in an unsupervised manner. Differentially expressed genes by cluster (cluster biomarkers) were identified by receiver operating characteristic (ROC) test or bimodal test. Significance cutoffs were AUC>0.6, ROC test and $p<0.05$ for bimodal test.

Gene ontology analysis was performed using biomarker lists for each clustered population identified by Seurat using GSEA molecular signature database analysis. Biomarkers were analyzed for statistical overrepresentation in biological process categories and semantically sorted using ReviGO.

CHAPTER 3: Heterogeneity of fetal germ cells increases with developmental age on the basis of germ cell fitness

<u>INTRODUCTION</u>

Metazoan development generates a broad diversity of tissues with highly divergent shapes and functions that all derive from a single initial cell. The cellular differentiation that creates such diversity involves sweeping changes in cell profiles to generate different lineages, but there is an emerging recognition that diversification does not cease once cells become lineage-restricted. Even within a cellular compartment, further differences such as cell cycle state (Altschuler et. al., 2010), niche (Goodell et. al., 2015), acquired mutations (Salk et. al., 2010), and even just stochastic variation in gene expression (Ansel et. al., 2008) can produce distinct subpopulations of cells that may be directed toward very different outcomes. When this same perspective is applied to a developing cell population that is dynamically transitioning between markedly distinct cell states, the potential for significant cellular heterogeneity is magnified with developmental time.

In the fetal period, the developmental journey of germ cells from specification through sex differentiation is replete with events that can increase heterogeneity and produce distinctive subpopulations of germ cells. Germ cells derive from a small population of founder cells (Saitou et. al., 2002) as early as e6.25. This initial population then undergoes proliferation and migration, which exposes them to different niches that can differentially regulate cellular behavior (Cantu et. al., 2016). Simultaneously, germ cells undergo extensive genome-wide epigenetic reprogramming to erase methylation marks and histone modifications (Seisenberger et. al., 2012), further exposing the germ cell population to potential variability. Finally, upon colonization of the gonads, germ cells undergo an additional major differentiation event through sex-differentiation to male or female lineages. In the male germline, this is accomplished through the concerted repression of female-associated meiosis and activation of male-specific programs (Suzuki et. al.,

2008). The complex regulation required for proper sex differentiation can produce heterogeneity among germ cells that results in subpopulation-specific proliferation and cell death (Sakashita et. al., 2015). Altogether, these varied events and transitions in fetal germ cell development provide numerous opportunities for an initially similar germ cell compartment to diversity.

In addition to developmental heterogeneity through potentially dissimilar responses to these cell state transitions, germ cells must also contend with the possibility of genetic heterogeneity through the action of transposable elements. These mobile DNA transposons are capable of random insertions that can modify gene expression as well as gene sequences (O'Donnell et. al., 2010). Transposons are normally held in check by DNA methylation (Molaro et. al., 2014) but the aforementioned massive demethylation event in early germ cell development establishes a window of vulnerability during which transposons are derepressed. The extent of genetic diversity produced by these suddenly activated transposons is not known, although the tools for assessing heterogeneity at a single cell level greatly increase the resolution by which we can inspect genetic changes in a population. Beyond investigating transposon-induced differences, understanding heterogeneity among all germ cells during this dynamic fetal period can provide new insight into the role of these varied developmental events in shaping the composition of germ cells that will eventually produce gametes. In particular, understanding differences among fetal germ cell populations can predict germ cell success or failure and reveal how these distinctions are potentially set up through developmental selection.

Here, we utilize single-cell sequencing to investigate heterogeneity in male germ cells during a period between e12.5 to e13.5 when germ cells both begin sex differentiation and undergo an apoptotic wave. In males, we have discovered that apoptotic selection is highest at e13.5 (Chapter 2) and that subpopulations of germ cells are at highly distinct risk for undergoing apoptosis. We seek to identify the origins of these e13.5 subpopulations by examining an earlier timepoint for similar cell profiles. Furthermore, this approach will reveal how other developmental

events aside from apoptosis are influential in diversifying germ cells to produce additional levels of germ cell hierarchies over developmental time. We also integrate transposon profiling to enrich our transcriptional categorization of germ cell heterogeneity. We discover that precociously differentiating germ cell subpopulations exist during this period and may represent a more fit germ cell population due to increased transposon resistance. By combining these findings with clonal labeling, we uncover new dimensions of germ cell heterogeneity that can be assessed longitudinally to better define what contributes to germ cell fitness and which populations will prevail over this developmental journey.

RESULTS

Male germ cell differentiation is heterogeneous between e12.5 and e13.5 due to differential Nodal signaling and transposon-regulating gene expression

As germ cells mature upon colonizing the fetal gonads, they must undergo a significant cell state transition between e10.5 to e13.5 to become male germ cells (Yamaguchi et. al., 2013). This is achieved by large-scale transcriptional changes that include deactivation of migratory programs, upregulation of proliferation-related genes, and increased sensitization to apoptosis. The timing and breadth of these numerous changes produce an intricate developmental scale to classify the extent of male maturation. This complexity is further amplified by an emerging recognition that germ cells do not complete male differentiation as a unified, homogenous population. We have investigated the germ cell compartment during this developmental period by single-cell RNA sequencing and discovered that, at e13.5, male germ cells stratify into transcriptionally distinct subpopulations (please refer to Chapter 2). These data suggest a dichotomy between the most mature male-differentiated germ cell subpopulation and more sex-indifferent, apoptosis-susceptible subpopulation of germ cells. We proposed a linkage between differentiation status and favorable survival outcome as a potential mechanism for germ cell quality control. These results indicate that e13.5 is a critical timepoint for recognizing differences in male germ cell developmental states. To identify the origin of the transcriptional changes that underlie this emergent heterogeneity, we performed single-cell RNA sequencing on a e12.5 male germ cell population as a companion dataset to our e13.5 analysis. We hypothesized that the most mature e13.5 male germ cells would begin male differentiation relatively earlier than other germ cell populations, which would be detectable at e12.5 through the precocious expression of male-differentiation markers.

We isolated 2,517 e12.5 germ cells from Oct4-GFPΔPE fetal testes for analysis on the 10X Chromium platform. We processed this populations simultaneously with the e13.5 population

47

described in chapter 2, and submitted both populations paired-end sequencing on the Illumina HiSeq 4000. We first inquired if transcriptionally distinctive populations could be identified in an unguided manner using differentially expressed genes within this dataset. We determined that 708 genes were differentially expressed among e12.5 germ cells (Table 3.S1), which produced significantly discrete subpopulations (Fig 3.1A) after principal component analysis and cluster detection.

To investigate our hypothesis that e12.5 germ cells contain a precociously differentiating subpopulation, we examined the expression of differentiation markers among the bioinformatically-detected subpopulations (Fig 3.1B). *Nanos2*, a marker of late male germ cell differentiation with described onset at e13.5 (Suzuki et. al., 2008), was absent in the entirety of e12.5 germ cells. However, *Dazl*, a dynamically expressed germ cell differentiation marker that increases from e11.5 onwards, was significantly elevated in population 4 relative to all other populations. From our e13.5 single cell analysis in Chapter 2, we identified *Rhox6/9* as a set of genes that are sharply downregulated during the e13.5 transition between immature and more mature male germ cells. Expression of both *Rhox6* and *Rhox9* decreased in this same *Dazl* high population 4, confirming that these cells likely represent the earliest male-differentiating cells at e12.5. *Rhox6/9* were also decreased in population 5, which features a small increase in *Dazl* expression and may represent an intermediate population that has also begun to male-differentiate but slightly lags behind population 4.

We have also identified the Nodal signaling pathway as a key mediator of male differentiation during this transitional period. Nodal signaling initially activates *Lefty1/2* transcription (Chen et. al., 2004) and we detect that both Lefty genes are indeed upregulated in the same populations 4 and 5 at e12.5 (Fig 3.1C). From the expression of these genes, we can place these populations on the male differentiation timeline as the earliest of e12.5 germ cells to receive   Nodal   signals

Figure 3.1

Figure 3.1. **Male germ cell differentiation is heterogeneous between e12.5 and e13.5 by Nodal signaling and transposon-regulating genes** (A) t-SNE plot of 2,517 e12.5 male germ cells with clustered population by differential gene expression. (B) Ln-2 normalized expression of differentiation genes by e12.5 clustered populations. (C) Ln-2-normalized expression of Nodal-responsive *Lefty* genes by e12.5 clustered populations. (D) t-SNE plot of combined e12.5 and e13.5 populations with original population ID from each stage overlaid. (E) tSNE plot for combined e12.5 and e13.5 datasets with single-cell expression for markers of male-differentiation including transposon-regulating genes.

driving male commitment. These precocious e12.5 populations may then continue on to be the first germ cells expressing *Nanos2* as a male-committed germ cell at e13.5.

To directly compare the e12.5 and e13.5 germ cells by single-cell RNA expression, we combined both datasets and performed differential gene expression and clustering on the resulting mixed population. Given our prior observations at e13.5 that a gradient of male differentiation exists between immature *Trp53*^{high} cells and mature, male-differentiate *Nanos2*^{high} cells (Chapter 2), we predicted that the transcriptional state of our precocious e12.5 populations 4 and 5 would more closely resemble the majority of e13.5 germ cells than the developmentally lagging *Trp53*^{high} population at e13.5. Surprisingly, the combined e12.5 and e13.5 dataset robustly maintained a clear distinction between cells from either timepoint (Fig 3.S1A), with only a few scattered cells found among cells of the opposite timepoint.

Using the cluster identities defined by our separate analyses at e12.5 and e13.5, we sought to identify the relative positioning of these distinct differentiation states. We reasoned that the e12.5 populations 4 and 5 and the e13.5 *Trp53*^{high} population all expressed relatively high Nodal-responsive Lefty genes and may therefore be the most transcriptionally similar. While these populations did not overlap on the combined tSNE-distribution, they did occupy neighboring space (Fig 3.1D). In contrast, the most differentiated population at e13.5 characterized by high *Nanos2* expression was relatively more distant from e12.5 population 4 and 5. The similarity between the *Trp53*^{high} population and precocious e12.5 populations implies that the distinctive transcriptional profile associated with high *Trp53* at e13.5 may reflect a significant developmental delay. Although we found *Trp53* expression to be heterogeneous at e13.5, *Trp53* was homogenous in e12.5 germ cells (Fig 3.S1B) and similar in expression level. These results suggest that variation in *Trp53* may be associated with developmental stage, with more immature germ cells expressing higher levels.

Figure 3.S1
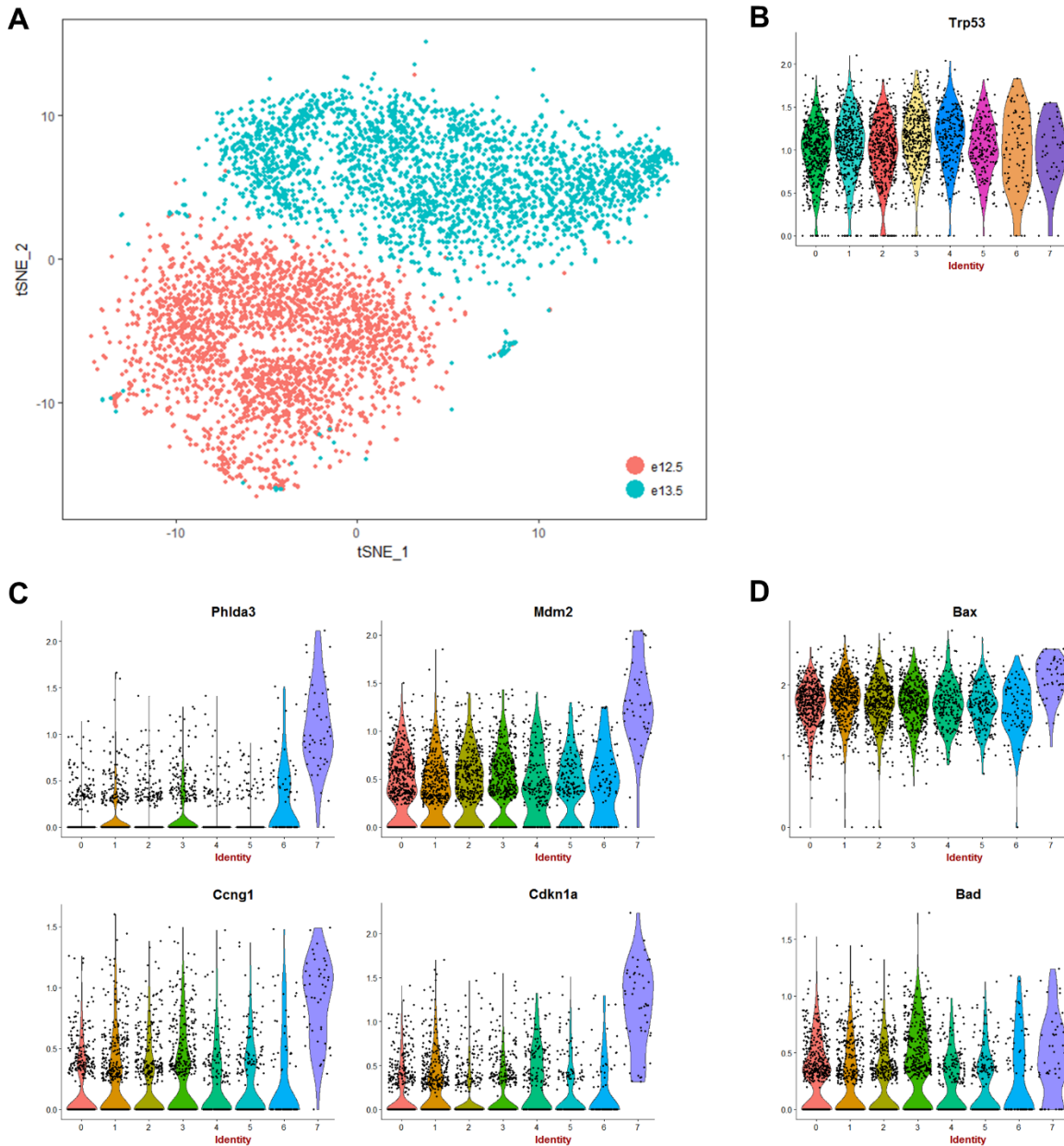
Figure 3.S1. (A) t-SNE plot of combined e12.5 and e13.5 populations. The t-SNE distribution was recalculated for the mixed dataset. Cells are labeled by original timepoint. (B) *Trp53* expression is homogenous across e12.5 clusters. (C) p53-responsive genes are enriched in a single e12.5 subpopulation. (D) pro-apoptotic genes are enriched in a single e12.5 subpopulation.

Interestingly p53-responsive genes were highly enriched in one germ cell population at e12.5 (Fig 3.S1C) and readily identified as the most significant markers of this population by Wilcoxon rank sum testing (Table 3.S1). While this population 7 did not express higher levels of *Trp53*, the upregulation of downstream targets suggest that posttranslational activation of existing p53 may distinguish this population. These p53 targets were previously established as for their role in promoting p53-mediated apoptosis (Fridman et. al., 2003) and we detected higher expression of master apoptotic genes Bad and Bax in the same e12.5 subpopulation (Fig 3.S1D). Together, these results imply that, as early as e12.5, p53 activity may be potentiating cell death in an apoptosis-sensitive population. Although we observed apoptosis to peak at e13.5 (Chapter 2), this suggests that a subset of e12.5 germ cells are already primed to rapidly execute an apoptotic cascade.

Lastly, we investigated whether single-cell differences in the expression of male differentiation markers could reveal the developmental trajectory of germ cells from an immature e12.5 to male-committed e13.5 state. As predicted, *Rhox6/9 l*evels differ between e12.5 and e13.5 cell populations, but the *Trp53^{high}* e13.5 population most resembled the comparatively homogenous e12.5 population in the expression of these differentiation markers (Fig 3.S1E). We also examined *Lefty1/2* expression as a readout of Nodal signaling between these two timepoints. While Lefty1 was highest in the e13.5 population, *Lefty2* was highest in e12.5 cells, with the *Trp53^{high}* cells expressing a similar level of *Lefty2* as most e12.5 germ cells. *Lefty1* and *Lefty2* can be differentially regulated by non-Nodal signaling (Muller et. al., 2012), which may explain the e13.5 specific enrichment of *Lefty1*. This combined transcriptional analysis reaffirms that *Trp53^{high}* e13.5 cells are most developmentally similar to e12.5 germ cells, which are themselves less heterogeneous at a population level than e13.5 germ cells.

Figure 3.S1

E
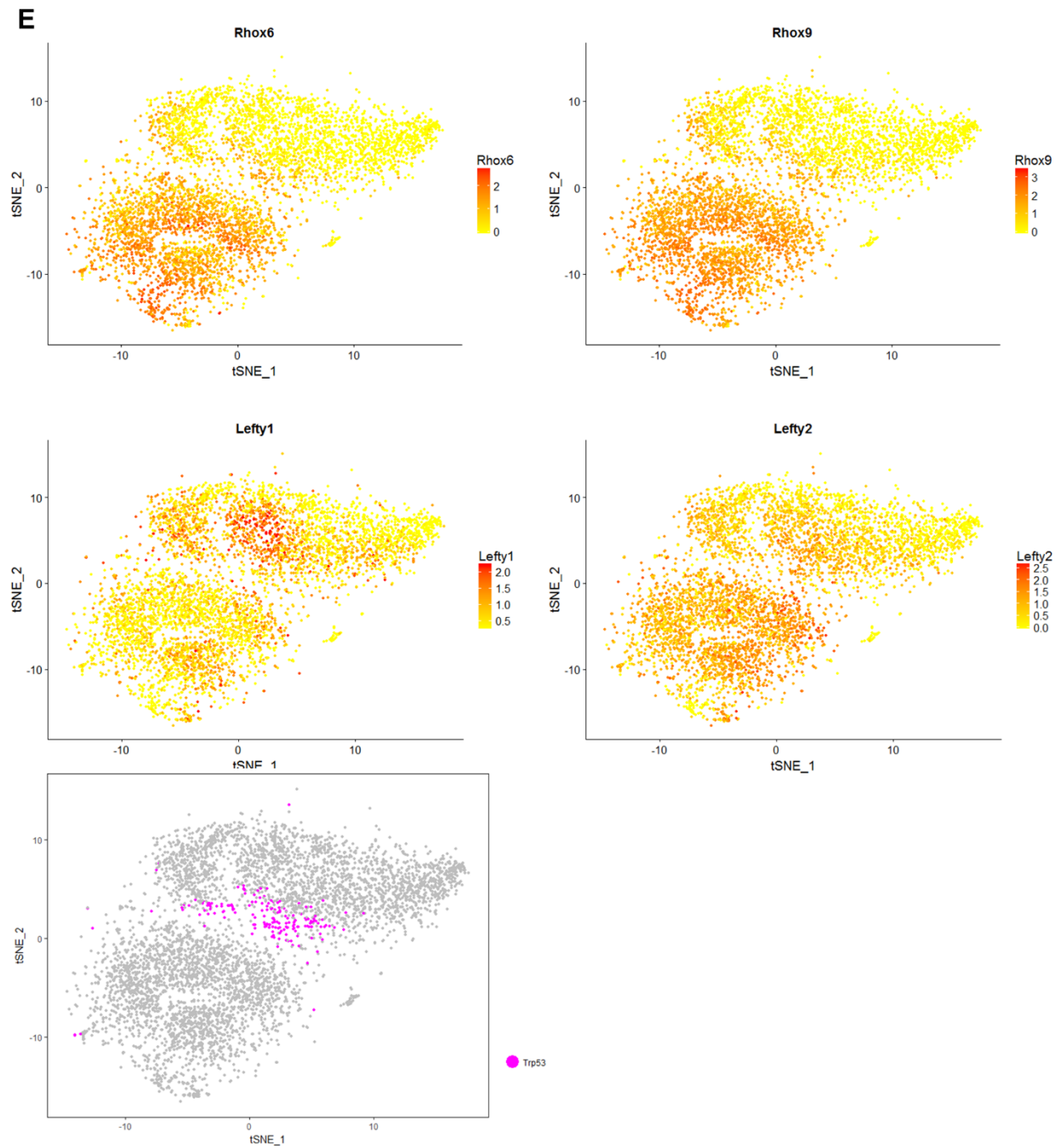
Figure 3.S1. (E) tSNE plot for combined e12.5 and e13.5 datasets with single-cell expression of differentiation genes, *Rhox6/9* and Nodal-responsive genes *Lefty1/2*. *Trp53*high cells from e13.5 are highlighted.

In Chapter 2, we identified several transposon-regulating genes as significant markers of the most mature *Nanos2^{high}* e13.5 population. While *Nanos2^{high}* cells were the most transcriptionally distinct of all e13.5 germ cells, *Nanos2* is expressed at a very low level among e12.5 cells (Fig. 3.1E). We sought to determine if expression of these transposon regulating genes could precede *Nanos2* expression and male-commitment, particularly because transposon suppression by DNA methylation is removed during global demethylation that begins as early as e10.5 and continues through e13.5. As this represents a window of vulnerability in which transposon expression may be deregulated, we hypothesized that transposon-regulating genes may be upregulated as a compensatory part of male germ cell differentiation. As expected, *Nanos2* was absent in all but a narrowly clustered group of germ cells in the combined e12.5/e13.5 population, which we confirmed were only e13.5 germ cells. We examined expression of *Tdrd5, Piwil2, and Mael*, which are all necessary components of the piRNA pathway for transposon regulation (Yabuta, et. al., 2011, Clark et. al., 2014) and notable markers of the *Nanos2^{high}* population we have transcriptionally characterized. Unlike *Nanos2*, there was scattered expression of these genes in the e12.5 population, although none of the three genes significantly marked a e12.5 subpopulation. For all three transposon-regulating genes, expression was overall higher in e13.5 cells than e12.5 cells, suggesting that these genes are markers of more mature male germ cells.

Transposon expression is elevated in the most developmentally advanced male germ cells

Transposable elements are of particular interest to germ cell development, as the failure to properly regulate TEs leads to genomic instability and reproductive failure (Bourc'his et. al., 2004). TEs are normally suppressed by several mechanisms such as histone marks, methylation, and the piRNA pathway, but the fetal period is especially critical due to epigenetic reprogramming. PGCs undergo significant genome-wide DNA demethylation from e7.5 through e12.5, providing a window of vulnerability during which demethylated TEs can be expressed (Kim et al., 2014). To

counteract this, piRNA biogenesis is first activated around e13.5 to provide another mechanism to suppress TEs.

Our discovery of differential expression of piRNA-related genes in e13.5 germ cells – Piwil2, Mael, and Tdrd5 – is significant because mutations in any of the above phenocopy each other and result in aberrantly high LINE-1 expression and male sterility. The association with high expression of these genes in a Nanos2^{high} population suggests that TE repression is not a widely-found property among e13.5 germ cells; rather, it is restricted to only the most male-differentiated population. Given that DNA demethylation is extensive at e13.5 (Seisenberger et. al., 2012), this differential expression of TE-regulating genes predicts that some populations of e13.5 germ cells may be move vulnerable to TE-expression. We therefore sought to evaluate TE-expression at a single-cell level to determine if the transcriptionally distinct populations we identified were also distinctive in their levels of TE expression. We mapped reads for e12.5 and e13.5 male germ cell single-cell RNA seq to a transposon reference genome and integrated this with our transcriptional profiling. This also enabled us to assess which different families of TEs might be expressed in our identified germ cell populations. Failure to regulate LINE-1 TEs is specifically catastrophic in germ cells (Yang, et. al., 2016) so variation in LINE-1 expression may further distinguish successful from failing germ cells. Based on our finding of a developmental dichotomy at e13.5 with Nanos^{high} cells expressing the highest levels and *Trp53^{high}* cells expressing the lowest levels of these transposon-regulating genes, we anticipated that transposon expression would be significantly reduced in the cells that represented the most mature male germ cells. Conversely, we hypothesized that immature germ cells, particularly *Trp53^{high}* e13.5 and all e12.5 populations, would harbor the highest amounts of TEs.

At e12.5, only three TEs were distinctive across all cell populations (Fig 3.S2A, Fig 3.S2B), and two of these encoded ERVK-family member TEs rather than LINE-1s. At e13.5, LINE-1s were found to be differentially expressed and associated with a specific population. However, contrary

to our hypothesis, we discovered that LINE-1-encoding TEs were actually most highly expressed in the *Nanos^high^* population and even statistically significant as a marker that could identify that mature population (Fig 3.2A). This particular family of LINE-1 TEs, L1Md_A is notable for being the youngest and most active TE in mice (Sookdeo et. al., 2013). L1Md_A TEs are also subjected to the highest degree of regulation by both methylation and piRNAs (Inoue et.al, 2017). L1Md_A levels were lower but equivalent in the other e13.5 populations (Fig 3.2B). At e12.5, L1Md_A expression was similarly homogenous across all populations (Fig 3.2C) (Fig 3.S2C). It is surprising that LINE-1 transposons were not highly expressed in these e13.5 and e12.5 populations given their relative lack of associated transposon-regulating genes as well as being mostly demethylated. Instead, elevated LINE-1 expression appears to be associated with only the most advanced, male-differentiated population at e13.5. We confirmed that the frequency of LINE-1-positive cells varies with age by immunofluorescence staining for LINE-1 ORF1p protein. LINE-1 is initially undetected at e12.5 (Fig 3.S2D) but begins to be heterogeneously expressed at e13.5, when small clusters of germ cells begin to express higher levels relative to all other germ cells (Fig. 3.2A). By e15.5, most germ cells express high levels of ORF1p relative to earlier timepoints in a homogeneous manner across the entire population.

Differential LINE-1 transposon expression is clonal and associated with smaller clones

Differential transposon expression among germ cell populations potentially is a reflection of differential development. We observed heterogeneous expression of L1 transcript and protein at e13.5. Intriguingly, immunofluorescence staining also revealed that germ cells with high LINE-1 staining tend to appear in clusters. This distribution is similar to our observations of clustered apoptosis in similarly staged germ cells (Chapter 2), although we do not observe a relationship between LINE-1 expression and apoptosis (data not shown). Given our finding that clonal

Figure 3.2

A

TE_gene	myAUC	avg_logFC	cluster
TE_L1Md_A	0.738	0.423838	Nanos2hi
TE_MMERGLN-int	0.796	0.861744	2
TE_MER34A1	0.739	0.566709	2
TE_L1_Mus1	0.711	0.130409	2
TE_MMETn-int	0.775	0.551453	3
TE_MMETn-int	0.75	0.530362	Trp53hi

B

C

D
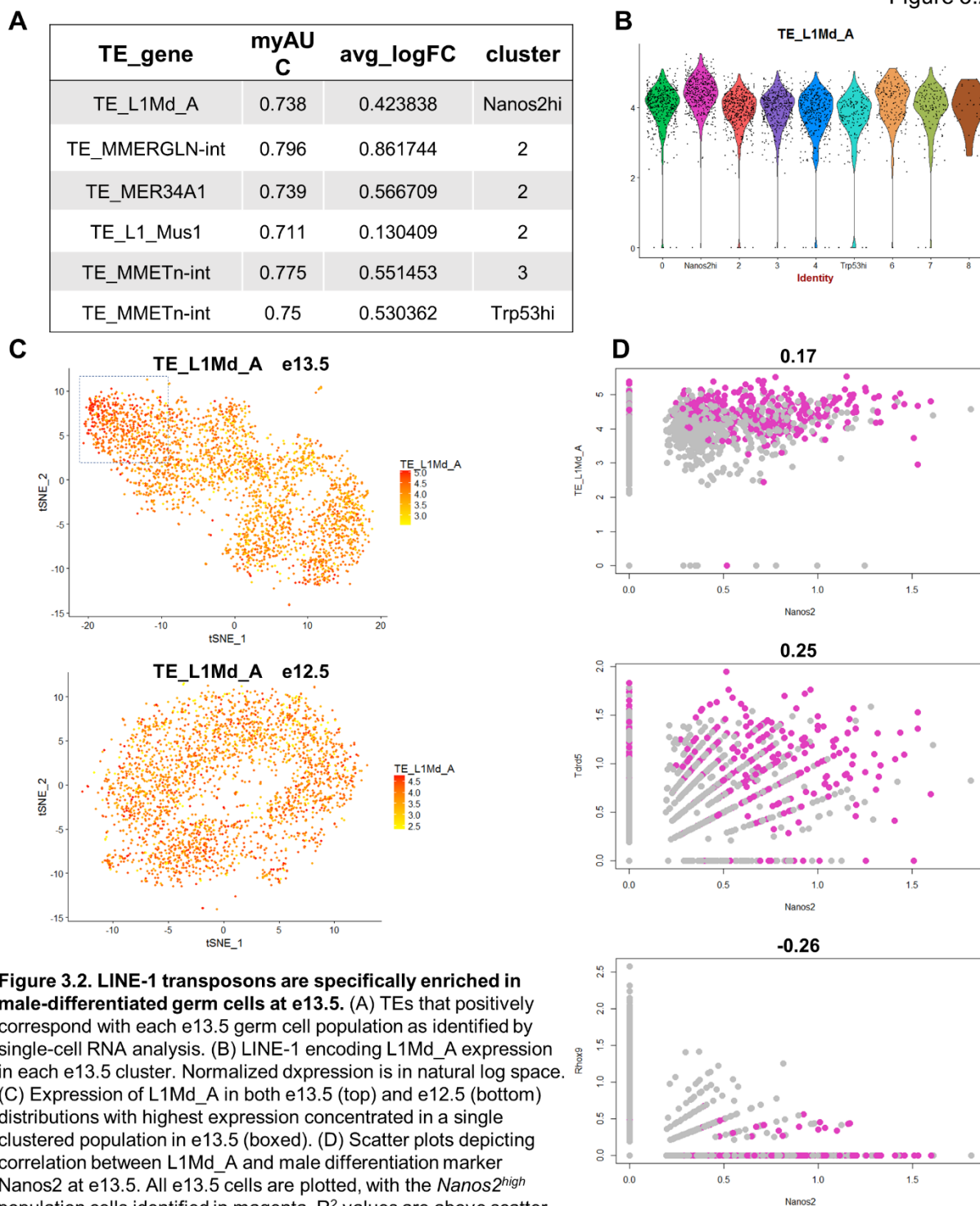
Figure 3.2. LINE-1 transposons are specifically enriched in male-differentiated germ cells at e13.5. (A) TEs that positively correspond with each e13.5 germ cell population as identified by single-cell RNA analysis. (B) LINE-1 encoding L1Md_A expression in each e13.5 cluster. Normalized dxpression is in natural log space. (C) Expression of L1Md_A in both e13.5 (top) and e12.5 (bottom) distributions with highest expression concentrated in a single clustered population in e13.5 (boxed). (D) Scatter plots depicting correlation between L1Md_A and male differentiation marker Nanos2 at e13.5. All e13.5 cells are plotted, with the *Nanos2high* population cells identified in magenta. R^2 values are above scatter plots. For comparison, Nanos2 expression is compared to a transposon-regulating gene *Tdrd5* as well as an anticorrelated marker of sex-undifferentiated germ cells, *Rhox6*. Cells plotted on axes are those with insufficient reads (dropouts).

57

Figure 3.S2

A

gene	myAUC	power	avg_logFC	cluster
TE_B1_Mm	0.718	0.436	0.255412	4
TE_RLTR1B	0.759	0.518	1.114934	7
TE_RLTR1B-int	0.716	0.432	0.758078	7

B

C
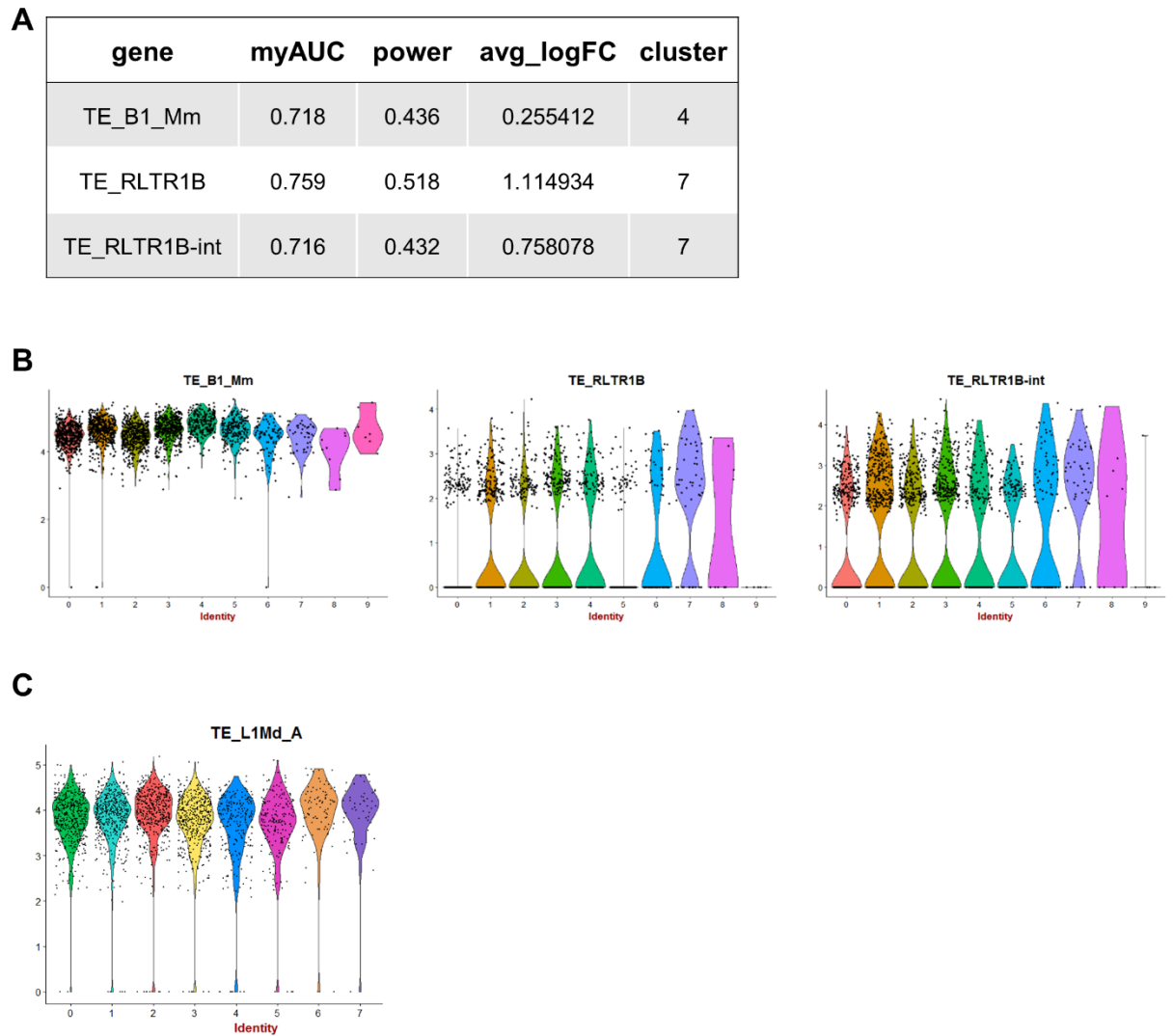
Figure 3.S2. (A) Table of TE markers associated with transcriptionally clustered populations at e12.5. (B) Expression of TE markers from S2A in each e12.5 cluster. Normalized expression is in natural log space. (C) L1Md_A expression across e12.5 clustered populations is homogenous.

Figure 3.S2

D
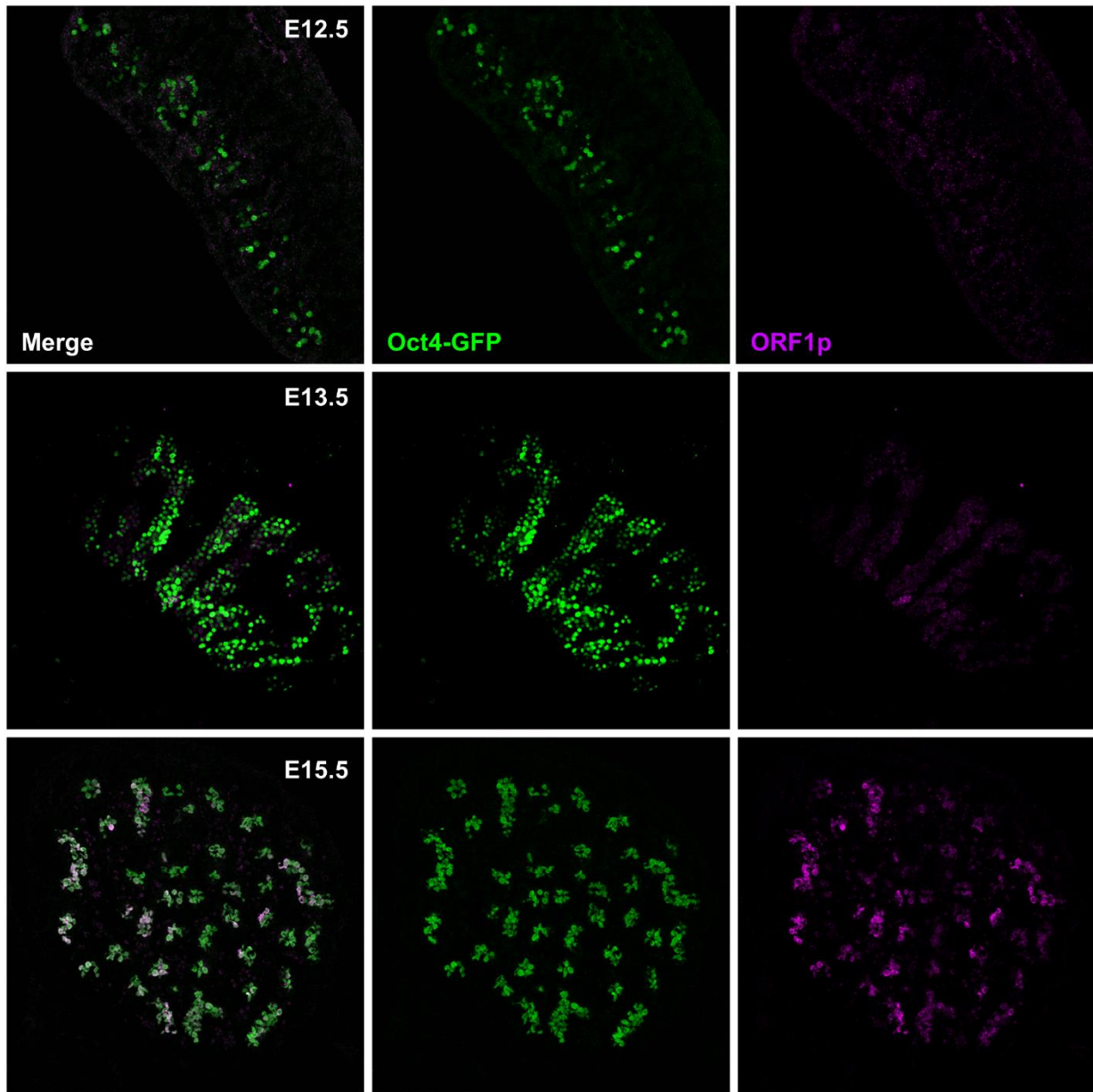
Figure 3.S2. (D) Orf1p expression increases with germ cell maturation from e12.5 through e15.5 to become more homogenous. Heterogeneous expression can be observed at e13.5 when small clusters of germ cells express Orf1p much more highly than other germ cells at the same stage.

variation underlies differential apoptosis, we wondered if the clustered arrangement of LINE-1 high cells was also due to a clonal property.

We examined LINE-1 expression at e13.5 on a Confetti background at a sufficiently low dose to allow for distinguishing individual clones (Fig 3.3A). We noted that high LINE-1 expressing cell clusters often overlapped with clonal boundaries. To more precisely measure LINE-1 expression within clones, and to allow for comparisons between clones, we first outlined each clone and then computationally separated individual cells to extract average LINE-1 values by cell (Fig 3.3B). When we considered clones by average LINE-1 expression across all constituent cells of the clone, we observed that clones were heterogeneous for LINE-1, with the distribution featuring a long tail containing high-LINE-1 expressing clones. While individual clones differed by LINE-1, we noted that most individual cells within a clone expressed similar levels of LINE-1. Such a result suggests that clonally related cells regulate LINE-1 expression similarly to produce this intraclonal homogeneity. However, due to the presence of intercellular bridges among clonally related cells, we cannot rule out that cell-to-cell similarity is enforced by LINE-1 products equally diffusing throughout a clone.

Based on our prior observation that LINE-1 expression is highest in cells that are also highest for *Nanos2*, a key marker of male differentiation at e13.5, we predicted that high-LINE-1 clones would resemble mature male-differentiated cells. One of the most significant cell state changes that accompanies male-differentiation during the fetal period is mitotic arrest around e13.5 (Western et. al, 2008). We confirmed that the e13.5 *Nanos2^{high}* population sharply downregulates *Mki67*, a cell cycle marker (Fig 3.S3A). We also observe specifically heightened expression of the cell cycle inhibitor *Cdkn1b* (data not shown). If *Nanos2^{high}* clones are mitotically arrested, this predicts that such clones would cease to grow in cell number sooner, due to earlier entry into male-differentiation and mitotic arres, while less mature clones would continue growing at that same point in time. We therefore examined the relationship between clone size and LINE-

1 expression, taking LINE-1 expression as a readout for developmental maturity. We found a weak negative correlation between clone size and LINE-1 expression (Fig 3.3D) but noted that only 1 LINE-1 high clone was larger than 10 cells by e13.5 (20%), whereas LINE-1 low clones feature 16 clones that were larger than cells (57%). While this was not statistically significant (p=0.2235), this analysis is limited to 37 clones in total. From an initial labeling with Confetti at e10.5, this potential ceiling for LINE-1-high clones suggests that more rapidly maturing clones would begin expressing *Nanos2* earlier and enter mitotic arrest having completed fewer rounds of proliferation than *Nanos2*-low clones. We also observed that cell cycle progression is synchronized within clones (Fig 3.S3B), reinforcing the model of distinct behavior across different arising from similar cellular behaviors within clones. The alternate scenario, wherein LINE-1 high clones are smaller due to apoptosis, is unlikely as we do not observe a relationship between apoptosis and high LINE-1 expression (data not shown).

Figure 3.3

A

B

C

Clonal ORF1P normalized to Hoechst

D
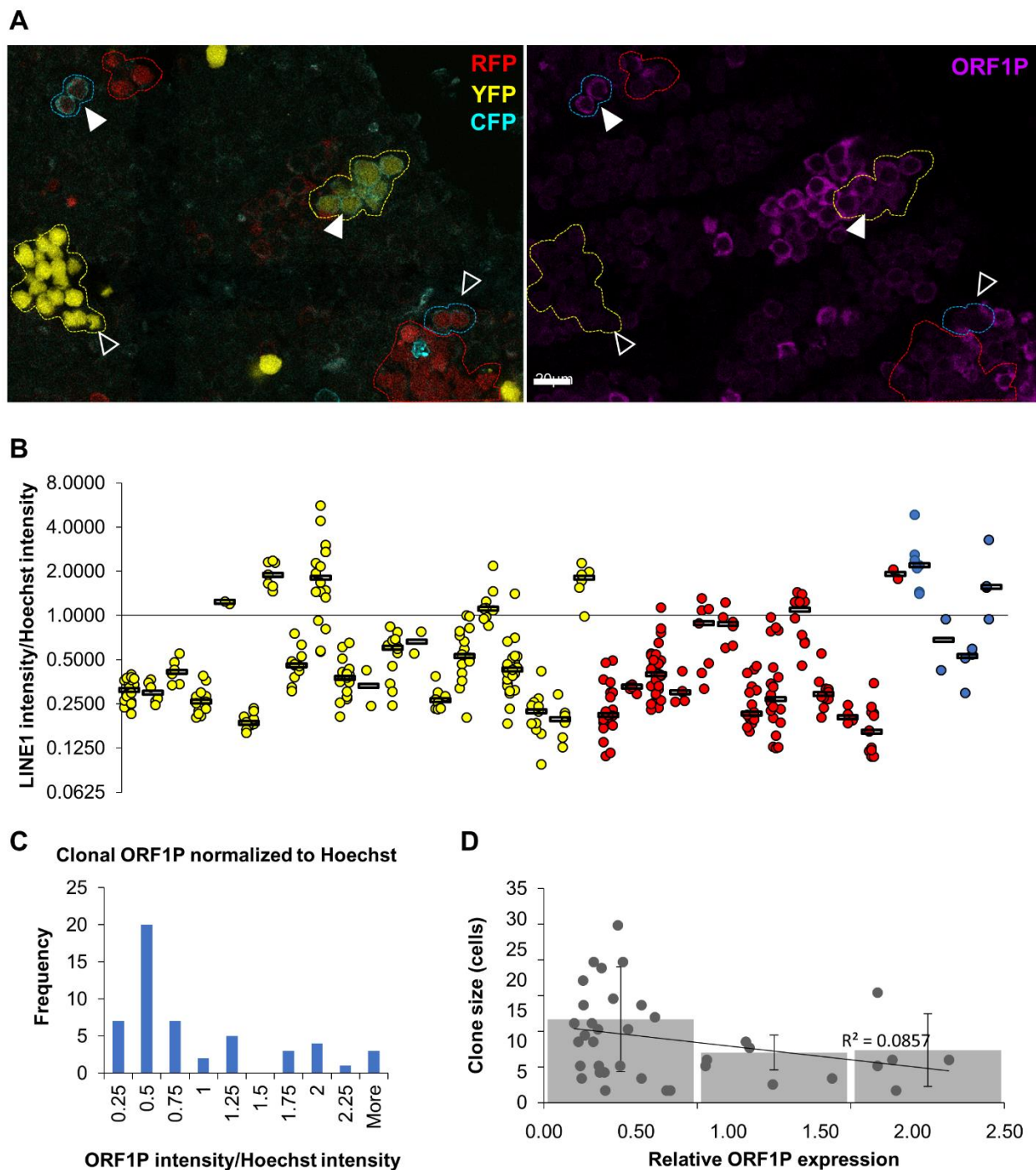
Figure 3.3. ORF1P expression is clonally heterogeneous (A) Immunofluorescence staining for ORF1P in e13.5 *Pou5f1-Cre-ER;Confetti* testes. Clonal ORF1P expression is depicted by outlined clones, with high ORF1P expression (white arrowheads) and low ORF1P (black arrowheads) (B) Quantification of ORF1P staining for each individual cell (dots) of a clone. Each clone is displayed as an individual column of cells. Black bars indicated median ORF1P intensity for each clone. Intensity values are presented on a log2 scale. (C) Histogram of the number of clones categorized by clonal ORF1P expression. (D) Relationship between clone size and ORF1P.

Figure 3.S3

A

B
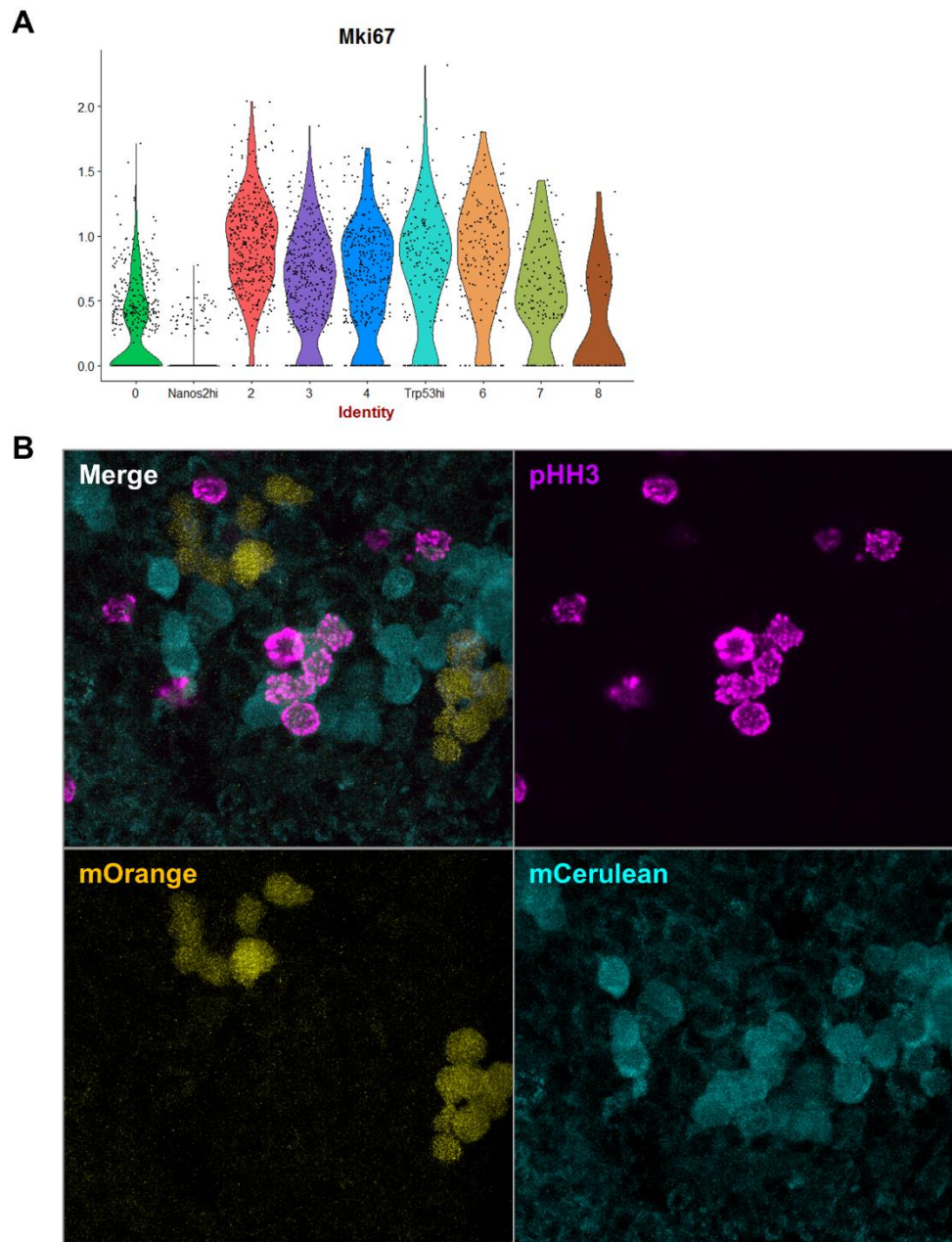
Figure 3.S3. (A) *Mki67* expression across the range of e13.5 clonal identities, including *Nanos2high* and *Trp53hi*. (B) Specific G2/M marker phospho-histone H3 is expressed in a group of clonally related cells.

DISCUSSION

The developmental journey of germ cells does not cease upon their arrival in the gonadal ridge; rather, the post-migratory fetal period involves extensive cell state changes that prepare PGCs for gametogenesis. In males, these include extensive epigenetic reprogramming (Seisenberger et. al., 2012), acquisition of a male sexual identity (Suzuki et. al., 2008), and heightened proliferation followed by mitotic arrest (Western et. al., 2008). These changes produce complex variations in cell states throughout a germ cell population that can lead to very divergent outcomes. Our recent work investigating germ cell heterogeneity at e13.5 revealed that survival or apoptosis is one such dichotomy that results from variable differentiation. By characterizing germ cells at single-cell resolution, we identified two transcriptionally distinct subpopulations that represent the leading and lagging edges of a developmental spectrum, as well as a variety of intermediate populations. While this approach can powerfully illuminate developmental diversity at the single timepoint, the origins of these germ cell subpopulations and their compositions over time remained unclear. Investigating this question requires examining multiple timepoints in a longitudinal study.

Here, we examined an earlier timepoint at e12.5 to ascertain the heterogeneity and developmental status of germ cell subpopulations. In particular, we compared these subpopulations to the two diametrically opposed cell identities we transcriptionally defined in e13.5 male germ cells. Given the importance of regulating transposable elements during this period of epigenetic resetting, we extended our single-cell analysis to include the expression of transposons during the e12.5 to e13.5 transition. This revealed specific transposons that further define our previously described states of differentiation. We further determined that differential expression of L1 transposons is a clonal property, suggesting each clonally-related cell population of fetal germ cells proceeds through male maturation as an individual unit.

Germ cells become increasingly heterogeneous during male differentiation

Our prior analysis of e13.5 male germ cells identified two distinct transcriptional states: what appears to be a developmentally advanced, male-differentiated population (*Nanos2^high*) and an immature, apoptosis-susceptible population (*Trp53^high*) lacking expression of many male-differentiation markers. We hypothesized that the *Trp53^high* population at e13.5 was developmentally stunted and predicted its resemblance to germ cells at an earlier stage. We utilized a single cell RNA sequencing spanning e12.5 to e13.5 to elucidate the developmental trajectory between the two timepoints as well as identify the where upon this timeline the of *Trp53^high* population exists. This could also resolve whether *Trp53^high* represented such an extreme developmental deviation that it would branch off from the timeline altogether.

As would be expected, the combinatorial approach revealed more homogeneity among germ cells at e12.5 germ cells compared to e13.5, suggesting that developmental differences begin to accelerate apart during this transition period. While the majority of e12.5 germ cells were developmentally similar, two populations stood out for their expression of genes characteristic of a Nodal signaling response. Because Nodal facilitates a rapid transition between undifferentiated and male-differentiated germ cell states during this period (Wu et. al., 2013), we hypothesized that this e12.5 population corresponds to precociously developed germ cells, as suggested by the early activation of male differentiation genes.

As this incipient Nodal-responsive population represented an intermediate between e12.5 and e13.5, we wondered how it would compare to the e13.5 *Trp53^high* population. The combined e12.5 and e13.5 single cell analysis indicated that the mature e12.5 and *Trp53^high* populations overlapped only minimally. The distinction between these stages could reflect the extensive transcriptional changes associated with the e12.5 to e13.5 transition. Despite the lack of overlap, the mature e12.5 and e13.5 *Trp53^high* populations were the most proximal in t-SNE space, suggesting some degree of similarity. A pseudotime analysis using developmental markers would

more precisely map these populations onto a transcriptionally-inferred trajectory. This would also reveal whether e12.5 germ cells must transition through the *Trp53^high* state to reach a more mature e13.5 state or alternatively whether the Trp53high state represents a significant departure from the normal developmental path. Based on similar expression of *Trp53* and apoptosis-related genes between the general e12.5 population and e13.5 *Trp53^high* germ cells, we anticipate that normal development starting at e12.5 indeed proceeds toward a *Trp53^high* state before activating *Nanos2* and male differentiation.

Our identification of distinct differentiating populations raises a question over the fate of individual populations over developmental time. Does a precocious Nodal-responsive population at e12.5 continue on to become the precocious *Nanos2^high* population at e13.5? Such a result would fit a conveyor belt model of differentiation, whereby initial differences that separate individual cells into different populations are maintained throughout development, with earliest-differentiating cells remaining developmentally ahead of lagging populations. Alternatively, membership in these initially-defined populations could be unstable, with cells differentiating further at variable rates toward disparate outcomes. A clonal labeling approach – especially one that can be inducibly pulsed to restrict labeling to only qualified cells at a given moment – could begin to track population fates to generate a rich cell atlas of developmental time.

Differential transposon regulation in maturing male germ cells

Using single-cell RNA sequencing, we have identified several gene networks that are dynamically regulated as germ cells begin male differentiation between e12.5 and e13.5, including piRNA related genes involved in transposon regulation. Because germ cells are globally demethylated during this period, the piRNA pathway assumes responsibility for suppressing transposons and its expression steadily increases from e13.5 onward (Kuramochi-Miyagawa et.

al., 2004). From this, we reasoned that diminished transposon expression would be evident in the most male-differentiated germ cells at e13.5, whereas more immature germ cells would feature higher levels of transposons.

We investigated this paradigm by incorporating transposon expression into our single-cell transcriptomic analysis and were surprised to discover that the reverse was true: male-differentiated germ cells marked by *Nanos2* expression were uniquely distinguished by increased expression off L1Md_A, a LINE-1 family member transposon. This particular transposon represents the youngest and most active LINE-1 family in regard to transposition activity in mice (Sookdeo et. al., 2013), so its upregulation seemingly conflicts with these *Nanos2*^{high} population also expressing higher levels of transposon regulators. Why might the most mature germ cell populations at e13.5 begin expressing uniquely high levels of transposons when transposon regulation by the piRNA pathway is a feature of mature germ cells? A key clue may lie in the method of piRNA biogenesis in this prepachytene stage.

In the fetal period corresponding to the prepachytene stage, piRNAs are notably enriched for sense transcripts from transposable elements, suggesting that they derive directly from transposon transcripts (Aravin et. al., 2008). These piRNAs would then bind to MILI, the protein product of Piwil2 that we detect is coexpressed with L1Md_A at e13.5, to generate secondary antisense piRNAs that guide targeted DNA methylation of specific TEs. This process, known as the ping-pong cycle, establishes durable methylation-mediated suppression of TEs from the fetal stage through spermatogenesis. Due to the ping-pong cycle being initiated by sense transcripts, abundant initial fetal expression of a particular TE would lead to its methylation and repression in later adulthood. This model suggests that the early expression of transposons can therefore educate the piRNA machinery to fine-tune its targeting and ensure that hyperactive transposons, such as L1Md_A, are repressed.

It remains to be seen whether germ cell populations that first differentiate and express heightened *Nanos2* and transposons will ultimately be more efficient at suppressing these transposons. The consequence of differential transposon expression in fetal germ cells at later stages in the adult is currently unknown, although mutants in transposon-regulating genes such as *Mili, Miwi2, Mael, and Mov10l* suffer reproductive failure later in spermatogenesis (Molaro et. al., 2014, Goodier et. al., 2016, Castaneda et. al., 2014). In that regard, it is possible that early differentiating male germ cells may enjoy a later fitness advantage due to more robust transposon suppression that results from the earlier initial expression of TEs. Transient labeling of the earliest *Nanos2*-expressing germ cells would mark this early male population and permit a later evaluation of its fitness as well as its potentially superior transposon regulation via increased methylation of transposons.

We also note that, although ORF1p expression is initially heterogeneous at e13.5, it is more homogeneous by e15.5 (Fig. 3.S2), suggesting that most germ cells attain equal levels of L1 mRNA. This may be the result of slower-differentiating germ cells catching up to the precocious *Nanos2^{high}* cells that first male-differentiate at e13.5 and are first to express L1 mRNAs. If initial L1 expression is associated with priming antisense piRNA production via the ping-pong cycle, this evidence suggests that eventually antisense L1 transcripts are more evenly produced across all germ cells by e15.5. However, given the earlier expression of L1 in *Nanos2^{high}* cells, we would expect that L1 methylation would be heterogeneous at e15.5 due to more time allotted for the initial *Nanos2^{high}* germ cell populations to establish piRNA-mediated L1 methylation.

Single-cell studies have illuminated the diversity of transcriptional states comprising a cell population. In germ cells, we have used this approach over developmental time and with transposon profiling to more comprehensively categorize germ cell states. These states may also reflect clonal differences that can produce distinct outcomes for reproductive success among germ cell populations.

MATERIALS AND METHODS

Mice

For WT embryo collection, CD1 females were mated to Oct4-ΔPE-GFP[Szabo] males (MGI: 4835542). For clonal labeling, *R26R-Confetti[Snippert]* (MGI:104735) and *R26R-Rainbow[Rinkevich]* mice (gift from I. Weissman, Stanford University) were outcrossed onto CD1 to generate mixed background homozygous females and then crossed to heterozygous *Pou5f1-cre/Esr[Greder]* (MGI:5049897) males for Tamoxifen-inducible germ-cell specific labeling after e8.5.

Wholemount and Section Imaging

Tissues were fixed in 4% PFA for 2h, washed with PBS, and blocked with 2% BSA, 0.1% Triton X-100 in PBS for 3 hours. Primary antibodies incubation was performed in 0.2% BSA, 0.1% Triton X-100 in PBS for 2 or more days at 4°C, followed by washing with 0.1% Triton X-100 in PBS. Primary antibodies used were [Tra98, Abcam (ab82527), 1:200; ORF1P, gift of Bortvin lab, , 1:1000;].

Secondary antibody incubation was performed in 0.2% BSA, 0.2% BSA, 0.1% Triton X-100 in PBS. Tissues were washed with PBS and dehydrated through a 25%, 50%, 75%, 100%, 100% methanol series. Tissues were cleared with a 2:1 benzyl benzoate:benzyl alcohol (BABB) solution and imaged in BABB with a *10x*/0.4 *dry* HCX PL APO CS objective on a Leica SP8 upright confocal microscope.

For section immunofluorescence, tissues were fixed in 4% PFA for 2h, washed with PBS, and dehydrated overnight in 30% sucrose at 4C. Tissues were embedded in OCT and flash-frozen and stored at -80C. Thick cryosections were cut at 25um and 50um; otherwise, sections were cut at 8um thickness and affixed to Superfrost Plus slides (Fisher Scientific). Sections were washed

with PBS and incubated overnight at 4C with primary antibody in 5% donkey serum, 0.5% Triton X-100. Sections were washed with PBS and incubated with secondary antibody for 1h at room temperature. Slides were mounted with Vectashield and imaged on a SP5 Leica confocal microscope. For antibodies requiring antigen retrieval, sections were immersed in 10mM sodium citrate and heated until boiling. Sections were washed with PBS and stained with primary antibody as described.

Single cell RNA seq

For e12.5 male germ cell collection, WT testes from timed matings were collected simultaneously with e13.5 male germ cells for single-cell RNA sequencing (Chapter 2). Wild-type testes from timed matings were dissected in cold PBS and nongonadal tissue removed. Testes were digested in 0.25% trypsin/EDTA at 37C for 20 minutes with trituration every 10 minutes, followed by the addition of 1mg/ml DNAse and further digestion for 10 minutes. An equal volume of fetal bovine serum was added to halt digestion and the digest was strained through a single-cell filter. Dead cells were labeled with Sytox Blue and live germ cells were obtained by sorting on GFP$^+$, Sytox$^-$ into 0.04% BSA. Cells were processed for 10X sequencing by the UCSF Institute for Human Genetics. Cell by gene matrices were obtained by performing CellRanger analysis on 10x reads. For transposon reference, transposon reference was downloaded from the Hammell lab (Cold Spring Harbor). Single cell expression data was analyzed using Seurat to identify differentially expressed genes and perform principal component analysis. Statistically significant principal components ($p<0.05$) were used to cluster cells in an unsupervised manner. Differentially expressed genes by cluster (cluster biomarkers) were identified by receiver operating characteristic (ROC) test, bimodal test, and Wilcoxon rank sum test. Significance cutoffs were AUC>0.6, ROC test and $p<0.05$ for bimodal and Wilcoxon rank sum test. An AUC score>0.6 was used to identify markers that were reliable, positive classifiers of a cluster, with AUC scores

closer to 1.0 as examples of perfect classifiers. For transposon analysis, multimodal Seurat analysis was used with transposon expression added as a data slot to the precalculated transcriptional data. Fold changes and normalized gene expression was expressed in natural log space as a default output of Seurat. For fold change calculations pertaining to cluster markers, the mean expression across all cells of one cluster was compared to the mean expression of all other cells in non-log space, and then the fold difference was expressed in natural log space.

Gene ontology analysis was performed using biomarker lists for each clustered population identified by Seurat using GSEA molecular signature database analysis. Biomarkers were analyzed for statistical overrepresentation in biological process categories and semantically sorted using ReviGO.

Chapter 4: CONCLUSION AND FUTURE DIRECTIONS

Reproduction is often thought of as the product of numerous random mixings – random combinations of chromosomes in haploid gametes, random crossing over events during meiosis, all culminating in hypothetically random pairing of gametes – but the long and complex span of reproductive development that precedes gametogenesis provides many opportunities for developmental selection to nonrandomly act upon gamete precursors. In fact, lineage tracing experiments have begun to reveal nonrandom patterns of germ cell success that translate into unequal gamete representation (Ueno et. al., 2009, Kanatsu-Shinohara et. al., 2016). Furthermore, apoptosis is a hallmark of germ cell development, and cell death is an inherent bottleneck for a population. If germ cells are selectively enriched or eliminated, that would have significant downstream effects on which gametes are later generated and passed on. These findings pose the question: how does reproductive development select for certain germ cells and how does this impact the gamete pool?

This thesis investigated the premise of germ cell selection by focusing on the events of germ cell development in the male mouse embryo. This period is notable for intense and dynamic changes that guide a nascent germ cell population through specification, expansion, elimination, and differentiation – all of which present opportunities for selection or differential action on a germ cell population with more population diversity than previously appreciated.

We first focused on an apoptotic wave that specifically eliminates male fetal germ cells between e12.5 to e15.5, as apoptosis represents a clear developmental bottleneck and source of potential selection. In Chapter 2, we identified a high incidence of apoptotic germ cells organizing in local clusters that suggested a nonrandom, environment-independent basis for elimination. We integrated clonal labeling to define these apoptotic clusters as clonally related germ cells, which further argued for an intrinsic, heritable trait that is selected against. We investigated germ cell populations at a single-cell level during peak apoptosis at e13.5 and identified two divergent

subpopulations in regard to apoptotic susceptibility. These populations differed by p53 and Nodal signaling networks and likely represented two extremes for male sex differentiation. Together, these findings suggested that apoptotic selection discriminates against clonal populations with intrinsically impaired sex differentiation.

We built on these findings in Chapter 3 by seeking to understand how such population variation in sex differentiation arises over developmental time. We extended our single-cell analysis to e12.5 and identified a precocious sex-differentiating population that we predicted would enjoy a selective advantage during later germ cell apoptosis. We also described transposon regulation and expression as germ cell characteristics that varied with these heterogeneous sex-differentiating populations. Our work argues for a novel understanding of germ cells as a diverse collection of clonal populations that vary in sex differentiation capacity. We also offer a new perspective into fetal germ cell development as a selection process that enriches for the most fit populations.

Germ cell heterogeneity is due to variation in male maturation

Germ cell development in the fetal period is characterized by rapid transitions between diverse cell states, which encompass proliferation, mitotic arrest, migration, and global demethylation, to name a few. The wide range of cell states presents many opportunities for populations to become increasingly desynchronized, which is further exacerbated as finely tuned signaling from the niche is potentially missed by lagging populations. BMP signaling is one such critical PGC survival and differentiation factor that is expressed in a transient niche, and loss of this signal decreases PGC number (Dudley et.al, 2010). Importantly, decreased sensitivity to BMP signaling also resulted in the same reduction in PGC number, demonstrating that the concept of a transient niche can also involve the target cell's receptivity to an extrinsic factor. Therefore, such

a tight requirement of coordination can be thought of as a narrow developmental window in which differentiation cues are optimally transmitted to a dynamic population of cells.

In our own study of fetal male germ cells, we discovered that receptivity to Nodal signaling is another such example of a tightly regulated signaling window. Nodal signaling promotes the significant cell state change of male sex differentiation and we found a previously unknown heterogeneity among germ cell populations in their response to Nodal signaling as well as their progression through male sex differentiation. At our earliest observed stage of e12.5, we see this initial heterogeneity in the emergence of a precocious male differentiating population. At the later stage of e13.5, this initial heterogeneity expands into a stark dichotomy between mature male-differentiated germ cells and an immature population that is highly divergent from the mature population by several metrics, including apoptosis susceptibility and transposon expression. We propose that the precocious male-differentiating population represents the earliest population that is responsive to Nodal signaling and are first to become mature male germ cells. In contrast, germ cell populations that are initially delayed or relatively less capable in responding to Nodal signaling fall further behind, resulting in these populations becoming the most immature germ cells observed at e13.5. Therefore, an initial heterogeneity in responding to a cell state transition is exacerbated as sex differentiation further stratifies germ cells populations into the leading groups versus the deficient lagging groups. Our observation that apoptosis is heightened in the immature population suggests that germ cells that miss the initial window will eventually become so divergent that they are eliminated entirely.

Epigenetic reprogramming can generate heritable variation

Our findings using *Confetti* clonal labeling indicate that heterogeneous behavior varies from clone to clone but is intraclonally similar, meaning that identically colored nearby cells

behave similarly. Thus, heterogeneity appears to be clonal and therefore a heritable property. Because heritability is achieved through a genetic or epigenetic mechanism, we consider both possibilities as a source of heterogeneous clonal behavior.

Generally, the germline is protected from spontaneous mutation and exhibits a far lower mutation rate than other somatic tissues (Lynch 2010). One mechanism that protects the germline from mutation is a germ-cell enriched DNA damage response such as global genome repair (Lans et. al., 2010). Germ cells are also more likely to undergo apoptosis in response to DNA damage than somatic cells, providing another failsafe against the acquisition of mutations. These findings suggest that it is that spontaneous mutations are unlikely to be responsible for generating the diversity of germ cell populations we observe.

Epigenetically, germ cells undergo significant changes during the fetal period. Most notably, global DNA demethylation precedes the onset of male sex differentiation and is an intriguing candidate for generating heritable variation among germ cell populations. While our approach did not include examining the methylation status of the individual germ cell populations we characterized, the fact that DNA methylation is carefully regulated to control the timing of germ cell differentiation (Hargan-Calvopina, et. al, 2016) suggests that the precocious male-differentiating germ cell population may be more advanced in demethylation status and receptive to differentiation signals. Examining the methylation status and histone modifications of the *Nanos2^{high}* population can reveal the epigenetic differences that may give rise to the early differentiating population. Moreover, we predict that methylation status is both heterogeneous and clonal. In support of this, we note that LINE-1 expression of its protein product Orf1p appears to be highly clonal, and transposon expression during the fetal period is principally regulated by methylation status. Future studies integrating methylation analysis along with single-cell technologies such as single-cell RNA sequencing and clonal immunofluorescence can elucidate the extent by which methylation is clonal and also associated with clonal behaviors.

Selection among variable germ cells can improve germ cell outcomes

Our work here demonstrates that germ cell heterogeneity results from differences in male differentiation capacity and has significantly variable consequences for a population's success toward gametogenesis. We showed that p53 expression and apoptotic susceptibility is heightened in immature germ cell populations while mature male germ cells were the most protected. Male differentiation bestows several potentially beneficial characteristics on germ cells that reach this stage first. Transposon regulating genes are elevated in this population, which can ensure that genomic integrity is best safeguarded against insertions by transposable elements. This is especially pertinent considering that germ cells during the e12.5 to e13.5 period studied by this thesis are especially vulnerable to transposon expression due to extensive DNA demethylation. Germ cells can compensate for this increase in transposon susceptibility by activating piRNA pathway genes, which we observe in mature *Nanos2*^-high germ cells. The piRNA pathway lays down durable methylation at transposable element loci to ensure continued genomic integrity for all the progeny of a germ cell. Therefore, germ cells that attain a male-differentiated state first could more thoroughly defend against transposition.

A second advantage is that male differentiation is associated with mitotic arrest, which we confirmed by a greatly diminished expression of cell cycle markers in the *Nanos2*^high cells. Germ cells that fail to appropriately regulate cell cycle genes and enter mitotic arrest at e13.5 are more likely to form teratomas (Cook et. al, 2011, Kimura et. al., 2003). The increased susceptibility of immature germ cells to apoptosis may be one method of preventing a potentially tumorigenic population from continuing through to gametogenesis. LINE-1 transposon expression is also associated with germ cell tumors (Su et. al, 2007), which may be due to mutational insertion or a pluripotency-associated role of LINE-1 family members (Närvä et. al., 2012, Klawitter et. al., 2016). The combined contribution of dysregulated LINE-1 expression with impaired cell cycle control could also represent a cheater population – one that enjoys a proliferative advantage that

comes at the detriment of organismal success and genomic integrity. Further studies on an apoptosis-deficient background such as *Bax* could elucidate the consequences of unchecked immature male populations beyond the fetal period. The role of apoptotic selection may be intimately linked with the need to limit heterogeneous germ cell populations during a period when transposons and demethylation threaten to introduce undesirable additional variation into a tightly regulated population.

APPENDICES

Table 2.S1: Clustered differentially expressed markers for e13.5 germ cells

gene	myAUC	power	avg_logFC	pct.1	pct.2	cluster
Cdc20.1	0.754	0.508	0.505456	0.965	0.73	1
Hspa5	0.785	0.57	0.431771	1	0.979	1
Ccnb1.1	0.742	0.484	0.423363	0.995	0.836	1
Arl6ip1.1	0.76	0.52	0.409062	1	0.973	1
Ube2c.1	0.746	0.492	0.405926	1	0.976	1
Cks2.1	0.745	0.49	0.347472	1	0.994	1
Calr	0.733	0.466	0.322281	1	0.995	1
Ube2s.1	0.728	0.456	0.298965	1	0.999	1
Dynll1	0.84	0.68	0.284229	1	1	1
Pttg1	0.704	0.408	0.281977	0.993	0.912	1
Ccnb2	0.708	0.416	0.278513	0.988	0.949	1
Top2a.1	0.858	0.716	0.724126	0.988	0.908	2
Hn1.1	0.907	0.814	0.721313	0.991	0.907	2
Ube2c.2	0.886	0.772	0.715789	0.995	0.978	2
Cdc20.2	0.848	0.696	0.679706	0.986	0.742	2
Smc4.1	0.863	0.726	0.679518	0.988	0.92	2
Ccnb1.2	0.85	0.7	0.677415	0.988	0.848	2
Arl6ip1.2	0.85	0.7	0.66503	0.998	0.975	2
Tubb4b.1	0.849	0.698	0.609957	0.991	0.978	2
Lefty1	0.713	0.426	0.546036	0.871	0.655	2
Cdk1	0.818	0.636	0.545794	0.93	0.656	2
Ube2s.2	0.874	0.748	0.545712	1	0.999	2
Plk1.1	0.856	0.712	0.544271	0.892	0.314	2
Cenpa.1	0.835	0.67	0.525124	0.991	0.901	2
Aurka.1	0.834	0.668	0.517544	0.925	0.474	2
Nusap1.1	0.833	0.666	0.514925	0.934	0.533	2
Kpna2.1	0.83	0.66	0.503626	0.911	0.539	2
Cenpe	0.831	0.662	0.50126	0.979	0.781	2
Tpx2.1	0.827	0.654	0.499367	0.97	0.618	2
Hmgb2.1	0.851	0.702	0.494937	1	0.981	2
Hmmr.1	0.816	0.632	0.493695	0.948	0.636	2
Mis18bp1.1	0.834	0.668	0.488652	0.984	0.816	2
Prc1	0.816	0.632	0.478766	0.967	0.703	2
Incenp.1	0.813	0.626	0.476581	0.977	0.724	2
Cks2.2	0.831	0.662	0.47608	1	0.994	2
Cenpf.1	0.845	0.69	0.473143	1	0.997	2
Bub3.1	0.815	0.63	0.461425	0.977	0.89	2
Mki67.1	0.773	0.546	0.419911	0.963	0.631	2

gene	myAUC	power	avg_logFC	pct.1	pct.2	cluster
Birc5.1	0.795	0.59	0.413938	0.984	0.858	2
Tuba3a.1	0.755	0.51	0.398366	0.979	0.689	2
Nucks1.1	0.789	0.578	0.397021	0.974	0.831	2
Ccnf	0.801	0.602	0.374813	0.876	0.422	2
Kif23	0.795	0.59	0.363722	0.82	0.301	2
Malat1.1	0.759	0.518	0.351675	1	0.999	2
Blnk	0.741	0.482	0.334432	0.899	0.606	2
Spc25.1	0.749	0.498	0.327215	0.977	0.839	2
Cdca2	0.741	0.482	0.325317	0.927	0.674	2
Fzr1	0.755	0.51	0.324731	0.843	0.5	2
Smc1b	0.724	0.448	0.311139	0.988	0.96	2
Tuba1c	0.739	0.478	0.308077	0.787	0.37	2
Trim59	0.746	0.492	0.300036	0.796	0.371	2
Pttg1.1	0.708	0.416	0.291724	0.986	0.919	2
Knstrn	0.731	0.462	0.289295	0.815	0.483	2
Ccna2.1	0.72	0.44	0.285125	0.967	0.763	2
Eif1.1	0.773	0.546	0.272018	1	0.999	2
Kif11	0.733	0.466	0.271673	0.852	0.446	2
Aspm	0.737	0.474	0.267826	0.787	0.355	2
Cfl1.1	0.727	0.454	0.267275	0.995	0.994	2
Aurkb	0.727	0.454	0.264981	0.756	0.344	2
Kif20b	0.704	0.408	0.264237	0.953	0.776	2
Kif2c	0.714	0.428	0.26327	0.867	0.568	2
Hmgn2	0.707	0.414	0.25515	0.995	0.981	2
Cdca8.1	0.714	0.428	0.252342	0.981	0.975	2
Hist1h2ap	0.945	0.89	1.19816	0.987	0.414	3
Hist1h1b	0.95	0.9	1.190784	0.994	0.376	3
Hist1h1e	0.959	0.918	1.14684	0.987	0.34	3
Top2a.2	0.856	0.712	0.709063	1	0.91	3
Slbp.1	0.879	0.758	0.648266	1	0.926	3
Gmnn.1	0.86	0.72	0.623684	0.997	0.795	3
Hist1h2ae	0.891	0.782	0.619635	0.911	0.203	3
H2afx	0.847	0.694	0.5818	0.987	0.771	3
Hist1h1a	0.873	0.746	0.579882	0.848	0.17	3
A430005L14Rik	0.853	0.706	0.544545	0.984	0.762	3
Dek.1	0.87	0.74	0.537938	1	0.947	3
Smc4.2	0.819	0.638	0.537461	0.997	0.922	3
Tuba3a.2	0.811	0.622	0.533137	0.987	0.702	3
Dnajc9.1	0.848	0.696	0.503257	0.984	0.75	3
Fbxo5.1	0.831	0.662	0.494749	0.934	0.385	3
Nxt1	0.844	0.688	0.479603	0.987	0.914	3
Dut.1	0.855	0.71	0.475084	1	0.99	3

gene	myAUC	power	avg_logFC	pct.1	pct.2	cluster
Nasp.1	0.816	0.632	0.450614	1	0.972	3
Tipin.1	0.792	0.584	0.417758	0.987	0.866	3
Ezh2.1	0.785	0.57	0.408765	0.984	0.813	3
Tyms.1	0.782	0.564	0.402492	0.972	0.728	3
Usp1.1	0.786	0.572	0.387755	0.994	0.859	3
Esco2.1	0.774	0.548	0.383445	0.991	0.874	3
Mcm6	0.766	0.532	0.37296	0.987	0.862	3
Prim1.1	0.772	0.544	0.368934	0.943	0.682	3
Mcm5	0.756	0.512	0.363561	0.959	0.783	3
H3f3b	0.875	0.75	0.35669	1	1	3
Rfc3	0.758	0.516	0.35083	0.943	0.732	3
Mrpl18	0.763	0.526	0.342399	0.991	0.918	3
Atad2	0.748	0.496	0.339794	0.994	0.936	3
Cdk1.1	0.737	0.474	0.333107	0.934	0.669	3
U2af1.1	0.783	0.566	0.332795	1	0.996	3
Pcna	0.75	0.5	0.327151	0.877	0.562	3
Lig1.1	0.742	0.484	0.319329	0.997	0.952	3
Smc2.1	0.735	0.47	0.318503	0.997	0.97	3
Brca2	0.736	0.472	0.315832	0.927	0.683	3
Mcm3	0.737	0.474	0.313449	0.978	0.802	3
Hmgb2.2	0.708	0.416	0.312407	1	0.982	3
Birc5.2	0.732	0.464	0.311402	0.991	0.863	3
Stmn1.1	0.754	0.508	0.309876	1	0.999	3
Siva1.1	0.766	0.532	0.305951	1	0.992	3
Rpa2	0.742	0.484	0.301623	0.997	0.974	3
Ppil1	0.73	0.46	0.301253	0.978	0.898	3
Hist1h1d	0.737	0.474	0.29801	0.541	0.078	3
Dnmt1	0.716	0.432	0.295784	0.965	0.85	3
Incenp.2	0.714	0.428	0.294233	0.972	0.737	3
Rfc2	0.725	0.45	0.29052	0.921	0.672	3
Pold3	0.741	0.482	0.290188	0.883	0.627	3
Clspn	0.72	0.44	0.28971	0.93	0.705	3
Spc24.1	0.718	0.436	0.28914	0.965	0.769	3
Rad51ap1	0.733	0.466	0.288693	0.807	0.417	3
Ywhah	0.721	0.442	0.288156	0.959	0.756	3
Prc1.1	0.708	0.416	0.285979	0.94	0.72	3
Hells	0.745	0.49	0.283713	1	0.991	3
Fen1	0.725	0.45	0.283218	0.905	0.629	3
Syce2.1	0.716	0.432	0.28191	1	0.959	3
2700029M09Rik	0.721	0.442	0.281793	0.959	0.818	3
Dctpp1.1	0.779	0.558	0.281533	1	0.998	3

gene	myAUC	power	avg_logFC	pct.1	pct.2	cluster
Smc1a	0.708	0.416	0.281208	0.978	0.9	3
Pmf1	0.72	0.44	0.281025	0.991	0.902	3
Dhfr	0.709	0.418	0.280354	0.908	0.666	3
Rrm1	0.727	0.454	0.280105	0.924	0.659	3
Rfc4	0.708	0.416	0.278492	0.978	0.932	3
Ssna1	0.725	0.45	0.278474	0.978	0.874	3
Tk1	0.747	0.494	0.275491	0.696	0.238	3
Wdhd1	0.732	0.464	0.27263	0.782	0.389	3
Nup62	0.71	0.42	0.270913	0.962	0.812	3
Med9	0.713	0.426	0.265834	0.924	0.713	3
2810417H13Rik	0.73	0.46	0.265404	0.652	0.221	3
Rbm44	0.724	0.448	0.264609	0.712	0.318	3
Ranbp1.1	0.758	0.516	0.26045	1	0.999	3
Smc3	0.74	0.48	0.260415	1	0.996	3
Hist1h2ap.1	0.762	0.524	0.718276	0.798	0.451	4
Hist1h1b.1	0.768	0.536	0.681747	0.814	0.413	4
Slbp.2	0.848	0.696	0.624305	0.988	0.929	4
Ung	0.85	0.7	0.579748	0.972	0.781	4
Wbp5	0.78	0.56	0.55962	0.98	0.827	4
Fbxo5.2	0.81	0.62	0.537287	0.879	0.407	4
Gmnn.2	0.806	0.612	0.534348	0.98	0.802	4
Tipin.2	0.82	0.64	0.48222	0.984	0.869	4
Rrm2	0.816	0.632	0.480476	0.814	0.297	4
Mcm6.1	0.808	0.616	0.465368	0.972	0.867	4
Mcm3.1	0.814	0.628	0.45571	0.976	0.808	4
Mcm5.1	0.806	0.612	0.454009	0.968	0.787	4
Mcm4	0.809	0.618	0.432106	0.911	0.576	4
Ccne1	0.817	0.634	0.430046	0.781	0.223	4
Dhfr.1	0.784	0.568	0.420951	0.943	0.669	4
Ezh2.2	0.772	0.544	0.412071	0.968	0.819	4
Cdt1	0.793	0.586	0.39998	0.862	0.471	4
Clspn.1	0.755	0.51	0.395099	0.899	0.715	4
Cdc25a	0.767	0.534	0.392112	0.891	0.573	4
Dek.2	0.769	0.538	0.389671	0.996	0.949	4
Dut.2	0.79	0.58	0.385393	1	0.991	4
Mcm2	0.777	0.554	0.383956	0.964	0.835	4
Dtl	0.76	0.52	0.381907	0.858	0.556	4
Hells.1	0.799	0.598	0.377276	0.996	0.992	4
Hist1h2ae.1	0.731	0.462	0.376455	0.664	0.25	4
Nasp.2	0.744	0.488	0.357053	0.996	0.973	4
Tyms.2	0.74	0.48	0.356588	0.927	0.74	4

gene	myAUC	power	avg_logFC	pct.1	pct.2	cluster
Cdc45	0.743	0.486	0.347231	0.781	0.436	4
Pgp	0.757	0.514	0.346121	0.996	0.969	4
Chaf1a	0.759	0.518	0.342543	0.858	0.528	4
Rfc3.1	0.742	0.484	0.339671	0.939	0.739	4
Casp8ap2	0.741	0.482	0.338191	0.919	0.729	4
Hist1h1e.1	0.714	0.428	0.337957	0.761	0.383	4
Exo1	0.744	0.488	0.337124	0.802	0.485	4
2810417H13Rik.1	0.721	0.442	0.33545	0.632	0.236	4
Siva1.2	0.772	0.544	0.320113	1	0.992	4
Rpa2.1	0.748	0.496	0.318076	0.988	0.976	4
Cdca7	0.723	0.446	0.30711	0.842	0.578	4
Ppil1.1	0.734	0.468	0.303758	0.976	0.9	4
Rad51ap1.1	0.709	0.418	0.300001	0.741	0.435	4
1810037I17Rik	0.72	0.44	0.299719	0.964	0.872	4
Dnajc9.2	0.704	0.408	0.299631	0.943	0.761	4
Asf1b	0.732	0.464	0.298961	0.887	0.623	4
Brca1	0.733	0.466	0.293691	0.733	0.365	4
Syce2.2	0.734	0.468	0.293374	0.98	0.962	4
Fen1.1	0.701	0.402	0.291861	0.858	0.642	4
Tk1.1	0.716	0.432	0.291857	0.644	0.257	4
Pcna.1	0.73	0.46	0.291369	0.874	0.572	4
Chaf1b	0.725	0.45	0.285142	0.692	0.317	4
Topbp1	0.708	0.416	0.277244	0.96	0.789	4
Wdhd1.1	0.708	0.416	0.271866	0.733	0.406	4
Mms22l	0.708	0.416	0.270928	0.773	0.5	4
Wdr76	0.715	0.43	0.270227	0.717	0.377	4
Rad51	0.702	0.404	0.268368	0.907	0.716	4
Zmynd19	0.704	0.408	0.266097	0.955	0.852	4
Pim1	0.703	0.406	0.262452	0.964	0.887	4
Nxt1.1	0.704	0.408	0.260205	0.98	0.917	4
E2f8	0.738	0.476	0.256182	0.547	0.079	4
Arl6ip6	0.702	0.404	0.252399	0.846	0.612	4
Dtymk	0.709	0.418	0.25103	0.996	0.962	4
Rhox9	0.951	0.902	1.043709	0.989	0.353	5
Rhox6	0.908	0.816	0.884445	0.902	0.258	5
Rhox5	0.883	0.766	0.70985	0.989	0.923	5
Ckb	0.847	0.694	0.627378	0.978	0.785	5
Grn	0.822	0.644	0.506767	0.957	0.804	5
Fabp5	0.786	0.572	0.501563	0.875	0.491	5
Lefty2	0.776	0.552	0.493282	0.935	0.667	5
Dppa5a	0.878	0.756	0.49267	1	0.998	5

gene	myAUC	power	avg_logFC	pct.1	pct.2	cluster
Hmgn5	0.781	0.562	0.492525	0.87	0.556	5
L1td1	0.808	0.616	0.482669	0.94	0.566	5
Pdgfa	0.794	0.588	0.461845	0.951	0.643	5
Txn1.1	0.79	0.58	0.457538	1	0.928	5
Arpc1b	0.787	0.574	0.432513	0.897	0.603	5
Tdh	0.76	0.52	0.43195	0.946	0.766	5
Ung.1	0.761	0.522	0.421766	0.957	0.787	5
Nsmce4a.1	0.768	0.536	0.417079	0.962	0.882	5
Lgals1	0.733	0.466	0.409712	0.995	0.951	5
Ifitm3	0.749	0.498	0.373949	0.995	0.979	5
Gmnn.3	0.717	0.434	0.357053	0.962	0.808	5
Rest	0.771	0.542	0.353994	1	0.979	5
Grhpr	0.75	0.5	0.341488	0.967	0.84	5
Map1lc3b	0.79	0.58	0.339889	1	0.99	5
Dynll2	0.733	0.466	0.321525	0.989	0.906	5
Trp53	0.733	0.466	0.314233	0.978	0.903	5
Pmm1	0.768	0.536	0.31151	1	0.995	5
Klf2	0.723	0.446	0.311045	0.815	0.482	5
Cenpa.2	0.71	0.42	0.304615	1	0.909	5
Ybx1.1	0.77	0.54	0.303526	1	0.999	5
Prdx2	0.742	0.484	0.293067	0.995	0.988	5
Kcnk1	0.717	0.434	0.292705	0.511	0.105	5
Sub1	0.798	0.596	0.289831	1	1	5
Nans	0.707	0.414	0.287749	0.897	0.763	5
Pttg1.2	0.701	0.402	0.286406	0.995	0.925	5
Polr2g	0.707	0.414	0.286207	0.962	0.973	5
Lrpap1	0.709	0.418	0.274406	0.788	0.473	5
Pop5	0.72	0.44	0.274106	0.995	0.975	5
Plcd1	0.711	0.422	0.270513	0.511	0.108	5
Gstm1	0.751	0.502	0.259365	0.897	0.55	5
Sntb2	0.716	0.432	0.254737	0.745	0.428	5
Ube2l3	0.726	0.452	0.250711	1	0.995	5
Tfap2c	0.718	0.436	0.25048	0.576	0.16	5
Gtsf1	0.778	0.556	0.550534	0.765	0.397	6
Malat1.3	0.832	0.664	0.530545	1	0.999	6
Stk31.1	0.836	0.672	0.50439	1	0.959	6
Ifi27	0.801	0.602	0.494877	0.975	0.798	6
4930447C04Rik.1	0.794	0.588	0.467385	0.969	0.873	6
Rpl22l1	0.836	0.672	0.451183	1	1	6
Ptgr1.1	0.767	0.534	0.440249	0.914	0.609	6
Tex15	0.742	0.484	0.439684	0.883	0.635	6

gene	myAUC	power	avg_logFC	pct.1	pct.2	cluster
Nanos3	0.772	0.544	0.424896	0.87	0.634	6
Mael	0.739	0.478	0.412965	0.969	0.861	6
Tdrd5	0.779	0.558	0.405567	0.981	0.833	6
Taf7	0.736	0.472	0.402913	0.988	0.918	6
Nanos2	0.747	0.494	0.398514	0.722	0.319	6
Ogt	0.745	0.49	0.382771	0.944	0.787	6
Egr4.1	0.753	0.506	0.370718	0.809	0.458	6
Fkbp6	0.759	0.518	0.367172	0.994	0.957	6
Gmpr.1	0.737	0.474	0.36198	0.809	0.521	6
Trip12	0.737	0.474	0.339287	0.988	0.917	6
Dppa4	0.751	0.502	0.338808	1	0.987	6
Taf7l	0.728	0.456	0.338082	0.58	0.157	6
Spa17	0.72	0.44	0.337183	0.784	0.553	6
Bnc2.1	0.736	0.472	0.336785	0.864	0.608	6
Auts2	0.731	0.462	0.335016	0.901	0.689	6
Golgb1	0.716	0.432	0.33376	0.969	0.889	6
Dnd1	0.73	0.46	0.332975	0.994	0.957	6
Sox4	0.726	0.452	0.331834	0.981	0.9	6
Sycp3	0.723	0.446	0.331045	0.846	0.656	6
Sugt1	0.746	0.492	0.32716	1	0.967	6
Anxa7	0.734	0.468	0.32671	0.765	0.444	6
Abcb6	0.744	0.488	0.326674	0.84	0.518	6
Rsph9	0.744	0.488	0.32625	0.747	0.355	6
Gtsf1l	0.721	0.442	0.325234	0.679	0.33	6
D10Wsu102e	0.72	0.44	0.323944	0.963	0.879	6
Bbx	0.724	0.448	0.320269	0.994	0.959	6
Acly	0.725	0.45	0.316254	0.802	0.538	6
Rhox1	0.732	0.464	0.315945	0.907	0.719	6
Serf1.1	0.742	0.484	0.311476	0.988	0.957	6
Ddx25	0.707	0.414	0.308028	0.759	0.545	6
Lzts2	0.732	0.464	0.307985	0.784	0.462	6
Zmym3.1	0.727	0.454	0.302968	0.84	0.616	6
Ndufv3	0.732	0.464	0.298434	0.975	0.973	6
Ctdsp2	0.705	0.41	0.297127	0.864	0.759	6
Eva1b	0.701	0.402	0.295433	0.79	0.539	6
Rps27	0.789	0.578	0.294517	1	1	6
Kdm5b	0.721	0.442	0.28873	0.988	0.962	6
BC005561	0.704	0.408	0.288193	0.963	0.873	6
Mea1	0.733	0.466	0.282986	0.994	0.979	6
Topaz1	0.714	0.428	0.281042	0.654	0.332	6
Mrpl23.1	0.766	0.532	0.279433	1	1	6

gene	myAUC	power	avg_logFC	pct.1	pct.2	cluster
Atp6v1b2	0.701	0.402	0.274119	0.895	0.78	6
Npdc1	0.703	0.406	0.273704	0.543	0.171	6
Eef2	0.828	0.656	0.272969	1	1	6
Gabarap	0.704	0.408	0.268496	0.988	0.981	6
Ccdc53	0.703	0.406	0.262144	0.901	0.829	6
Snhg11	0.713	0.426	0.260322	0.611	0.223	6
Xlr5c	0.713	0.426	0.257573	0.593	0.195	6
Cox7a2l	0.738	0.476	0.257334	1	0.999	6
Cbx3	0.966	0.932	1.112509	1	0.896	7
Pdcd4	0.918	0.836	0.86254	0.983	0.857	7
Actb	0.922	0.844	0.729682	1	0.999	7
Upf1	0.785	0.57	0.587883	0.783	0.418	7
4933434E20Rik	0.799	0.598	0.505858	0.983	0.873	7
Hsf2	0.758	0.516	0.505129	0.783	0.479	7
Slc24a5	0.707	0.414	0.481441	0.6	0.319	7
Pfas	0.771	0.542	0.474667	0.8	0.499	7
Myef2	0.733	0.466	0.456759	0.733	0.464	7
Marf1	0.752	0.504	0.454903	0.7	0.319	7
Rrn3	0.72	0.44	0.359729	0.717	0.393	7
Slc39a1	0.741	0.482	0.351475	0.533	0.078	7
Notch2	0.725	0.45	0.344155	0.533	0.101	7
Lrrc8a	0.708	0.416	0.326715	0.583	0.229	7
Sdc4	0.724	0.448	0.315771	0.967	0.991	7
Ythdf2	0.703	0.406	0.312456	0.95	0.898	7
Gnb1	0.706	0.412	0.295938	0.95	0.977	7
Ssr1	0.712	0.424	0.27708	0.917	0.846	7
Stra8	0.812	0.624	0.969552	0.636	0.027	8
Smc1b.2	0.73	0.46	0.452693	1	0.964	8
Vamp3	0.704	0.408	0.402644	0.727	0.631	8
Sycp3.1	0.716	0.432	0.395219	0.773	0.667	8
Arhgap32	0.702	0.404	0.371912	0.682	0.466	8
Ddx4	0.756	0.512	0.368402	1	0.932	8
Syce1	0.727	0.454	0.354874	0.773	0.621	8
Camta1	0.747	0.494	0.354715	0.864	0.679	8
Tusc2	0.722	0.444	0.329948	0.773	0.59	8
Nudt4	0.71	0.42	0.32438	0.909	0.887	8
4932438A13Rik	0.708	0.416	0.320878	0.727	0.502	8
Polr2b	0.725	0.45	0.317743	0.864	0.811	8
Pcbd2	0.712	0.424	0.311456	0.818	0.682	8
Pigp	0.712	0.424	0.310866	0.909	0.929	8
Angel2	0.718	0.436	0.30742	0.773	0.677	8

gene	myAUC	power	avg_logFC	pct.1	pct.2	cluster
Nol11	0.716	0.432	0.295552	0.773	0.63	8

Table 3.S1: Clustered differentially expressed markers for e12.5 germ cells

gene	myAUC	power	avg_logFC	pct.1	pct.2	cluster
Hist1h2ap	0.821	0.642	0.611699	0.99	0.732	0
Hist1h1b	0.782	0.564	0.567369	0.956	0.601	0
Rrm2	0.772	0.544	0.382251	0.974	0.812	0
Slbp	0.768	0.536	0.347746	1	0.986	0
Ung	0.735	0.47	0.293553	0.998	0.971	0
Ccne1	0.722	0.444	0.308522	0.877	0.654	0
Hist1h1e	0.72	0.44	0.328899	0.942	0.662	0
Hist1h1a	0.714	0.428	0.274314	0.744	0.363	0
Top2a	0.853	0.706	0.494872	0.998	0.985	1
Prc1	0.829	0.658	0.510112	0.981	0.759	1
Plk1	0.822	0.644	0.469136	0.934	0.521	1
Cenpf	0.808	0.616	0.42994	1	0.993	1
Malat1	0.8	0.6	0.383871	1	0.999	1
Smc4	0.786	0.572	0.436708	0.99	0.916	1
Cdk1	0.786	0.572	0.414181	0.969	0.817	1
Cenpe	0.783	0.566	0.406533	0.977	0.76	1
Mis18bp1	0.779	0.558	0.384184	0.981	0.822	1
Bub3	0.779	0.558	0.369555	0.994	0.936	1
Aurka	0.764	0.528	0.371476	0.946	0.669	1
Tpx2	0.763	0.526	0.353969	0.973	0.795	1
Hn1	0.76	0.52	0.313743	1	0.988	1
Kpna2	0.757	0.514	0.343857	0.893	0.576	1
Nusap1	0.744	0.488	0.321209	0.928	0.649	1
Cdca2	0.744	0.488	0.320355	0.94	0.766	1
Incenp	0.74	0.48	0.317265	0.984	0.9	1
Aspm	0.739	0.478	0.27783	0.788	0.387	1
Fzr1	0.736	0.472	0.29352	0.845	0.486	1
Ube2c	0.724	0.448	0.304041	0.998	0.983	1
Mki67	0.713	0.426	0.296575	0.984	0.928	1
H2afx	0.711	0.422	0.324905	0.969	0.884	1
Cks2	0.707	0.414	0.261347	1	0.991	1
Hmmr	0.705	0.41	0.272709	0.934	0.688	1
Cdc20	0.701	0.402	0.286414	0.986	0.842	1
Hist1h1e	0.882	0.764	0.817323	0.979	0.656	2
Hist1h1b	0.865	0.73	0.807259	0.979	0.6	2
Hist1h2ap	0.825	0.65	0.665332	0.979	0.738	2
Hist1h1a	0.739	0.478	0.304333	0.785	0.358	2
Hist1h2ae	0.723	0.446	0.279649	0.707	0.287	2
H2afx	0.715	0.43	0.324527	0.979	0.883	2
Top2a	0.702	0.404	0.26079	0.994	0.986	2

gene	myAUC	power	avg_logFC	pct.1	pct.2	cluster
Hspa5	0.734	0.468	0.316854	1	0.991	3
Ccnb1	0.733	0.466	0.368713	0.996	0.953	3
Cdc20	0.728	0.456	0.396	0.976	0.846	3
Dtl	0.719	0.438	0.313369	0.955	0.805	3
Cks2	0.715	0.43	0.269664	1	0.991	3
Arl6ip1	0.875	0.75	0.631165	1	0.984	4
Ccnb1	0.856	0.712	0.566726	0.996	0.957	4
Ube2c	0.855	0.71	0.535673	1	0.985	4
Cdc20	0.844	0.688	0.599106	0.996	0.857	4
Tubb4b	0.809	0.618	0.366831	1	0.993	4
Hmmr	0.8	0.6	0.434517	0.979	0.71	4
Dazl	0.8	0.6	0.348437	1	0.995	4
Cenpf	0.791	0.582	0.393826	1	0.994	4
Mtdh	0.786	0.572	0.43262	0.992	0.962	4
Cks2	0.776	0.552	0.324845	1	0.992	4
Hn1	0.752	0.504	0.318303	1	0.989	4
Cenpe	0.74	0.48	0.348627	0.971	0.785	4
Mis18bp1	0.739	0.478	0.340568	0.962	0.842	4
Nusap1	0.724	0.448	0.294816	0.908	0.681	4
Lefty2	0.723	0.446	0.401477	0.983	0.925	4
Tpx2	0.723	0.446	0.307779	0.975	0.814	4
Lefty1	0.72	0.44	0.389738	0.908	0.707	4
Kif20b	0.712	0.424	0.279613	0.958	0.797	4
Aurka	0.706	0.412	0.265913	0.912	0.703	4
Luc7l3	0.701	0.402	0.253029	1	0.973	4
Rpl18a	0.877	0.754	0.254673	1	1	6
Rpl10a	0.838	0.676	0.252635	1	1	6
Eef2	0.817	0.634	0.307843	1	1	6
Id1	0.81	0.62	0.686703	0.716	0.204	6
Stra8	0.771	0.542	0.753188	0.568	0.039	6
Pla2g16	0.767	0.534	0.479657	0.602	0.128	6
Ifitm1	0.765	0.53	0.354158	1	0.998	6
Id3	0.756	0.512	0.447203	0.989	0.948	6
Rpl22l1	0.756	0.512	0.307932	1	1	6
Mdk	0.743	0.486	0.550545	0.716	0.407	6
BC048679	0.738	0.476	0.485332	0.898	0.817	6
Zglp1	0.72	0.44	0.44252	0.682	0.399	6
Bri3	0.716	0.432	0.375438	0.92	0.904	6
Atox1	0.716	0.432	0.269506	0.989	0.982	6
Grn	0.712	0.424	0.367466	0.989	0.966	6
Malat1	0.712	0.424	0.332847	1	0.999	6
H2afy	0.708	0.416	0.251314	1	0.997	6

gene	myAUC	power	avg_logFC	pct.1	pct.2	cluster
Mrpl23	0.706	0.412	0.273454	0.989	0.998	6
Nr6a1	0.704	0.408	0.316165	0.648	0.353	6
Tspan3	0.702	0.404	0.319197	0.966	0.942	6
Phlda3	0.963	0.926	1.013573	0.979	0.256	7
Cdkn1a	0.942	0.884	0.997197	1	0.399	7
Mdm2	0.935	0.87	0.866177	0.979	0.742	7
Ccng1	0.914	0.828	0.673122	0.979	0.443	7
Rps27l	0.886	0.772	0.389535	1	0.999	7
Plk2	0.867	0.734	0.580097	0.75	0.026	7
Dhx16	0.857	0.714	0.75018	0.938	0.562	7
1700007K13Rik	0.845	0.69	0.714098	0.812	0.219	7
Ddit4l	0.838	0.676	0.571214	0.708	0.047	7
Btg2	0.834	0.668	0.707449	0.771	0.246	7
Cd81	0.832	0.664	0.739336	0.812	0.273	7
Ddit4	0.827	0.654	0.558649	0.854	0.443	7
Crip2	0.817	0.634	0.532407	0.958	0.719	7
Hat1	0.799	0.598	0.406272	1	0.993	7
Pmm1	0.795	0.59	0.321081	1	0.996	7
Bloc1s2	0.794	0.588	0.4904	0.896	0.645	7
Cox6b2	0.79	0.58	0.6526	0.917	0.767	7
Bax	0.784	0.568	0.321918	1	0.996	7
Trp53inp1	0.782	0.564	0.446891	0.833	0.484	7
Baiap2	0.782	0.564	0.362415	0.854	0.443	7
Sdc4	0.781	0.562	0.538751	0.979	0.81	7
Aen	0.781	0.562	0.502041	0.917	0.705	7
Cald1	0.781	0.562	0.38061	0.625	0.094	7
Tubb6	0.776	0.552	0.370664	0.646	0.164	7
Ranbp3	0.771	0.542	0.485222	0.833	0.604	7
Dnajc9	0.771	0.542	0.377845	1	0.924	7
Sesn2	0.764	0.528	0.308985	0.75	0.326	7
Nudcd2	0.748	0.496	0.400141	0.938	0.8	7
Rbm38	0.745	0.49	0.36484	0.938	0.596	7
Zmat3	0.744	0.488	0.35092	0.604	0.161	7
Gfer	0.742	0.484	0.334032	0.938	0.947	7
Dstn	0.738	0.476	0.339385	0.979	0.928	7
Emd	0.734	0.468	0.315964	0.896	0.76	7
N4bp1	0.734	0.468	0.313219	0.917	0.788	7
Ckap2	0.728	0.456	0.325643	0.833	0.705	7
Eif3l	0.728	0.456	0.307351	1	0.985	7
Ctc1	0.727	0.454	0.404909	0.792	0.508	7
Gtse1	0.727	0.454	0.350421	0.833	0.506	7
Bud13	0.727	0.454	0.327852	0.729	0.369	7

gene	myAUC	power	avg_logFC	pct.1	pct.2	cluster
Ak1	0.726	0.452	0.276315	0.792	0.528	7
Ppm1d	0.721	0.442	0.291155	0.729	0.424	7
Nfyb	0.719	0.438	0.337359	0.875	0.732	7
Commd3	0.717	0.434	0.281147	0.896	0.799	7
1500009L16Rik	0.715	0.43	0.321485	0.896	0.553	7
Bbc3	0.714	0.428	0.321554	0.542	0.14	7
Rap2b	0.713	0.426	0.294237	0.625	0.277	7
Lzic	0.712	0.424	0.304379	0.75	0.473	7
Sap30bp	0.71	0.42	0.378004	0.75	0.513	7
Exoc4	0.71	0.42	0.287666	0.771	0.534	7
Hist1h2ap	0.706	0.412	0.396572	0.958	0.78	7
Akr1a1	0.703	0.406	0.250294	0.979	0.935	7
Nme4	0.702	0.404	0.328988	0.729	0.452	7
Gpx3	0.702	0.404	0.287635	0.542	0.194	7

REFERENCES

Altschuler, S.J., and Wu, L.F. (2010). Cellular heterogeneity: when do differences make a difference? Cell *141*, 559–563.

Ansel, J., Bottin, H., Rodriguez-Beltran, C., Damon, C., Nagarajan, M., Fehrmann, S., François, J., and Yvert, G. (2008). Cell-to-Cell Stochastic Variation in Gene Expression Is a Complex Genetic Trait. PLoS Genet *4*.

Aravin, A.A., Sachidanandam, R., Bourc'his, D., Schaefer, C., Pezic, D., Toth, K.F., Bestor, T., and Hannon, G.J. (2008). A piRNA pathway primed by individual transposons is linked to de novo DNA methylation in mice. Mol. Cell *31*, 785–799.

Aravin, A.A., Heijden, G.W. van der, Castañeda, J., Vagin, V.V., Hannon, G.J., and Bortvin, A. (2009). Cytoplasmic Compartmentalization of the Fetal piRNA Pathway in Mice. PLOS Genetics *5*, e1000764.

Benchimol, S. (2001). p53-dependent pathways of apoptosis.

Bensaad, K., Tsuruta, A., Selak, M.A., Vidal, M.N.C., Nakano, K., Bartrons, R., Gottlieb, E., and Vousden, K.H. (2006). TIGAR, a p53-inducible regulator of glycolysis and apoptosis. Cell *126*, 107–120.

Bondar, T., and Medzhitov, R. (2010). p53-mediated hematopoietic stem and progenitor cell competition. Cell Stem Cell *6*, 309–322.

Bourc'his, D., and Bestor, T.H. (2004). Meiotic catastrophe and retrotransposon reactivation in male germ cells lacking Dnmt3L. Nature *431*, 96.

Bowles, J., and Koopman, P. (2007). Retinoic acid, meiosis and germ cell fate in mammals. Development *134*, 3401–3411.

Bowles, J., Feng, C.-W., Spiller, C., Davidson, T.-L., Jackson, A., and Koopman, P. (2010). FGF9 suppresses meiosis and promotes male germ cell fate in mice. Dev. Cell *19*, 440–449.

Brennan, J., Norris, D.P., and Robertson, E.J. (2002). Nodal activity in the node governs left-right asymmetry. Genes Dev *16*, 2339–2344.

Bullejos, M., and Koopman, P. (2004). Germ cells enter meiosis in a rostro-caudal wave during development of the mouse ovary. Mol. Reprod. Dev. *68*, 422–428.

Cantú, A.V., Altshuler-Keylin, S., and Laird, D.J. (2016). Discrete somatic niches coordinate proliferation and migration of primordial germ cells via Wnt signaling. J Cell Biol *214*, 215–229.

Castañeda, J., Genzor, P., van der Heijden, G.W., Sarkeshik, A., Yates, J.R., Ingolia, N.T., and Bortvin, A. (2014). Reduced pachytene piRNAs and translation underlie spermiogenic arrest in Maelstrom mutant mice. EMBO J *33*, 1999–2019.

Chen, C., and Shen, M.M. (2004). Two Modes by which Lefty Proteins Inhibit Nodal Signaling. Current Biology *14*, 618–624.

Chipuk, J.E., Kuwana, T., Bouchier-Hayes, L., Droin, N.M., Newmeyer, D.D., Schuler, M., and Green, D.R. (2004). Direct activation of Bax by p53 mediates mitochondrial membrane permeabilization and apoptosis. Science *303*, 1010–1014.

Clark, J.P., and Lau, N.C. (2014). Piwi proteins and piRNAs step onto the systems biology stage. Adv Exp Med Biol *825*, 159–197.

Cook, M.S., Coveney, D., Batchvarov, I., Nadeau, J.H., and Capel, B. (2009). BAX-mediated cell death affects early germ cell loss and incidence of testicular teratomas in Dnd1Ter/Ter mice. Developmental Biology *328*, 377–383.

Cook, M.S., Munger, S.C., Nadeau, J.H., and Capel, B. (2011). Regulation of male germ cell cycle arrest and differentiation by DND1 is modulated by genetic background. Development *138*, 23–32.

Coucouvanis, E.C., Sherwood, S.W., Carswell-Crumpton, C., Spack, E.G., and Jones, P.P. (1993). Evidence That the Mechanism of Prenatal Germ Cell Death in the Mouse Is Apoptosis. Experimental Cell Research *209*, 238–247.

Dudley, B., Palumbo, C., Nalepka, J., and Molyneaux, K. (2010). BMP Signaling Controls Formation of a Primordial Germ Cell Niche within the Early Genital Ridges. Dev Biol *343*, 84–93.

de Felici, M.D., Carlo, A.D., Pesce, M., Iona, S., Farrace, M.G., and Piacentini, M. (1999). Bcl-2 and Bax regulation of apoptosis in germ cells during prenatal oogenesis in the mouse embryo. Cell Death Differ. *6*, 908–915.

Fridman, J.S., and Lowe, S.W. (2003). Control of apoptosis by p53. Oncogene *22*, 9030–9040.

Goodell, M.A., Nguyen, H., and Shroyer, N. (2015). Somatic stem cell heterogeneity: diversity in the blood, skin and intestinal stem cell compartments. Nature Reviews Molecular Cell Biology *16*, 299.

Greder, L.V., Gupta, S., Li, S., Abedin, M.J., Sajini, A., Segal, Y., Slack, J.M.W., and Dutton, J.R. (2012). Brief Report: Analysis of Endogenous Oct4 Activation during Induced Pluripotent Stem Cell Reprogramming Using an Inducible Oct4 Lineage Label. STEM CELLS *30*, 2596–2601.

Greenbaum, M.P., Iwamori, T., Buchold, G.M., and Matzuk, M.M. (2011). Germ Cell Intercellular Bridges. Cold Spring Harb Perspect Biol *3*, a005850.

Hajkova, P. (2011). Epigenetic reprogramming in the germline: towards the ground state of the epigenome. Philos Trans R Soc Lond B Biol Sci *366*, 2266–2273.

Hajkova, P., Ancelin, K., Waldmann, T., Lacoste, N., Lange, U.C., Cesari, F., Lee, C., Almouzni, G., Schneider, R., and Surani, M.A. (2008). Chromatin dynamics during epigenetic reprogramming in the mouse germ line. Nature *452*, 877–881.

Hamer, G., Roepers-Gajadien, H.L., Gademan, I.S., Kal, H.B., and De Rooij, D.G. (2003). Intercellular bridges and apoptosis in clones of male germ cells. Int. J. Androl. *26*, 348–353.

Hansson, K., Jafari-Mamaghani, M., and Krieger, P. (2013). RipleyGUI: software for analyzing spatial patterns in 3D cell distributions. Front Neuroinform *7*.

Hargan-Calvopina, J., Taylor, S., Cook, H., Hu, Z., Lee, S.A., Yen, M.-R., Chiang, Y.-S., Chen, P.-Y., and Clark, A.T. (2016). Stage-Specific Demethylation in Primordial Germ Cells Safeguards against Precocious Differentiation. Developmental Cell *39*, 75–86.

He, Z., Jiang, J., Kokkinaki, M., and Dym, M. (2009). Nodal signaling via an autocrine pathway promotes proliferation of mouse spermatogonial stem/progenitor cells through Smad2/3 and Oct-4 activation. Stem Cells *27*, 2580–2590.

Heaney, J.D., Anderson, E.L., Michelson, M.V., Zechel, J.L., Conrad, P.A., Page, D.C., and Nadeau, J.H. (2012). Germ cell pluripotency, premature differentiation and susceptibility to testicular teratomas in mice. Development *139*, 1577–1586.

Hiramatsu, R., Harikae, K., Tsunekawa, N., Kurohmaru, M., Matsuo, I., and Kanai, Y. (2010). FGF signaling directs a center-to-pole expansion of tubulogenesis in mouse testis differentiation. Development *137*, 303–312.

Houwing, S., Kamminga, L.M., Berezikov, E., Cronembold, D., Girard, A., van den Elst, H., Filippov, D.V., Blaser, H., Raz, E., Moens, C.B., et al. (2007). A role for Piwi and piRNAs in germ cell maintenance and transposon silencing in Zebrafish. Cell *129*, 69–82.

Inoue, K., Ichiyanagi, K., Fukuda, K., Glinka, M., and Sasaki, H. (2017). Switching of dominant retrotransposon silencing strategies from posttranscriptional to transcriptional mechanisms during male germ-cell development in mice. PLOS Genetics *13*, e1006926.

Jiang, P., Du, W., Heese, K., and Wu, M. (2006). The Bad Guy Cooperates with Good Cop p53: Bad Is Transcriptionally Up-Regulated by p53 and Forms a Bad/p53 Complex at the Mitochondria To Induce Apoptosis. Mol Cell Biol *26*, 9071–9082.

Kanatsu-Shinohara, M., Naoki, H., and Shinohara, T. (2016). Nonrandom Germline Transmission of Mouse Spermatogonial Stem Cells. Developmental Cell *38*, 248–261.

Kim, S., Günesdogan, U., Zylicz, J.J., Hackett, J.A., Cougot, D., Bao, S., Lee, C., Dietmann, S., Allen, G.E., Sengupta, R., et al. (2014). PRMT5 Protects Genomic Integrity during Global DNA Demethylation in Primordial Germ Cells and Preimplantation Embryos. Mol Cell *56*, 564–579.

Kimura, M., Itoh, N., Takagi, S., Sasao, T., Takahashi, A., Masumori, N., and Tsukamoto, T. (2003). Balance of Apoptosis and Proliferation of Germ Cells Related to Spermatogenesis in Aged Men. Journal of Andrology *24*, 185–191.

Klawitter, S., Fuchs, N.V., Upton, K.R., Muñoz-Lopez, M., Shukla, R., Wang, J., Garcia-Cañadas, M., Lopez-Ruiz, C., Gerhardt, D.J., Sebe, A., et al. (2016). Reprogramming triggers endogenous L1 and *Alu* retrotransposition in human induced pluripotent stem cells. Nature Communications *7*, 10286.

Knudson, C.M., Tung, K.S., Tourtellotte, W.G., Brown, G.A., and Korsmeyer, S.J. (1995). Bax-deficient mice with lymphoid hyperplasia and male germ cell death. Science *270*, 96–99.

Kopera, I.A., Bilinska, B., Cheng, C.Y., and Mruk, D.D. (2010). Sertoli-germ cell junctions in the testis: a review of recent data. Philos. Trans. R. Soc. Lond., B, Biol. Sci. *365*, 1593–1605.

Koubova, J., Menke, D.B., Zhou, Q., Capel, B., Griswold, M.D., and Page, D.C. (2006). Retinoic acid regulates sex-specific timing of meiotic initiation in mice. Proc. Natl. Acad. Sci. U.S.A. *103*, 2474–2479.

Koubova, J., Hu, Y.-C., Bhattacharyya, T., Soh, Y.Q.S., Gill, M.E., Goodheart, M.L., Hogarth, C.A., Griswold, M.D., and Page, D.C. (2014). Retinoic Acid Activates Two Pathways Required for Meiosis in Mice. PLOS Genetics *10*, e1004541.

Kumar, P., Tan, Y., and Cahan, P. (2017). Understanding development and stem cells using single cell-based analyses of gene expression. Development *144*, 17–32.

Kuramochi-Miyagawa, S., Kimura, T., Ijiri, T.W., Isobe, T., Asada, N., Fujita, Y., Ikawa, M., Iwai, N., Okabe, M., Deng, W., et al. (2004). Mili, a mammalian member of piwi family gene, is essential for spermatogenesis. Development *131*, 839–849.

Lans, H., Marteijn, J.A., Schumacher, B., Hoeijmakers, J.H.J., Jansen, G., and Vermeulen, W. (2010). Involvement of Global Genome Repair, Transcription Coupled Repair, and Chromatin Remodeling in UV DNA Damage Response Changes during Development. PLOS Genetics *6*, e1000941.

Lomonosova, E., and Chinnadurai, G. (2008). BH3-only proteins in apoptosis and beyond: an overview. Oncogene *27 Suppl 1*, S2-19.

Lynch, M. (2010). Evolution of the mutation rate. Trends Genet *26*, 345–352.

Maatouk, D.M., and Resnick, J.L. (2003). Continuing primordial germ cell differentiation in the mouse embryo is a cell-intrinsic program sensitive to DNA methylation. Developmental Biology *258*, 201–208.

Maatouk, D.M., Kellam, L.D., Mann, M.R.W., Lei, H., Li, E., Bartolomei, M.S., and Resnick, J.L. (2006). DNA methylation is a primary mechanism for silencing postmigratory primordial germ cell genes in both germ cell and somatic cell lineages. Development *133*, 3411–3418.

Maclean, J.A., Chen, M.A., Wayne, C.M., Bruce, S.R., Rao, M., Meistrich, M.L., Macleod, C., and Wilkinson, M.F. (2005). Rhox: a new homeobox gene cluster. Cell *120*, 369–382.

Mendis, S.H.S., Meachem, S.J., Sarraj, M.A., and Loveland, K.L. (2011). Activin A Balances Sertoli and Germ Cell Proliferation in the Fetal Mouse Testis. Biol Reprod *84*, 379–391.

Menke, D.B., Koubova, J., and Page, D.C. (2003). Sexual differentiation of germ cells in XX mouse gonads occurs in an anterior-to-posterior wave. Dev. Biol. *262*, 303–312.

Messerschmidt, D.M., Knowles, B.B., and Solter, D. (2014). DNA methylation dynamics during epigenetic reprogramming in the germline and preimplantation embryos. Genes Dev. *28*, 812–828.

Miles, D.C., Wakeling, S.I., Stringer, J.M., Bergen, J.A. van den, Wilhelm, D., Sinclair, A.H., and Western, P.S. (2013). Signaling through the TGF Beta-Activin Receptors ALK4/5/7 Regulates Testis Formation and Male Germ Cell Development. PLOS ONE *8*, e54606.

Molaro, A., Falciatori, I., Hodges, E., Aravin, A.A., Marran, K., Rafii, S., McCombie, W.R., Smith, A.D., and Hannon, G.J. (2014). Two waves of de novo methylation during mouse germ cell development. Genes Dev. *28*, 1544–1549.

Molyneaux, K.A., Stallock, J., Schaible, K., and Wylie, C. (2001). Time-lapse analysis of living mouse germ cell migration. Dev. Biol. *240*, 488–498.

Mori, C., Nakamura, N., Dix, D.J., Fujioka, M., Nakagawa, S., Shiota, K., and Eddy, E.M. (1997). Morphological analysis of germ cell apoptosis during postnatal testis development in normal and Hsp70-2 knockout mice. Dev. Dyn. *208*, 125–136.

Mork, L., Tang, H., Batchvarov, I., and Capel, B. (2012). Mouse germ cell clusters form by aggregation as well as clonal divisions. Mech. Dev. *128*, 591–596.

Müller, P., Rogers, K.W., Jordan, B.M., Lee, J.S., Robson, D., Ramanathan, S., and Schier, A.F. (2012). Differential diffusivity of Nodal and Lefty underlies a reaction-diffusion patterning system. Science *336*, 721–724.

Nagano, R., Tabata, S., Nakanishi, Y., Ohsako, S., Kurohmaru, M., and Hayashi, Y. (2000). Reproliferation and relocation of mouse male germ cells (gonocytes) during prespermatogenesis. Anat. Rec. *258*, 210–220.

Närvä, E., Rahkonen, N., Emani, M.R., Lund, R., Pursiheimo, J.-P., Nästi, J., Autio, R., Rasool, O., Denessiouk, K., Lähdesmäki, H., et al. (2012). RNA-Binding Protein L1TD1 Interacts with LIN28 via RNA and is Required for Human Embryonic Stem Cell Self-Renewal and Cancer Cell Proliferation. STEM CELLS *30*, 452–460.

O'Donnell, K.A., and Burns, K.H. (2010). Mobilizing diversity: transposable element insertions in genetic variation and disease. Mobile DNA *1*, 21.

Patel, A.P., Tirosh, I., Trombetta, J.J., Shalek, A.K., Gillespie, S.M., Wakimoto, H., Cahill, D.P., Nahed, B.V., Curry, W.T., Martuza, R.L., et al. (2014). Single-cell RNA-seq highlights intratumoral heterogeneity in primary glioblastoma. Science *344*, 1396–1401.

Pepling, M.E., and Spradling, A.C. (1998). Female mouse germ cells form synchronously dividing cysts. Development *125*, 3323–3328.

Perez, G.I., Knudson, C.M., Leykin, L., Korsmeyer, S.J., and Tilly, J.L. (1997). Apoptosis-associated signaling pathways are required for chemotherapy-mediated female germ cell destruction. Nat. Med. *3*, 1228–1232.

Popp, C., Dean, W., Feng, S., Cokus, S.J., Andrews, S., Pellegrini, M., Jacobsen, S.E., and Reik, W. (2010). Genome-wide erasure of DNA methylation in mouse primordial germ cells is affected by Aid deficiency. Nature *463*, 1101–1105.

Rinkevich, Y., Lindau, P., Ueno, H., Longaker, M.T., and Weissman, I.L. (2011). Germ-layer and lineage-restricted stem/progenitors regenerate the mouse digit tip. Nature *476*, 409–413.

Rodriguez, I., Ody, C., Araki, K., Garcia, I., and Vassalli, P. (1997). An early and massive wave of germinal cell apoptosis is required for the development of functional spermatogenesis. The EMBO Journal *16*, 2262–2270.

de Rooij, D.G. (2009). The spermatogonial stem cell niche. Microsc. Res. Tech. *72*, 580–585.

Rucker, E.B., Dierisseau, P., Wagner, K.-U., Garrett, L., Wynshaw-Boris, A., Flaws, J.A., and Hennighausen, L. (2000). Bcl-x and Bax Regulate Mouse Primordial Germ Cell Survival and Apoptosis during Embryogenesis. Mol Endocrinol *14*, 1038–1052.

Runyan, C., Schaible, K., Molyneaux, K., Wang, Z., Levin, L., and Wylie, C. (2006). Steel factor controls midline cell death of primordial germ cells and is essential for their normal proliferation and migration. Development *133*, 4861–4869.

Russell, L.D., Chiarini-Garcia, H., Korsmeyer, S.J., and Knudson, C.M. (2002). Bax-dependent spermatogonia apoptosis is required for testicular development and spermatogenesis. Biol. Reprod. *66*, 950–958.

Saba, R., Kato, Y., and Saga, Y. (2014). NANOS2 promotes male germ cell development independent of meiosis suppression. Developmental Biology *385*, 32–40.

Saitou, M., and Yamaji, M. (2012). Primordial Germ Cells in Mice. Cold Spring Harb Perspect Biol *4*, a008375.

Saitou, M., Barton, S.C., and Surani, M.A. (2002). A molecular programme for the specification of germ cell fate in mice. Nature *418*, 293.

Sakashita, A., Kawabata, Y., Jincho, Y., Tajima, S., Kumamoto, S., Kobayashi, H., Matsui, Y., and Kono, T. (2015). Sex Specification and Heterogeneity of Primordial Germ Cells in Mice. PLOS ONE *10*, e0144836.

Salk, J.J., Fox, E.J., and Loeb, L.A. (2010). Mutational Heterogeneity in Human Cancers: Origin and Consequences. Annu Rev Pathol *5*, 51–75.

Satija, R., Farrell, J.A., Gennert, D., Schier, A.F., and Regev, A. (2015). Spatial reconstruction of single-cell gene expression data. Nature Biotechnology *33*, 495.

Sax, J.K., Fei, P., Murphy, M.E., Bernhard, E., Korsmeyer, S.J., and El-Deiry, W.S. (2002). BID regulation by p53 contributes to chemosensitivity. Nat. Cell Biol. *4*, 842–849.

Schemmer, J., Araúzo-Bravo, M.J., Haas, N., Schäfer, S., Weber, S.N., Becker, A., Eckert, D., Zimmer, A., Nettersheim, D., and Schorle, H. (2013). Transcription Factor TFAP2C Regulates Major Programs Required for Murine Fetal Germ Cell Maintenance and Haploinsufficiency Predisposes to Teratomas in Male Mice. PLOS ONE *8*, e71113.

Seisenberger, S., Andrews, S., Krueger, F., Arand, J., Walter, J., Santos, F., Popp, C., Thienpont, B., Dean, W., and Reik, W. (2012). The Dynamics of Genome-wide DNA Methylation Reprogramming in Mouse Primordial Germ Cells. Molecular Cell *48*, 849–862.

Seki, Y., Yamaji, M., Yabuta, Y., Sano, M., Shigeta, M., Matsui, Y., Saga, Y., Tachibana, M., Shinkai, Y., and Saitou, M. (2007). Cellular dynamics associated with the genome-wide epigenetic reprogramming in migrating primordial germ cells in mice. Development *134*, 2627–2638.

Snippert, H.J., van der Flier, L.G., Sato, T., van Es, J.H., van den Born, M., Kroon-Veenboer, C., Barker, N., Klein, A.M., van Rheenen, J., Simons, B.D., et al. Intestinal Crypt Homeostasis Results from Neutral Competition between Symmetrically Dividing Lgr5 Stem Cells. Cell *143*, 134–144.

Sookdeo, A., Hepp, C.M., McClure, M.A., and Boissinot, S. (2013). Revisiting the evolution of mouse LINE-1 in the genomic era. Mobile DNA *4*, 3.

Soper, S.F.C., van der Heijden, G.W., Hardiman, T.C., Goodheart, M., Martin, S.L., de Boer, P., and Bortvin, A. (2008). Mouse Maelstrom, a component of nuage, is essential for spermatogenesis and transposon repression in meiosis. Dev Cell *15*, 285–297.

Spiller, C., Wilhelm, D., and Koopman, P. (2009). Cell cycle analysis of fetal germ cells during sex differentiation in mice. Biol. Cell *101*, 587–598.

Spiller, C.M., Feng, C.-W., Jackson, A., Gillis, A.J.M., Rolland, A.D., Looijenga, L.H.J., Koopman, P., and Bowles, J. (2012). Endogenous Nodal signaling regulates germ cell potency during mammalian testis development. Development *139*, 4123–4132.

Su, Y., Davies, S., Davis, M., Lu, H., Giller, R., Krailo, M., Cai, Q., Robison, L., and Shu, X.-O. (2007). Expression of LINE-1 p40 protein in pediatric malignant germ cell tumors and its association with clinicopathological parameters: A report from the Children's Oncology Group. Cancer Letters *247*, 204–212.

Suzuki, A., and Saga, Y. (2008). Nanos2 suppresses meiosis and promotes male germ cell differentiation. Genes Dev. *22*, 430–435.

Szabó, P.E., Hübner, K., Schöler, H., and Mann, J.R. (2002). Allele-specific expression of imprinted genes in mouse migratory primordial germ cells. Mech. Dev. *115*, 157–160.

Tian-Zhong, M., Bi, C., Ying, Z., Xia, J., Cai-Ling, P., Yun-Shan, Z., Mei-Wen, H., and Yan-Ru, N. (2016). Critical role of Emx2 in the pluripotency – differentiation transition in male gonocytes via regulation of FGF9/NODAL pathway. Reproduction *151*, 673–681.
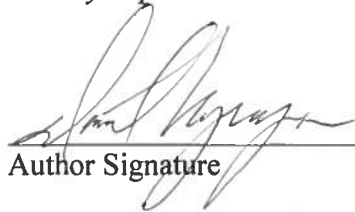
Ueno, H., Turnbull, B.B., and Weissman, I.L. (2009). Two-step oligoclonal development of male germ cells. PNAS *106*, 175–180.

van Boxtel, A.L., Chesebro, J.E., Heliot, C., Ramel, M.-C., Stone, R.K., and Hill, C.S. (2015). A Temporal Window for Signal Activation Dictates the Dimensions of a Nodal Signaling Domain. Developmental Cell *35*, 175–185.

Wang, R.A., Nakane, P.K., and Koji, T. (1998). Autonomous cell death of mouse male germ cells during fetal and postnatal period. Biol. Reprod. *58*, 1250–1256.

Western, P.S., Miles, D.C., van den Bergen, J.A., Burton, M., and Sinclair, A.H. (2008). Dynamic regulation of mitotic arrest in fetal male germ cells. Stem Cells *26*, 339–347.

Wu, Q., Kanata, K., Saba, R., Deng, C.-X., Hamada, H., and Saga, Y. (2013). Nodal/activin signaling promotes male germ cell fate and suppresses female programming in somatic cells. Development *140*, 291–300.

Xu, Y. (2003). Regulation of p53 responses by post-translational modifications. Cell Death Differ. *10*, 400–403.

Yabuta, Y., Ohta, H., Abe, T., Kurimoto, K., Chuma, S., and Saitou, M. (2011). TDRD5 is required for retrotransposon silencing, chromatoid body assembly, and spermiogenesis in mice. The Journal of Cell Biology *192*, 781–795.

Yamaguchi, S., Hong, K., Liu, R., Inoue, A., Shen, L., Zhang, K., and Zhang, Y. (2013). Dynamics of 5-methylcytosine and 5-hydroxymethylcytosine during germ cell reprogramming. Cell Res. *23*, 329–339.

Yang, F., and Wang, P.J. (2016). Multiple LINEs of retrotransposon silencing mechanisms in the mammalian germline. Semin Cell Dev Biol *59*, 118–125.

Yao, H.H.-C., DiNapoli, L., and Capel, B. (2003). Meiotic germ cells antagonize mesonephric cell migration and testis cord formation in mouse gonads. Development *130*, 5895–5902.

(2015). Front-matter. In Sertoli Cell Biology (Second Edition), M.D. Griswold, ed. (Oxford: Academic Press), pp. i–iii.

Publishing Agreement

It is the policy of the University to encourage the distribution of all theses, dissertations, and manuscripts. Copies of all UCSF theses, dissertations, and manuscripts will be routed to the library via the Graduate Division. The library will make all theses, dissertations, and manuscripts accessible to the public and will preserve these to the best of their abilities, in perpetuity.

Please sign the following statement:

I hereby grant permission to the Graduate Division of the University of California, San Francisco to release copies of my thesis, dissertation, or manuscript to the Campus Library to provide access and preservation, in whole or in part, in perpetuity.

Author Signature

DEC 22, 2017

Date